STRUCTURE AND ORIGIN OF THE CYGNUS SUPERBUBBLE

NIKOLAY G. BOCHKAREV and TATIANA G. SITNIK

Sternberg State Astronomical Intitute, Moscow, U.S.S.R.

(Received 15 June, 1984)

Abstract. This paper summarizes and analyzes the results of radio optical, infrared, and X-ray observations of a large sector of the sky in the constellation Cygnus ($\alpha \approx 19^h20^m$–22^h, $\delta = 30$–$50°$; $l^{II} = 65$–$90°$, $|b^{II}| \lesssim 10°$). This region is associated with an extended X-ray source referred to as the Cygnus superbubble. About a quarter of the superbubble region is occupied by the extensively investigated multicomponent thermal radio source Cyg X. The region contains eight OB-associations which, when projected on the sky, duplicate the outline of the X-ray superbubble. These associations contains 110 stars of high luminosity (about 40 Wolf–Rayet and Of stars). The observations suggest that the X-ray superbubble is not a single object. Between 50 and 75% of its X-ray emission can be ascribed to discrete sources, the rest being probably due to regions of coronal gas about 100 pc in diameter, created by stellar winds and, possibly, supernova explosions in individual associations. The objects that produce the X-ray and optical radiation of the presumed superbubble are located at distances from 0.5 to 2.5 kpc from the Sun in the Carina-Cygnus spiral arm. The eastern portion of the region presumed superbubble contains the associations Cyg OB7 and Cyg OB4 and is generally less than 1 kpc distant, while the western portion contains the associations Cyg OB1, 2, 3, 8, and 9 and is 1 to 2 kpc distant.

1. Introduction

In recent years, a great deal of attention has been given to studies of the large-scale structure of the interstellar medium. The major impetus to these studies was given by three observations: (1) The discovery of the coronal gas from the UV lines of high-charge nitrogen and oxygen ion absorption in the interstellar medium (Jenkins and Meloy, 1974; York, 1974, 1977). (2) The realization that long-lived large caverns filled with hot rarefied coronal gas may arise from supernova explosions (Cox and Smith, 1974; McKee and Ostriker, 1977). (3) The existence of strong stellar winds around stars with the highest luminosity (Pikel'ner and Shcheglov, 1968; Avedisova, 1971, 1977; Dyson and deVries, 1972; Castor *et al.*, 1975; Weaver *et al.*, 1977; and others).

This is precisely what has prompted investigations of large-scale bubble structures in our and other galaxies. Numerous H II shells about 100 pc in size and several H II shells up to about 1 kpc in size have been found in the Magellanic clouds (Goudis and Meaburn, 1978; Meaburn, 1980). Some spiral galaxies have been found to contain H II bubble regions up to about 300 pc in diameter (see Sharov's (1982) summary of data on M31 and M33).

Heiles (1979, 1984) discovered about 50 supershells of neutral hydrogen in the Galaxy, while Georgelin *et al.* (1979) observed 13 giant H II shells. Also described were

Astrophysics and Space Science **108** (1985) 237–302. 0004–640X/85/1082–0237$09.90.

two large bubbles, one in the oscillations Orion and Eridanus, associated with the star formation complex in Orion (Reynolds and Ogden, 1980; Goudis, 1982), and the other, associated with Sco-Cen association and the North Polar Spur (Weaver, 1979). They are close to 300 pc in size. Both bubbles are sources of soft X-ray emission.

Cash *et al.* (1980) observed a large ($13 \times 18°$) horseshoe-shaped region in the Cygnus constellation emitting soft X-rays. It has become known as the Cygnus superbubble. According to Cash *et al.* (1980), its size is about 450 pc, which makes it the largest bubble in the Galaxy.

Our work was focused on structural analysis of the interstellar medium in a large sector of the sky ($65° \leq l^{II} \leq 90°$, $-10° \leq b^{II} \leq 8°$, $19^h20^m \leq \alpha \leq 22^h$, $30° \leq \delta \leq 50°$) in the constellation Cygnus which covers the superbubble observed by Cash *et al.* (1980). The main purpose of the analysis was to find out whether the superbubble is a single structure and to discover the source of its X-ray emission.

The region that contains the X-ray superbubble is a gigantic cluster of gas, dust, and high-luminosity stars. Within the region at distances of up to 2.5 kpc from the Sun are eight young stellar associations including about 110 stars of high luminosity and a variety of nebulae of different characteristics. The region is characterized by a high density of radio sources, both thermal and nonthermal. The western portion of the superbubble is superimposed on the Cyg X region extensively investigated in the radio, IR, and optical ranges. Thus, the region of the sky of interest contains a great variety of objects forming a projected picture of high complexity. None the less, all interpretations of the X-rays emitted by the superbubble have been based on the assumption that it is a single structural unit (Higdon, 1981; Abbott *et al.*, 1981; Blinnikov *et al.*, 1982). Notably, the discoverers of the superbubble ascribe its existence to sequential explosions of 30 to 100 supernovae over a period of three to ten million years in the dense Cyg OB2 association. Blinnikov *et al.* (1982) attribute its origin to the supernova-like explosion of a supermassive star ($2000 M_\odot$). According to Abbott *et al.* (1981), the Cyg OB2 association surrounded by highly rarefied gas and, therefore, Cyg OB2 bubble can be very large.

Analysis of observational data has led us to the conclusion that the observed giant ring of X-ray emission is essentially a projection on the celestial sphere of several physically separated discrete sources at different distances from the Sun (r = 0.5–2.5 kpc).

The basic data on the Cygnus superbubble are summarized in Section 2. Section 3 deals with the position of the superbubble in the Galaxy. The sections that follow describe at length the emission from the region of interest in different ranges of the electromagnetic spectrum: radio (Section 4), optical (Section 5), infrared (Section 6), and X-ray (Section 7). The discussion (Section 8) is concerned with the origin of the diffuse component of the superbubble's X-ray emission. Section 9 summarizes data on the spatial location of the objects making up the Cygnus superbubble. Section 10 delves briefly into the possible origin of the stellar associations responsible for the diffuse component of the X-rays emitted by the superbubble. Finally, Section 11 sets forth the main conclusions of this paper.

2. Basic Observational Data on Cygnus Superbubble

2.1. X-RAY OBSERVATIONS

The gigantic region emitting soft X-rays and having a horseshoe shape 13 × 18° in size (Figure 1) was discovered by Cash *et al.* (1980), with the aid of a system of proportional counters on board the X-ray satellite HEAO-1, operating in the range of 0.1 to 3 keV. The angular resolution was 1°.55 × 2°.95. The resulting emission spectrum was narrow (with steep slopes on both low- and high-energy sides). The bulk of the energy is emitted in the range of 0.5 to 1 keV.

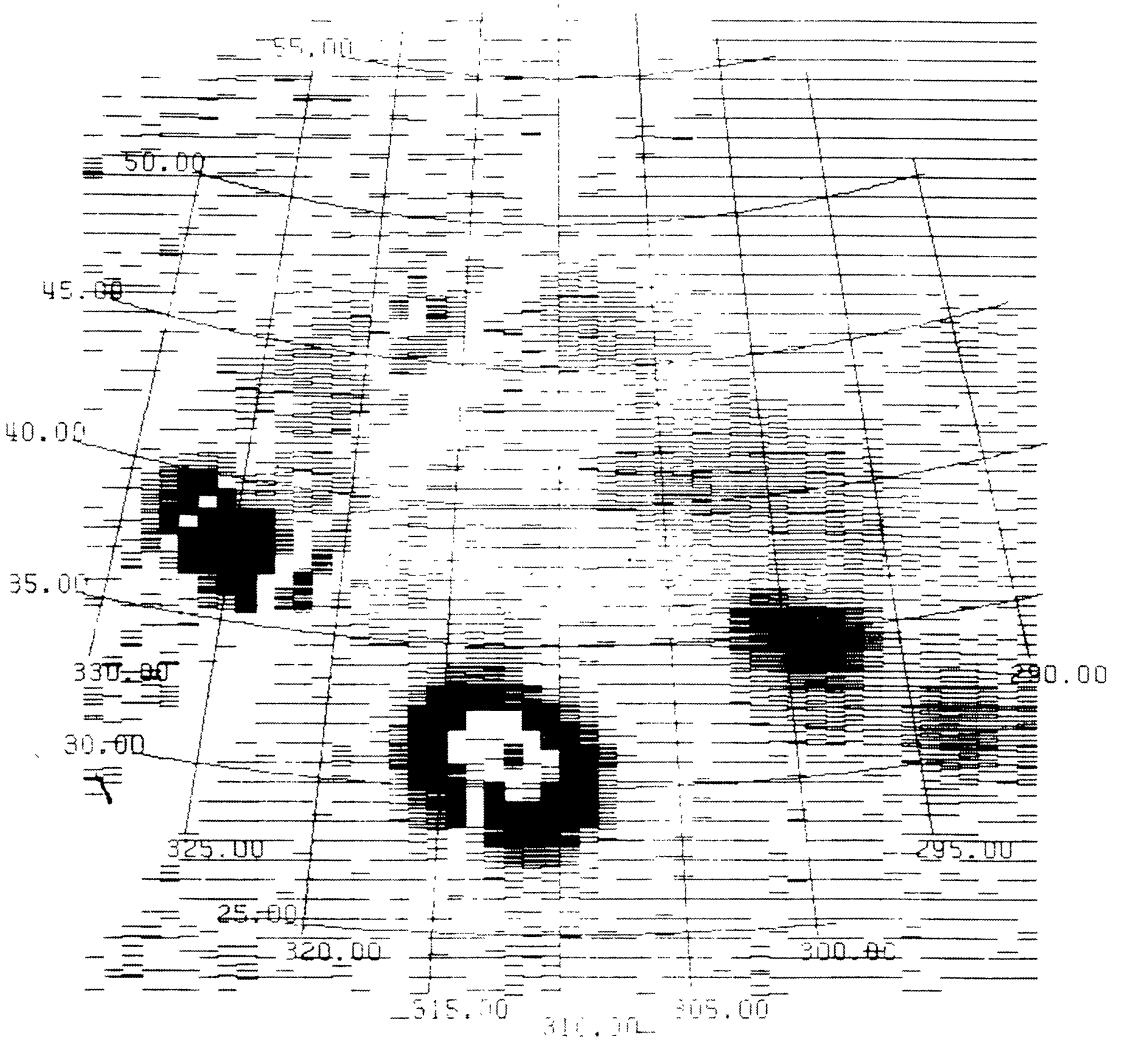

Fig. 1. X-ray picture of the Cygnus superbubble (Cash *et al.*, 1980) from satellite HEAO-1 data. The density of the hatching on the picture is proportional to the logarithm of the number of the accumulated photons. Equatorial coordinates are shown. The right ascension is given in degrees. The four darkest spots correspond to the intense sources of soft X-rays, subtracted by Cash *et al.* (1980) from the emission produced by the superbubble. The sources are Cyg X-2 (325, +38), Cyg Loop (313, +31), Cyg X-1 (299, +35), and G 65.2 + 5.7 (293, +32). Visible on the north-eastern edge of the ring is Cyg X-6. The spot with its center at (302, +41) is Cyg X-7. The picture was kindly supplied by Webster Cash.

The X-ray emission region extends along the galactic plane and has the following coordinates: $l^{II} = 70–88°$, $b^{II} = -8 - +5°$ ($\alpha = 19^h30^m–21^h50^m$, $\delta = 30–47°$). Portions of this large ring: namely, extended courses Cyg X-6 and Cyg X-7, were detected earlier (Coleman *et al.*, 1971; Davidsen *et al.*, 1977).

Cash (1980) compared the observed X-ray spectrum with that of optically thin hot plasma and found the temperature of the emitting gas to be $T = (1.6–2.5) \times 10^6$ K. He observed a column density $N_H = (5.6–9) \times 10^{21}$ cm^{-2}. (The indicated ranges correspond to a 90% level of significance.) The X-ray flux is F_x (0.5–1 keV) = 1.3×10^{-9} erg cm^{-2} s^{-1}, which, when corrected for interstellar absorption, becomes 10^{-8} erg cm^{-2} s^{-1}. The correction for interstellar absorption is highly uncertain (see Section 8.1).

The distance to the superbubble was rather arbitrarily assumed to be 2 kpc on the basis of:

(a) the high value of N_H, which implies that the distance to the X-ray source cannot be less than 0.5 to 0.8 kpc; and

(b) the possible linkage of the superbubble with the highly compact Cyg OB2 association which includes several stars of very high luminosity.

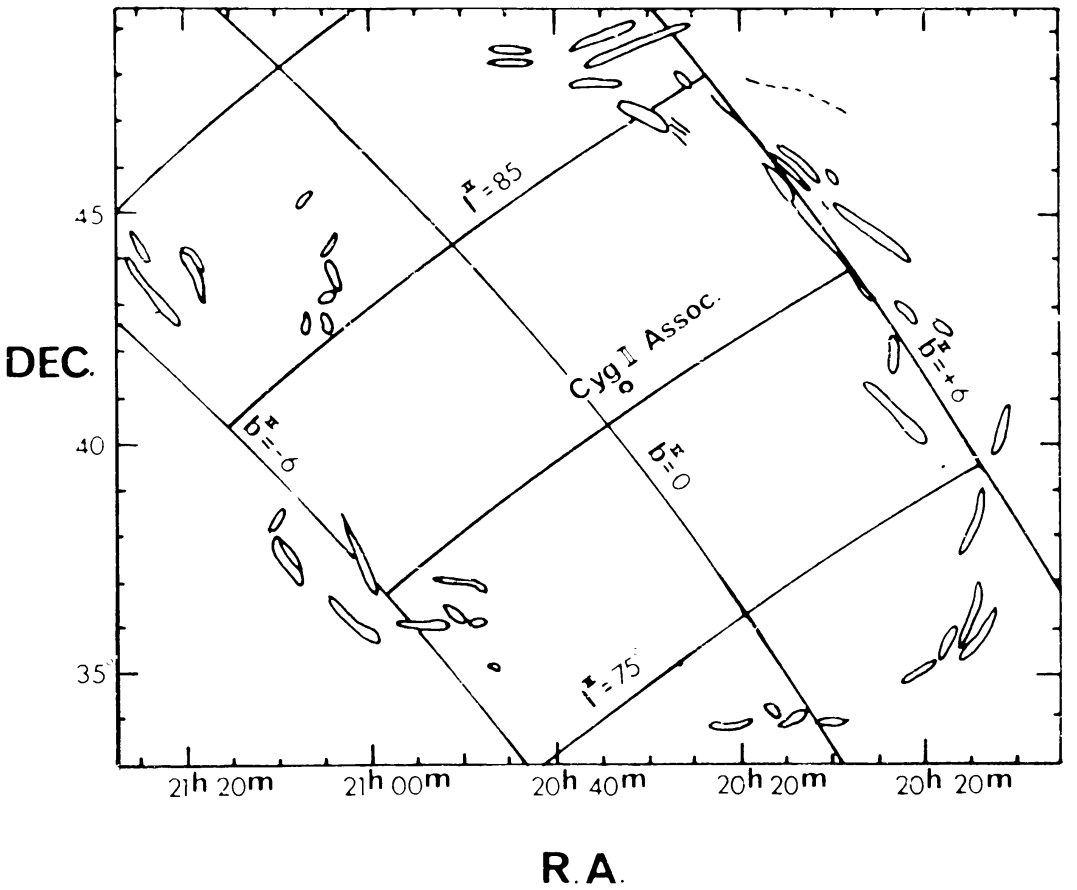

Fig. 2. System of elongated emission gas filaments 15 × 13° in size around radio source Cyg X and associations Cyg OB2, pointed out by Ikhsanov (1960b) and Dickel *et al.* (1969).

The following parameters were determined for an object at this assumed distance: X-ray luminosity of the superbubble, $L_x \approx 5 \times 10^{36}$ erg s^{-1}; size of the emitting region, $D = 450$ pc; volume emission measure $MV = \int N_e^2 \, dV = 1.5 \times 10^{59}$ cm^{-3}; gas concentration in the emitting region ≈ 0.02 cm^{-3} (Cash *et al.*, 1980).

The horseshoe shape of the superbubble X-ray emission is attributed by Cash *et al.* (1980) to the X-ray absorption by the Great Rift – a large dust cloud responsible for the visible bifurcation of the Milky Way. Further discussion of the X-ray observational data of the superbubble is deferred to Section 7.1.

2.2. System of optical filaments

The optical emission from the region of interest has a complex structure. Ikshanov (1960b) and Dickel *et al.* (1969) distinguished a giant system of gas filaments (for more detail, see Section 5.2) around the Cyg OB2 association, which form an oval 13 × 15° in size, stretching along the galactic plane (Figure 2).

Cash *et al.* (1980) emphasized the coincidence of the system of filaments around Cyg X and the observed X-ray superbubble. The approximate conformity of the positron of the filaments to the X-ray structure prompted Cash *et al.* (1980), Abbott *et al.* (1981), Higdon (1981), and Blinnikov *et al.* (1982) to regard the superbubble as a single structure.

3. Position in the Galaxy

3.1. Local spiral arm

Toward the constellation Cygnus ($l^{II} \approx 70$–$85°$) against which the superbubble is projected, is a local spiral arm referred to as the Orion or Carina-Cygnus arm. The Sun is located on the inner edge of this arm, hence, the position of the X-ray superbubble on the sky coincides with the arm cross-section.

The arm is discernible by the position of hot stars and diffuse nebulae (Bok, 1959), by the distribution of the obscuring matter (a review of earlier studies was made by Kaftan-Kassim (1961) by radio observations of natural hydrogen (McCutcheon and Shuter, 1970), by young star clusters (Humphreys, 1976), by examination of CO molecules, and by the position of the H II regions (Scoville and Solomon, 1975; Burton *et al.*, 1975).

According to McCutcheon and Shuter (1970), the line-of-sight remains within the local spiral arm in direction $l^{II} = 70$–$85°$, at least over the first 4 kpc from the Sun. Since evaluations of the distance to both the Cygnus superbubble (Cash *et al.*, 1980) and the stars and nebulae that may be associated with it (see Section 5) yield values ranging from 0.5 to 2.5 kpc (at any rate not exceeding 4 kpc), the superbubble region must be entirely located in the spiral arm.

Figure 3 presents a map derived by McCutcheon and Shuter (1970), showing the distribution of interstellar atomic hydrogen in the direction of Cygnus. The local spiral arm and two Perseus arms can be seen.

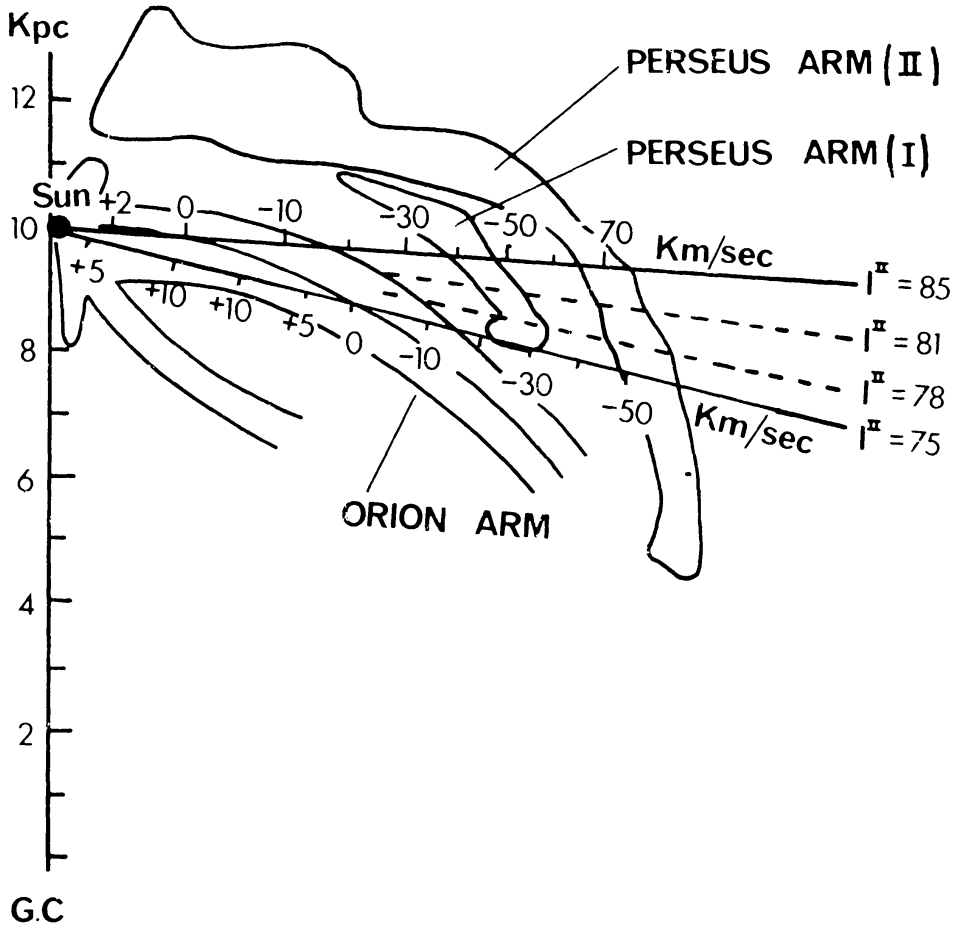

Fig. 3. Position of the local (Orion) spiral arm derived from observations of the 21 cm hydrogen line (McCutcheon and Shuter, 1970). GC is the galactic center. Also shown are the Perseus arm and the variation of radial velocities as a function of distance toward the region of interest.

The nature and properties of the local spiral arm seem to differ widely from those of other spiral arms. The many attempts made in recent years to construct a system of spiral arms for the Galaxy as a whole suggest that the Sun falls almost exactly in the middle between the major spiral arms so that the local arm does not fit into the grand design of the Galaxy. Such a conclusion was drawn by Georgelin and Georgelin (1976) from radio observations of the most prominent H II region in the Galaxy. The Orion arm which includes the Orion nebula and the numerous nebulae in the constellation Cygnus (which are of interest here) is far behind the other in terms of parameters of the brightest H II regions. Proceeding from studies into the kinematics of stars in the galactic disk, Byl and Ovenden (1978), Mishurov *et al.* (1979), Pavlovskaya and Suchkov (1980) reconstructed the position of spiral density waves and demonstrated that the entire local arm lies between the spiral density waves. Uranova (1985a) found that the distribution of obscuring matter in the local arm changes abruptly on the outer side and changes smoothly toward the inner one, which is hard to reconcile with the density-wave theory for a spiral arm.

Thus, the combination of young objects stretched toward Carina-Cygnus does not seem to define a 'usual' spiral arm resulting from a typical spiral shock wave. There is

a possibility of its being a side branch or a bar between main arms. This problem was treated at greater length by Bochkarev (1984a, c). In Section 10.1 we shall consider the possible relationship between some structural features of the region of interest in the constellation Cygnus and other large-scale formations in the local arm, on the one hand, and the absence of a spiral density wave in it, on the other.

Although it is likely that the local arm does not contain a spiral shock wave, it certainly does contain a group of young objects extending along the line-of-sight. The effects of projection may create an illusion of a single object whereas, in fact, we are dealing with a group of spatially separated and physically unrelated features. A similar crowding of gaseous nebulae and young objects is also observed in the constellation Carina (Walborn, 1973). The reason for high density of young objects in Carina may be the same – the line-of-sight is tangential to the local spiral arm.

3.2. Determination of distances toward Cygnus

The galactic longitudes of the superbubble region in Cygnus are in the neighbourhood of 90° ($65° \leq l^{II} \leq 90°$). In these directions, at a distance of up to 3–4 kpc, the differential galactic rotation results (see Figure 3), only in low radial velocities $|v| \lesssim 10$ km s^{-1}, a value similar to the dispersion of interstellar cloud velocities in the Galaxy. This creates difficulties in interpreting velocity data in the superbubble region; kinematic distances are unreliable and cannot be used to construct the spatial structure of the region.

Much more reliable are the distances derived from stellar photometric data, although they may contain serious errors because of the pronounced inhomogeneities in the distribution of interstellar light extinction in this region. It is quite possible that many young stars of this region (bright members of the Cyg OB2 association, for example), are still inside the gas-dust cocoons in which these stars were born (Reddish, 1968). The complex structure of the distribution of obscuring matter in the region of Cygnus (see Section 5.5), makes it very difficult to make accurate determinations of the distances of the involved stars.

4. Radio Emission from the Region of Interest

The region of the constellation Cygnus is characterized by strong radio emission of a complex structure. Bolton and Westford (1950) demonstrated that near the strongest extragalactic source Cyg A there is an extended radio-emitting region named Cyg X by Piddington and Minnett (1952). At present, the name Cyg X is normally applied to a region of the sky defined by coordinates $20^h \leq \alpha \leq 21^h$, $38° \leq \delta \leq 45°$. Cyg X occupies about a quarter of the region under investigation. In addition to Cyg X, many other strong radio sources can be seen in the above direction. This can be inferred, for example, from Figure 4 which shows the survey made by Berkhuijzen (1971) at 820 MHz with an angular resolution of 1°.2. Analysis indicates that the radio sources of this region include both thermal and nonthermal ones.

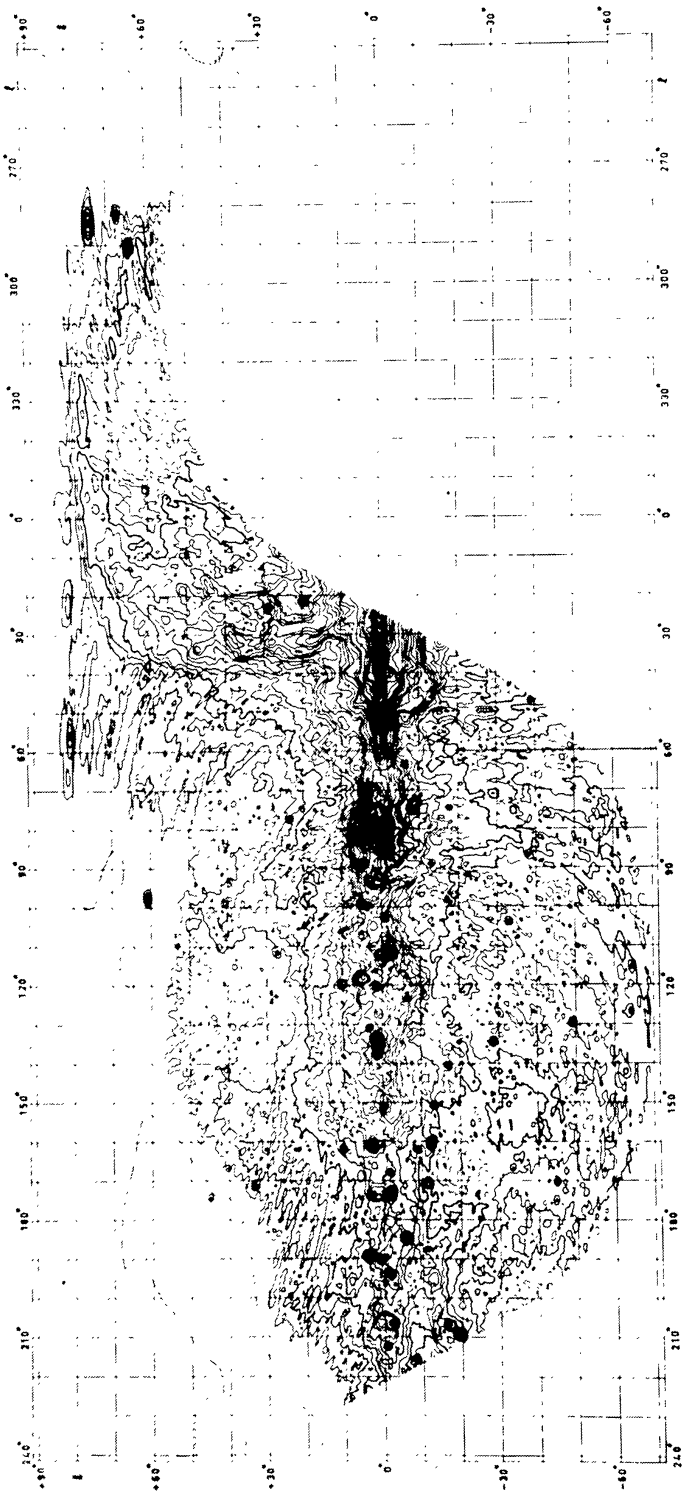

Fig. 4. The sky viewed at 820 MHz with an angular resolution of about 1°2 (Berkhuijzen, 1971). The Cygnus superbubble region ($l^{II} = 65–90°$, $|b| < 10°$) is marked by aggregation of a large number of sources.

4.1. Supernova remnants

Eight sources produce nonthermal spectra and are remnants of supernovae (Milne, 1979). The best known and strongest among them is the Cyg Loop located in the southern part of the region. Of all the SN remnants in the area of interest, the Cyg Loop and the recently discovered G 65.2 + 5.7 (Gull *et al.*, 1977; Shyder *et al.*, 1978) are closest to the Sun and have the largest angular dimensions. Three other objects (HB21, W63, and DR4) are less than 2 kpc distant from the Sun, while the others are farther.

Table I lists the equatorial coordinates, angular dimensions, distances, designations of supernova remnants, and references to information sources.

TABLE I

Supernova remnants in Cygnus region

Source	α_{1950}	δ_{1950}	Angular dimension θ (min of arc)	Distance R (kpc)	Designation	Reference
G65.2 + 5.7	19^h31^m	31°10′	240 × 200	0.9–1.2		Gull *et al.* (1977), Lozinskaya and Sitnik (1978)
G65.7 + 1.2	19^h45^m	30°00′	18.6	5.8	DA495	Milne (1979)
G74.0 − 8.6	20^h50^m	30°53′	180	0.8	Cyg Loop	Milne (1979)
G74.9 + 1.2	19^h45^m	40°00′	6.5	7.3	CTB87	Milne (1979)
G78.1 + 1.8	20^h21^m	40°04′	62	1.6	DR4	Milne (1979)
G82.2 + 5.4	20^h17^m	45°30′	77	1.3	W63	Milne (1979)
G84.2 − 0.8	20^h40^m	45°00′	18	6.2		Milne (1979)
G89.0 + 4.7	20^h43^m	50°30′	105	1.1	HB21	Milne (1979)

The optical emission of these supernova remnants will be discussed in Section 5.1, and the X-ray emission in Section 7.3.

4.2. Continuous thermal radio emission. Cyg-X region

The western part of the superbubble, marked by the most intense radio emission, is associated with the composite radio source Cyg X. The region under consideration also include several extended thermal radio sources such as the S119 nebulae, for example. (Some of these will be treated at greater length in the next section, in the context of their optical emission.)

Since the Cyg-X region coincides with a large part of the superbubble, it is necessary to consider the results of radio observations of this region.

A comprehensive summary of the Cyg-X region observations made before 1976 can be found in Goudis' (1976) work. The continuously emitting radio source Cyg X was investigated at frequencies of 408 MHz (Mathewson *et al.*, 1960), 610.5 MHz (Yang and West, 1964; Wendker, 1967), 1414 MHz (Pike and Drake, 1964), 2965 MHz

(Wendker, 1970), 3200 MHz (Higgs *et al.*, 1964), 5000 MHz (Downes and Rinehart, 1966), and 6600 MHz (Higgs, 1966). These observations, made in most cases with a resolution of 10′ to 20′ have shown that Cyg X has a complex structure. It includes the well-known star formation region W75 as well as sources W66, W67, and W80. Downes and Rinehart (1966) distinguished 27 objects in it (Figure 5). Only one of them (DR4) is known for sure to be a supernova remnant. Twenty-three objects are H II regions. Most of them are also far IR sources (see Section 6). Wendker (1970), in turn, identified 78 radio sources in the Cyg-X region.

The emission measures of the H II regions are EM = 3000–50 000 pc cm^{-6} (Goudis, 1976) with individual condensations characterized by EM of up to 5×10^6 in

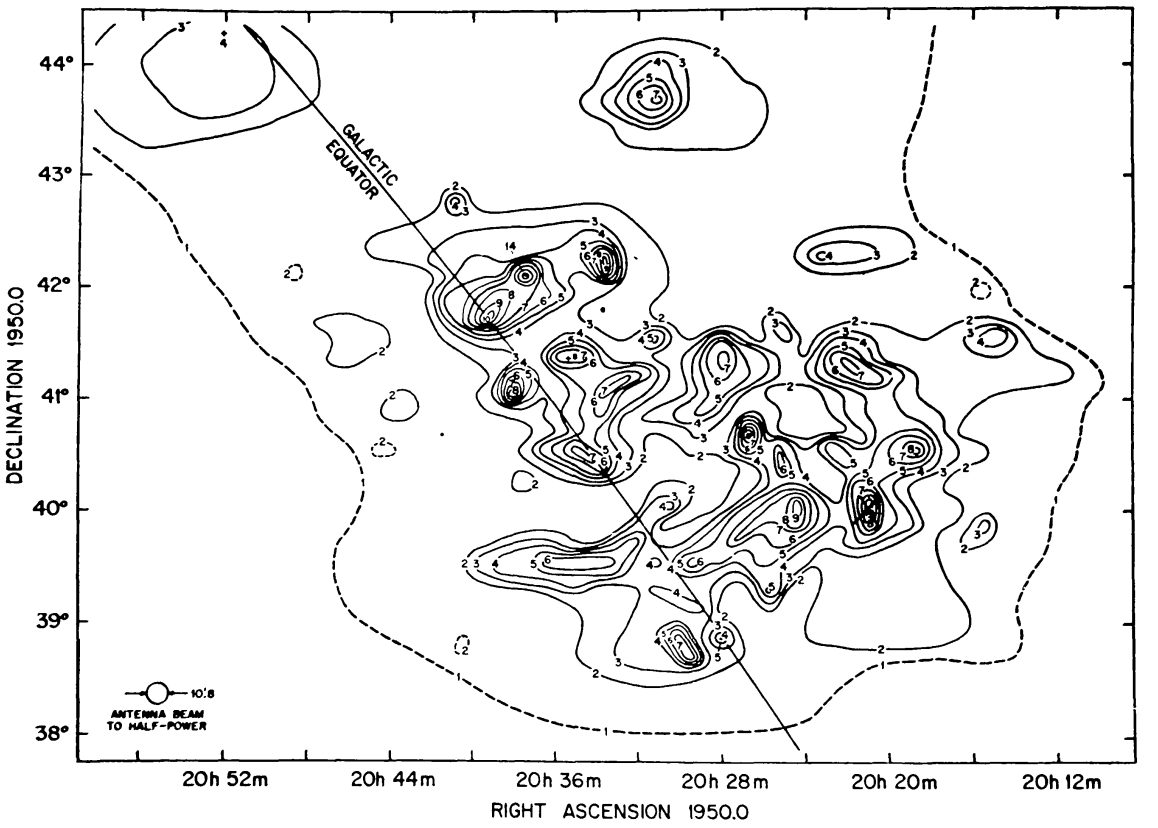

Fig. 5. Contour map of the radio continuum at 5000 MHz in the Cyg-X region (Downes and Rinehart, 1966).

DR5 = W67 = IC 1318b, c (Dickel *et al.*, 1974) and a plurality of extremely bright condensation with EM = (1–9) $\times$ 10^7 pc cm^{-6} (Goudis, 1976) in DR21 which forms part of the W75 complex. The typical densities of the extended components of the H II regions are $\langle N_e^2 \rangle^{1/2}$ = 15–100 cm^{-3}, and their masses are $M_{\mathrm{H\,II}}$ = 100–5000 M$M_\odot$.

Such a complex might be regarded as a single entity if all of its components were spatially close to one another. Should this have been so, the Cyg-X region could have been interpreted within the framework of the interstellar 'blister' model (Icke, 1979, 1981). However, the Cyg-X region is most likely to be extended along the line-of-sight,

covering a distance much longer than its transverse dimension. Such an assumption seems to be quite natural in view of the fact that the line-of-sight toward Cyg X is tangent to the local spiral arm (Bolton and Westford, 1950; Scheuer and Ryle, 1953; Westerhout, 1958). To throw light on the subject, one must know the spatial distribution of the objects in Cyg X. The kinematic distances toward Cyg X are not ideal distance indicators (see Section 3.2). Distribution of Cyg X objects may be determined from the obscuring matter distribution in the Galaxy and the interstellar extinction for each nebula. Shklovskii (1960) noticed that the interstellar absorption up to the H II regions emitting in both optical and radio ranges can be determined by comparing surface brightnesses in these two ranges (see Section 5.5). The first attempts to determine the distance in this manner has been made by Ikshanov (1960a). The more detailed investigations carried out by Dickel *et al.* (1969) and Dickel and Wendker (1978) (see Section 5.5) suggest that the nebulae in Cyg X are distributed in the local spiral arm at distances ranging from at least 1 to 2.4 kpc. The same conclusion follows from Cyg X observations in radio-absorption lines (see Section 4.3).

At the same time, after having excluded the radio emission from all discrete sources, Wendker (1970) detected in the Cyg-X region an extended object about 6° in size (the center coordinates are $\alpha \approx 20^{h}25^{m}$, $\delta \approx 40°30'$), which is possibly connected with a single large-scale object. Its brightness temperature at 2695 MHz is about 1 K. The position of this object correlates well with the Cyg OB2 association. Its nature will be discussed in Section 10.3.

4.3. Observations in recombination, molecular radio, and 21 cm atomic hydrogen lines

The region of interest is characterized by intense emission in the 21 cm line (Kaftan-Kassim, 1961; McCutcheon and Shuter, 1970), in the 2.6 mm CO line (Scoville and Solomon, 1975; Burton *et al.*, 1975), and in recombination radio lines. The Cyg-X region was investigated in hydrogen lines H 109α (Schraml and Mezger, 1969; Reifenstein *et al.*, 1970; Terzian and Parrish, 1973), H 158α (Dieter, 1967), H 166α, H 192α, H220α (Pedlar and Davies, 1972), and helium line He 85α (Churchwell *et al.*, 1974), while its individual components were also studied in other recombination radio lines. These observations corroborate that most of the 29 sources examined in this region are thermal ones. Their radial velocities with respect to the local standard of rest fall into the range $-15 \text{ km s}^{-1} \leq V_{LSR} \leq 14 \text{ km s}^{-1}$, except for those in line H 109α emitted by the source DR7, where V_{LSR} is about -40 km s^{-1} (Reifenstein *et al.*, 1970; Terzian and Parrish, 1973). The DR7 source is likely to be more distant than others and simply projected on the region under consideration. The kinematic distance to this source is 8 kpc, which is suggestive of its position in the Perseus arm.

In the Cyg-X region, OH absorption ($\lambda = 6$ cm) was detected at velocities of $-6 \text{ km s}^{-1} \leq V_{LSR} \leq 12 \text{ km s}^{-1}$ from 17 sources (Goss, 1968; Pashchenko, 1973). For 15 sources, $V_{LSR} \geq -3 \text{ km s}^{-1}$. For the sources DR7 and DR23, absorption components with $V_{LSR} = -5.7 \text{ km s}^{-1}$ were observed. These correspond to the greatest kinematic distances among the 17 sources. In the case of DR7, three line

components with $V_{LSR} = -5.7$, $+5.0$, and $+12.2$ km s^{-1} were observed at once (Pashchenko, 1973), which indicates that it 'shines' through three dark clouds and is indeed a distant object.

Observations of the radial velocities of the OH absorption line in the North America–Pelican complex located in the Cygnus superbubble region also give $V_{LSR} \geq +1$ km s^{-1} (Jefferts *et al.*, 1970; Turner, 1973). Corresponding to these are the velocities observed in the recombination radio lines of these nebulae (Pedlar and Matthews, 1973; Pedlar and Davies, 1972). This indicates that one of the absorbing molecular clouds is associated with these nebulae and the Great Rift. Besides, there is a possibility of another absorbing cloud being in front of them (see also Section 5.5).

Observations (Wilson *et al.*, 1974) of the CO emission line ($\lambda = 2.6$ mm) give velocities coinciding with those determined from OH absorption to within 1–4 km s^{-1}, except for source DR22. In the direction of the latter, an additional component is seen in the CO line with V_{LSR} of about -11 km s^{-1}, which does not correspond to the velocity determined from OH absorption, and there is no CO emission with $V_{LSR} = +5.0$ km s^{-1} corresponding to OH absorption. The additional CO emission must be due to farther cloud. Besides, emission in some other molecular radio lines was observed in several cases.

Thus, radio observations in CO emission, OH absorption, and CH emission lines ($\lambda = 9$ cm, resolution 15′, Rydbeck *et al.*, 1976) indicate that there are three molecular clouds present in the direction to the Cyg X radio source. The nearest cloud has $V_{LSR} \approx 12$ km s^{-1}, which corresponds to a distance less than 1.5 kpc, whereas the V_{LSR} of the others are $+5$ km s^{-1} and (-2 to -3) km s^{-1}. In some instances, similar velocities are also observed in recombination radio lines, which seems to indicate that the various components of Cyg X are associated with these clouds. The sources constituting Cyg X may be formed by the thermal emission from the ionized edges of these clouds (Icke, 1979, 1981).

In five cases, neutral atomic hydrogen absorption lines at $\lambda = 21$ cm were seen against the background of Cyg-X radio-emission (Davies and Matthews, 1962; Sato, 1968). The absorption lines cover a wide range of velocities; the components of highest velocity are associated with the emission sources of greatest intensity. The large spread of velocities in DR21 ($-20 \leq V_{LSR} \leq +18$ km s^{-1}), probably indicate expansion of this H II region. The velocities of other sources were found to be within the same range. Positive velocities are predominant, indicating small distances to the absorbing H I clouds. The 21 cm absorption and emission data suggest that Cyg X is associated with the local arm (Kaftan-Kassim, 1961; McCutcheon and Shuter, 1970).

Heiles (1979) found 14 giant shells of neutral hydrogen in the constellation Cygnus. Three shells GS 087 + 03 + 19 (angular dimensions: $8.^{\circ}5 \times 3.^{\circ}6$) and GS 088 + 04 + 17 (angular dimensions: $3 \times 3^{\circ}$) in the eastern part and CS 075 − 01 + 39 ($5.5 \times 3^{\circ}$) in the western part are at distances ranging from about 0.5 to 2.6 kpc. Heiles (1979) estimated the distance to the first two shells to be around 0.5 kpc, as suggested by the radial velocities of $+19$ and $+17$ km s^{-1}.

The remaining shells are more than 4 kpc distant from the Sun, and if the estimated

distances are correct, are not likely to be associated with the superbubble observed in X-ray emission. It is, therefore, difficult to accept the suggestion made by Cash *et al.* (1980) that the GS 081 − 05 − 37 shell (with a radial velocity of -37 km s^{-1}) is linked with the stellar association Cyg OB2 which has the distance ~ 2 kpc from the Sun (see Figure 3).

4.4. Summary

The radio-emission from the region of interest arises from a great variety of objects primarily within 1 to 2.5 kpc of the Sun. These include 8 supernova remnants, 3 neutral hydrogen supershells, and many H II regions scattered at different distances from the Sun within the local spiral arm. Radio observations reveal three molecular clouds in the same region. In addition, there seems to be an extended (about 6° in diameter) source of continuous radio-emission, most probably of thermal nature, in the neighborhood of the stellar association Cyg OB2. No continuous large-scale structures of nonthermal radio-emission have been detected in this region. This is a strong argument against the supposed connection of the X-ray superbubble in Cygnus with a remnant of one or several supernovae, since the principal feature which allows supernova remnants to be distinguished from other shell structures is their non-thermal radio-emission.

5. Optical Emission

The Cygnus region is essentially a giant gas-dust complex which contains a large number of high luminosity stars. It is shown in Figure 6 which is a photomosaic of red-Palomar maps.

5.1. Bright emission nebulae in Cygnus

In the western part of Figure 6, the interstellar gas forms a sizeable filamentary structure of sinuous shape, extending along the galactic plane over about 18°. In addition to the main, brightest structure clearly visible in Figure 6, the Palomar maps show, above and under this structure, similar but weaker, mostly diffuse formations with the same crests and valleys (barely visible in Figure 6). Typical crest dimensions vary from 3 to 5°. The most prominent crest is observed in the region $20^{h}00^{m} \leq \alpha \leq 20^{h}20^{m}$ and $35° < \delta < 40°$ (Figure 6).

In the considered sky sector, there are also several bright extensively studied emission nebulae. Their coordinates are given in Table II. Prominent in the north-eastern part are the North America (NGC 7000 = S117 = Sh234) and Pelican (IC 5067) nebulae representing a single bright H II region divided by a less distant filament of obscuring matter. Seen farther east is filamentary nebula S119 = Sh240 blown out by the stellar wind from 68 Cyg (for further details, see Section 7.5).

The southern portion of the region features wisps of the Veil nebula which is identical with the well-known supernova remnant Cyg Loop which has an angular diameter of 3°.

In the western portion of the region prominent against a sinuous background are

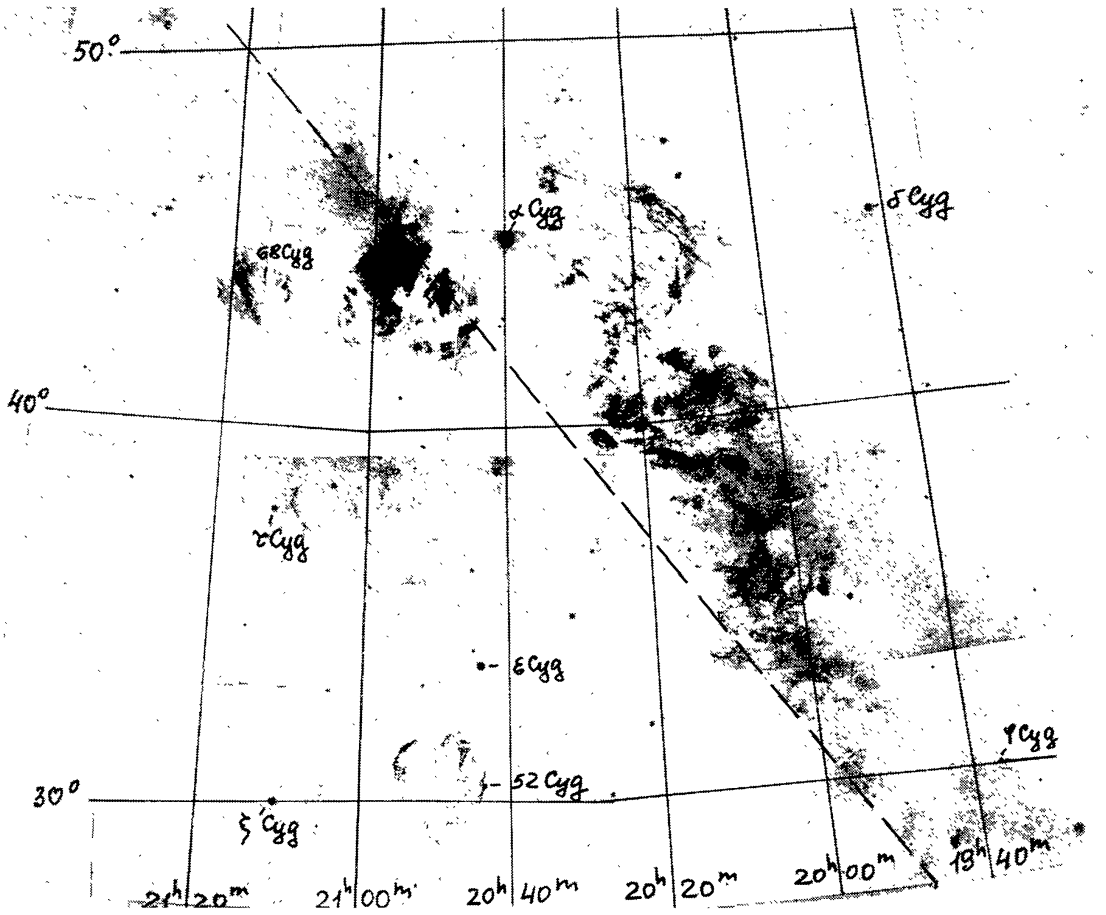

Fig. 6. Photomosaic of Red-Palomar sky survey showing the Cygnus region. The dashed diagonal from the left upper to the right lower corner indicates the galactic equator. At the top are the North-America and Pelican nebulae. Nebula S119 appears further to the left. Visible at the bottom are bright filaments of the Cyg Loop. Some bright stars of the constellation Cygnus are marked.

blisters of the H II region IC 1318a, b, c, divided into three parts by filaments of obscuring matter which are projected on it, as well as a nebula near γ Cyg. In the latter object the H II region and the less distant star γ Cyg are projected on the supernova remnant DR4 which is about 2 kpc away. The south-western part contains the bright dense nebula NGC 6888 (see Section 7.5) formed by the stellar wind from the WN6 star HD 192 163. The region of interest also features faint optical filaments of the supernova remnants HD 21, W63, and G 65.2 + 5.7 (see Table I). The filaments of W63 are projected on a complicated structure and defy any identification (Lozinskaya *et al.*, 1975). The filaments associated with G 65.2 + 5.7 must have been discovered by Struve (1957). They were described as supernova remnants by Gull *et al.* (1977).

5.1.1. *The Results of Interferometer and Spectral Observations of the Nebulae*

Some nebulae in this region were observed by the interference method in the Hα emission line. For the supernova remnants Cyg Loop and G 65.2 + 5.7, the velocities of both gas filaments (from the maximum Hα-profile) and the diffuse gas (from the Hα-line wings, Bychkov and Lebedev, 1979) were determined. For the other objects

1985Ap&SS.108..237B

TABLE II

Bright nebulae in Cygnus region

Ref. no.	Proper name	W	DR	NGC (IC)	Sharpless	Shain, Gaaze	α_{1950} δ_{1950}	l^{II} b^{II}	Angular dimension (arc min)	Distance (kpc)	Reference
1	North America	80	27	NGC 7000	S117	Sh234	20^h55^m 44°30′	86° −0°.5	~200′	1.0	Becker (1964), Georgelin and Georgelin (1970)
2	Pelican			IC 5067			20^h50^m 44°	84°.5 0°		1.0	Georgelin and Georgelin (1970)
3					S119	Sh240	21^h45^m 43°43′	88° −4°	~120	0.72	Savage and Jenkins (1972)
4	Cyg Loop (Veil)			NGC 6992–6995 NGC 6960			 20^h49^m 30°53′	74° 8°.6	~180	0.8	Milne (1979)
5		67	5	IC 1318b, c			20^h24^m 40°	79° 0°.7	30 × 60	1–1.5	Ikhsanov (1960a)
6	Near γ Cyg	66	4				20^h21^m 40°04′	79° 1°.5	21	1.5–2.1	Milne (1979)
7				NGC 6888			20^h10^m 38°17′	75°.8 1°.6	20 × 15	1.5–2.3	Lozinskaya (1980)

TABLE III

Radial velocities of some nebulae in Cygnus region

Object	α	δ	V (km s^{-1})	ΔV[a] (km s^{-1})	Reference
G65.2 + 5.7	19^h31^m	31°10′	16	100–150	Lozinskaya and Sitnik (1978)
W63	20^h17^m	45°30′	4	45	Lozinskaya *et al.* (1975)
Near W63			4		Lozinskaya *et al.* (1975)
IC 1318a	20^h17^m	43°00′	~ −4		Courtès *et al.* (1966)
DR4	20^h21^m	40°04′	9	40	Lozinskaya *et al.* (1975)
Near DR4			−2		Lozinskaya *et al.* (1975)
IC 1318b	20^h24^m	41°30′	~ −2		Courtès *et al.* (1966)
IC 1318c	20^h36^m	41°45′	0		Courtès *et al.* (1966)
HB21	20^h43^m	50°30′	22	20–110	Lozinskaya (1972)
Cyg Loop	20^h50^m	30°53′	16	20–115	Doroshenko *et al.* (1982)
S117	20^h58^m	44°00′	~1		Courtès *et al.* (1966)
S119	21^h45^m	43°43′	6	45	Esipov *et al.* (1982)

[a] ΔV is the width of the profile Hα line produced by the gas of the nebula, at half peak intensity.

listed in the first column of Table III, only the velocities of the filaments usually associated with the low-shift gas components were measured. The equatorial coordinates of the objects are given in the second and thirs columns of Table III, the fourth column represents the mean radial velocity with respect to the LSR. The last column gives the sources of velocity data. As can be seen from Table III, the radial velocities range from −2 to 16 km s^{-1}. This velocity range coincides with that determined by radio methods and mentioned in Section 4.3. Such a coincidence attests to the fact that the optical nebulae lie in the same region as the radio ones. Sometime, values of expansion velocities (the fifth column of Table III) seem to stay within the range of 10 to 15 km s^{-1} and cannot be measured by the instruments used for obtaining the data of Table III.

Reynolds (1980) scanned the galactic plane in the Hα-line ($0° < l^{II} < 240°$) with a Fabry–Pérot interferometer sensitive to emission with $EM \approx 2$ cm^{-6} pc. The Hα profiles observed in the region $68° < l^{II} < 90°$ have broad wings which correspond to high velocities. They cannot be explained in terms of a spiral structure or differential galactic rotation. According to Reynolds (1980), this region is characterized by peculiar motions of about 50 km s^{-1}. This velocity is typical for diffuse gas. Filaments have a velocity of 2 to 3 km s^{-1}.

Spectral observations of filaments in the Cyg-X region had prompted Sabbadin (1976) to regard it as an old supernova remnant of the S147 and Cyg Loop types. This conclusion was drawn as a result of comparison of the relative intensities of 12 filaments of this region in the Hα, [N II], and [S II] lines. According to their intensity ratios, filaments in the Cyg-X region occupy an intermediate position between H II regions and supernova remnants. The results of their observations in the region having coordinates $20^h08^m < \alpha < 20^h36^m 36° < \delta < 45°$ (to the right of α Cyg) are as follows:

$$1.55 < I(\mathrm{H}\alpha)/I(\mathrm{N\,II}] < 4\,, \qquad 0.65 < I([\mathrm{S\,II}])/I([\mathrm{N\,II}]) < 1.32\,,$$

$$1.26 < I(\mathrm{H}\alpha)/I([\mathrm{S\,II}]) < 4.2\,.$$

However, as was mentioned in Section 4.1, no extended sources of nonthermal radio-emission have been found in the region. Furthermore, the regions of line intensity ratios, in the case of H II regions and supernova remnants, overlap to such an extent that we find it impossible to give preference to any one of these possibilities, proceeding from the above ratios.

5.2. Extended ring-emission formations

The Cygnus region contains many long narrow emission filaments that have received attention from many investigators. Morgan (1955) joined patches of filaments in the region with coordinates $\alpha \approx 21^h$ and $\delta \approx 38°$ into an arcuate with dimensions $\approx 5°$. Struve (1957) identified a number of ring and arcuate structures, including Morgan's arc, and filaments that later turned out to be supernova remnant G 65.2 + 5.7. He found also the arc oriented almost at a right angle to the galactic plane in the region $l^{II} \sim 90°$, $b^{II} = -2$ to $8°$ and confining the X-ray emission region from the outside. If, as was pointed out by Struve (1957), this arc could have been extended, it would have encircled the entire constellation Cygnus.

5.2.1. *Ring Nebulae Around Associations*

Brand and Zealey (1975) distinguished in the constellation Cygnus a whole series of large-scale ring formations of gaseous nature, which they named Cyg 1, 2, 3, and 4. Numerical data for these objects are listed in Table IV. Their position correlates well with that of the stellar associations in the eastern part of the region of interest (see Section 5.3), and it may be assumed that each association is surrounded by its own system of filaments. The most prominent of them is Cyg 1 around association Cyg OB1, having an elliptical shape (Figure 7). Its dimensions are $3 \times 4°$, which corresponds, at the association's distance of 1.8 kpc, to 95×125 pc. (Its extended shape with respect to the galactic plane can be explained if it has been formed by the stellar wind from the stars of association Cyg OB1. The stars probably were born one after another as the star-formation wave traversed the molecular cloud from which these stars originated. The result is that the association and the nebula are extended along the galactic plane.)

TABLE IV

Loop structures around stellar associations in Cygnus region

Proper name	l^{II}, b^{II}	Angular diameter	Stellar association
		Emission structure	
Cyg 3	73°, +2°	2°	Cyg OB3
Cyg 1	76°, +1°	3°	Cyg OB1
Cyg 2	78°, +1°.5	2°	Cyg OB9
Cyg 4	80°, +1°	15°	Cyg OB2
		Dust structure	
Cyg 5	80°, +1°	8°	Cyg OB2

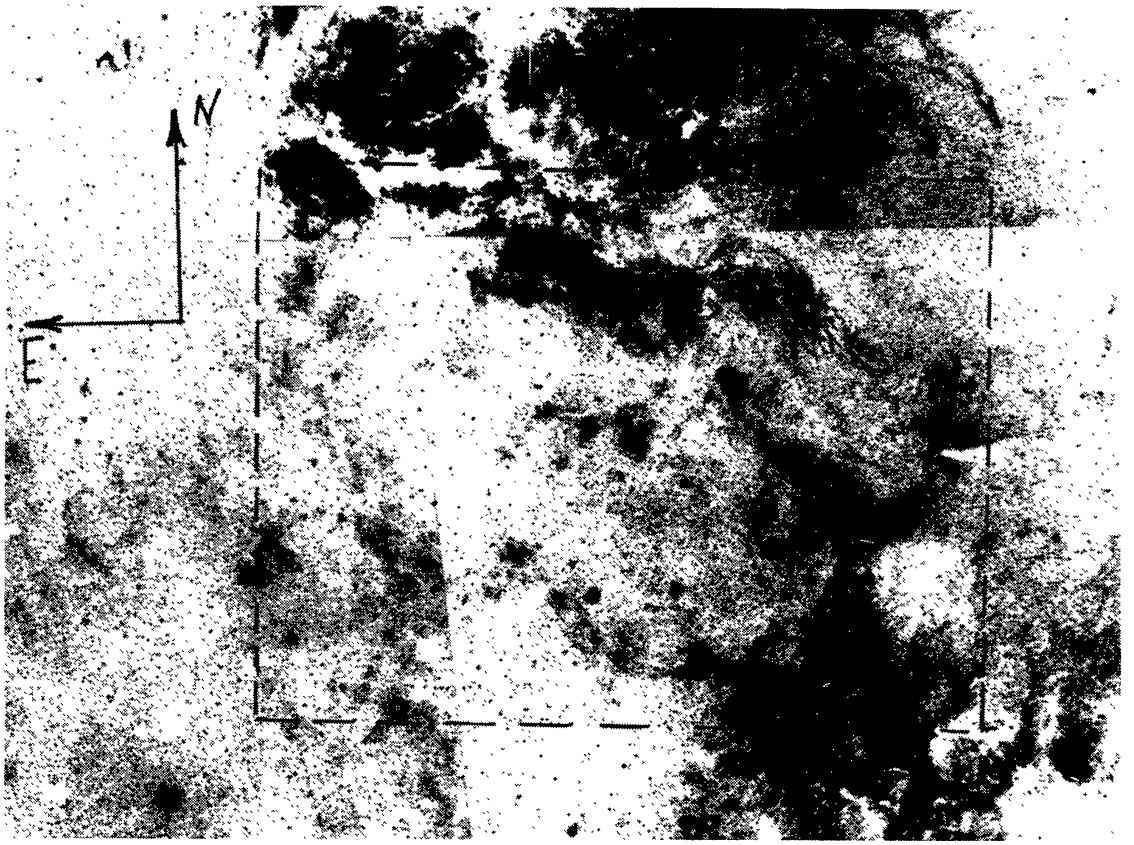

Fig. 7. Emission ring nebula Cyg I around association Cyg OB1, described by Brand and Zealey (1975) (inside of the dash line).

The emission loop structure Cyg 2 (Brand and Zealey, 1975) with dimensions of about 2° surrounds stellar association Cyg OB9. Emission structure Cyg 3 (~2°) is connected with association Cyg OB3. Brand and Zealey link to association Cyg OB2, the emission structure Cyg 4 about 15° in size (obviously coinciding with the ring of optical filaments mentioned in Section 2.2, see also below) and dust structure Cyg 5 (~8°). The nature of these ring structures will be discussed in brief in Section 10.2.

5.2.2. *The Ring of Emission Filaments Around the Cyg-X Region*

This giant system of filaments, slightly stretched in the galactic plane and having dimensions of 13 × 15°, was regarded by Ikhsanov (1960b) and Dickel *et al.* (1969), as a single structure (see Figure 2). As we have already mentioned, some workers tie the X-ray superbubble with the ring of optical filaments (Section 2.2).

This system of filaments was investigated by Kapp-herr and Wendker (1972), who compared the surface radio brightness of the filaments (observed with the angular resolution of 11′) with the calibrated values of the surface brightness of optical filaments in an Hα filter. For that purpose, the data published by Dickel and Wendker (1977) on absolute Hα-photometry data were being used whenever it was possible. In other cases, the surfaces emission brightness were estimated roughly from red Palomar photographs. The results of narrow-band surface photometry were averaged over the 11′ region, and

the derived values were compared with the radio data. This is a good way to determine the interstellar extinction toward the nebula (for more detail, see Section 5.5). The ring of filaments, identified by Dickel *et al.* (1969), was shown to be not a single structure; its various parts differ so widely in distance that they are located on either side of the Great Rift.

We believe that the elongation of the filamentary system along the galactic plane is another strong argument against speculations that these filaments owe their origin to a process initiated by a single centre. Since the assumed dimensions of the system of filaments (≈ 450 pc according to Cash *et al.*, 1980) are comparable with or greater than the thickness of the gaseous galactic disk (200–300 pc, Kaplan and Pikel'ner, 1979), one would expect stretching of the filamentary system across the galactic plane. Meanwhile, the observed orientation of the filament system is a natural consequence of the projection on the celestial sphere of many objects located in different place along the galactic plane (the arm is about 0.5 to 1 kpc wide along the plane and about 300 pc thick across the plane). Moreover, because the arm is convoluted, its projection on the sky will also be stretched along the galactic plane.

The same arguments seem to apply to the orientation along the galactic plane of the X-ray superbubble (Figure 1) which was connected by Cash *et al.* (1980) with the above-described ring of optical filaments.

It should also be noted that the ring of optical filaments was selected by Dickel *et al.* (1969) in a rather arbitrary manner. They included in the ring filaments of the nebula S119, which is a well-known separate source (Figures 2 and 6). It is also likely that some filaments from the south-western part of the ring are connected with the bubble around association Cyg OB1 (emission structure Cyg 1, see Table IV).

In the region under investigation one can also distinguish a filamentary system extending across the galactic plane. It includes filaments to the west of stars τ Cyg and α Cyg with coordinates $\alpha = 20^{h}10^{m}$–$20^{h}30^{m}$, $\delta = 42$–$46°$, and $\alpha = 20^{h}50^{m}$–$21^{h}10^{m}$, $\delta = 37$–$41°$. The latter region corresponds to Morgan's arc of filaments. It can be easily imagined that these filaments are patches of an elliptical shell extending across the galactic plane over about 10°. The shell includes, although far from the geometric center, the dense association Cyg OB2 which may have created such a system of filaments by its unusually strong (Abbott *et al.*, 1981) stellar wind. It is also possible that physically associated with the same region is the extended radio source discovered by Wendker (1970) and mentioned in Section 4.2 (see also Section 10.3). However, the hypothesis about the physical connection of the above-mentioned system of filaments certainly calls for observational verification based on analysis of both radio and optical data. Preliminary examination of Cyg X radio maps does not contradict that hypothesis, but of course is not sufficient to prove it.

5.3. Stellar Associations

The Cygnus region contains eight young stellar associations Cyg OB1, OB2, OB3, OB4, OB7, OB8, OB9, and NGC 6991. Together, these associations contain about 50 high-luminosity stars of class O. Some characteristics of these associations (galactic and

TABLE V

Stellar associations in Cygnus region

Association	l^{II}, b^{II}	α, δ	Distance (kpc)	Dimensions (pc)	O	B	A	Age ($\times 10^6$ yr)
Cyg OB3	71°3–73°8 1°2–3°4	20^h05^m 35°	2.29	90	9	15		8.3
Cyg OB1	74°0–77°0 −0°6–2°8	20^h15^m 37°	1.82	100	12	28		7.5
Cyg OB8	76°3–79°2 2°1–5°4	20^h10^m 40°30	2.29	130	4	10		3.0
Cyg OB9	77°0–79°0 0°8–2°2	20^h20^m 40°	1.2	40	7	7		8.0
Cyg OB2	80°1 0°9	20^h30^m 41°	1.82		13	2		5.0
Cyg OB4	81°0–84°0 −8°3–−6°3	21^h15^m 38°	1.00	50			1	
Cyg OB7	84°0–96°0 −4°9–9°0	21^h02^m 49°	0.83	170	3	6	1	13.0
NGC 6991	87°5 1°5							

Listed in columns 6, 7, and 8 is the number of high-luminosity stars (Humphreys, 1978).

equatorial coordinates, photometric distances from the Sun, dimensions, number of high-luminosity stars of classes O, B, and A) are listed in Table V. The ninth column gives our estimates of ages of the associations made by the methods proposed by Lucke (1978) – that is, based on the number of stars in the top of the Main Sequence of the Hertzsprung–Russell diagram, having the highest absolute magnitude (M_V) for a given association.

Associations Cyg OB3, OB1, OB8, OB9, and OB2 are located in the western part of the region, in the 'crests' and 'valleys' of the above-described sinuous filamentary structure (see Figure 8 and Table V). The solid lines in Figure 8 indicate emission filaments, while the dashed circles mark the approximate boundaries of the associations (but not the surrounding ring nebulae).

The parameters of the major associations are considered in brief in what follows.

Cyg OB2 is the most prominent association in this region and, probably, the Galaxy as a whole. It was studied in detail by Reddish *et al.* (1966). The distance to this association is about 2 kpc (Humphreys, 1978; Reddish *et al.*, 1966). It is a compact (29 × 7 pc) cluster of at least 3000 stars of which no less than 300 are Main-Sequence OB stars surrounded by gas-dust cocoons with a typical obscuration of about 3^m (Table V gives only the brightest stars, primarily supergiants, listed by Humphreys, 1978). There are several superluminous OB supergiants. Six of them are among the 15 brightest stars of the Galaxy (Humphreys, 1978). Five stars of this association have

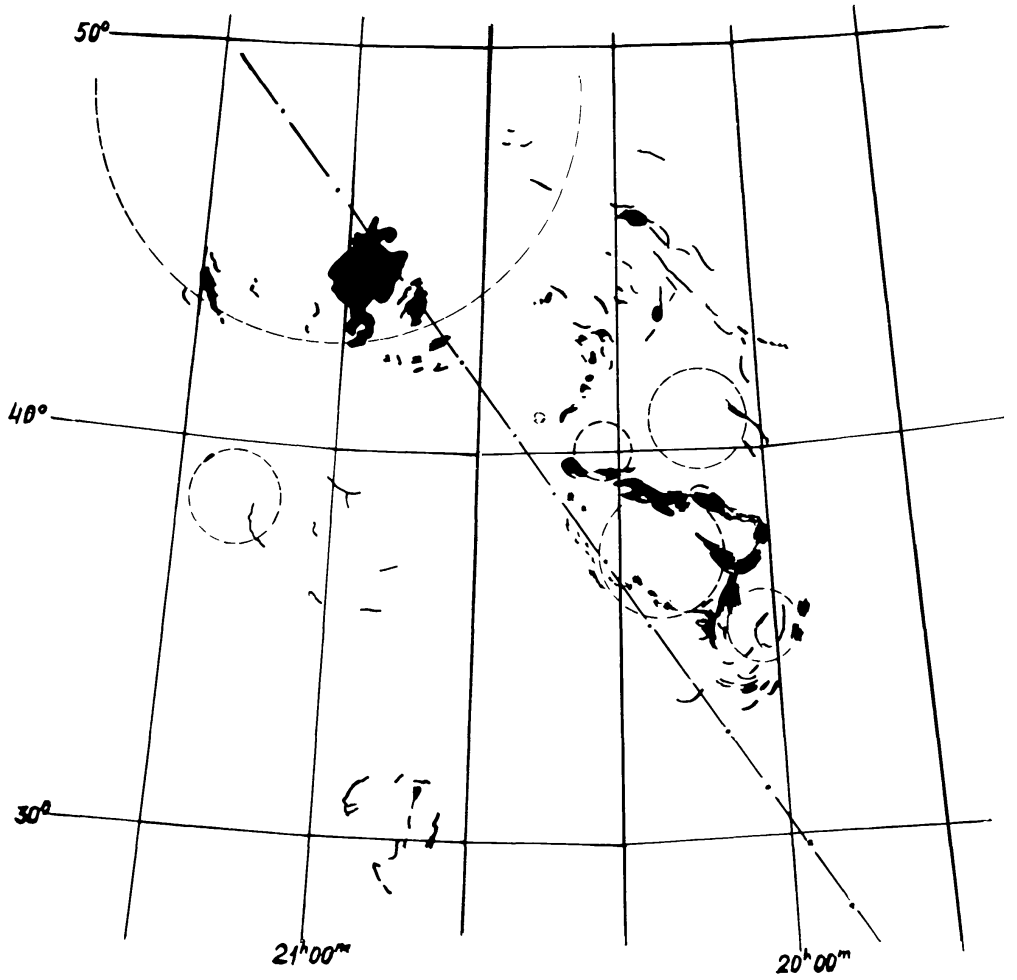

Fig. 8. Distribution of stellar associations against the background of bright filaments in the Cygnus region. The approximate boundaries of the associations (but not the ring nebulae around them) are indicated by dash circles. The dash-dot line marks the galactic equator.

been found to emit soft X-rays (see Section 7.4). In Cyg OB2, three Wolf–Rayet stars have been found (Reddish, 1968). The total mass of the stars has been estimated by Reddish *et al.* (1966) to be $(0.58–2.7) \times 10^4 M_\odot$, while the mass of the circumstellar shells is $(1.0–3.6) \times 10^4 M_\odot$ – that is, the total mass of the association is $(1.6–6.3) \times 10^4 M_\odot$. According to its parameters, the association is similar to the young globular clusters of the Magellanic clouds. The interstellar light extinction in its direction is 4 to 6^m (Dickel and Wendker, 1978).

Brand and Zealey (1975) ascribe the emission loop structure Cyg 4 with dimensions of 15° to association Cyg OB2 (see Section 5.2 and Table IV). The association is also surrounded by dust structure Cyg 5 having dimensions of 8°. The traces of the dust ring according to Brand and Zealey (1975) are visible against the North-America nebula. Also possibly connected with the association is the filamentary system which has dimensions of 8–10° and extends across the galactic plane (Section 5b) as well as the extended radio source described by Wendker (1970) (Sections 4.2 and 10.3).

Cyg OB1. This association comprises several bright stars characterized by strong stellar winds, including five Wolf–Rayet stars, three Of stars, and P Cyg. Cyg OB1 is surrounded by emission ring nebula Cyg 1 (Figure 7).

Cyg OB7. The eastern part of the region of interest contains stellar associations Cyg OB7 which is the nearest to the Sun and has dimensions of about 12°. It includes the O6f star 68 Cyg surrounded by the bright nebula S119 (see Sections 5.1 and 7.5). This is the oldest stellar association in the constellation Cygnus (see Table V).

The combination of the above stellar associations in the Cygnus region is projected on the sky in the form of a ring with the Great Rift in the middle. As can be seen from Table V, most of the associations are spatially close to one another ($r \approx 1.5$–2 kpc).

5.4. High-luminosity stars with strong stellar wind

The number of OB2 stars in Cygnus is high: 110 high-luminosity stars are concentrated there (Humphreys, 1978). All of them seem to be sources of soft X-ray emission. X-ray emission must be the most intense from 55 supergiants of early spectral classes.

The density of Wolf–Rayet stars with strong stellar winds in this region is two to three times greater than the average density of these stars in the Galaxy: the region, with extent about 18° along the galactic equator, contains 20 W–R stars of the 158 galactic W–R stars listed by Hucht *et al.* (1981). Most of the W–R stars lie within $72° < l^{II} < 81°$ and belong to stellar associations Cyg OB1 and Cyg OB2. Some of these stars are projected on the region where association Cyg OB3 is located.

The Cygnus region contains 16 out of about 90 galactic Of stars also characterized by a strong stellar wind (Lozinskaya and Lomovskij, 1982; Lozinskaya, 1982).

5.5. Interstellar extinction

For a better understanding of the complex picture of gaseous nebulae observed in optical emission, one must know well the distribution of obscuring matter in space. The region of interest is characterized by large amounts of interstellar extinction (Lynds, 1962). Investigation of the optical obscuration in the Cygnus region was started in the twenties (Wolf, 1923, 1925). The basic studies of the distribution of obscuring matter in the region are listed in Table VI.

According to Ikhsanov (1959), the dust in the direction toward Cygnus shows the usual ratio between color excess E_{B-V} and the interstellar extinction A_V: $R = A_V/E_{B-V} = 3.0 \pm 0.2$.

5.5.1. *Distribution of Obscuring Matter Along the Galactic Plane*

The region of interest gives rise to the Great Rift dissecting the Milky Way near the galactic plane from the constellation Cygnus to the galactic center and beyond. The Great Rift is a giant gas-dust complex associated with the North-America and Pelican nebulae. The edge of obscuring matter of the Great Rift, closest to the Sun, is at distances ranging from 500 to 800 pc (Miller, 1937; Vanäs, 1941). With the galactic longitude l^{II}, decreasing from 85–90° to 60°, the edge gradually recedes (Uranova, 1968; Lucke, 1978; see Figure 9). The far edge of the Great Rift is at a distance of 1600

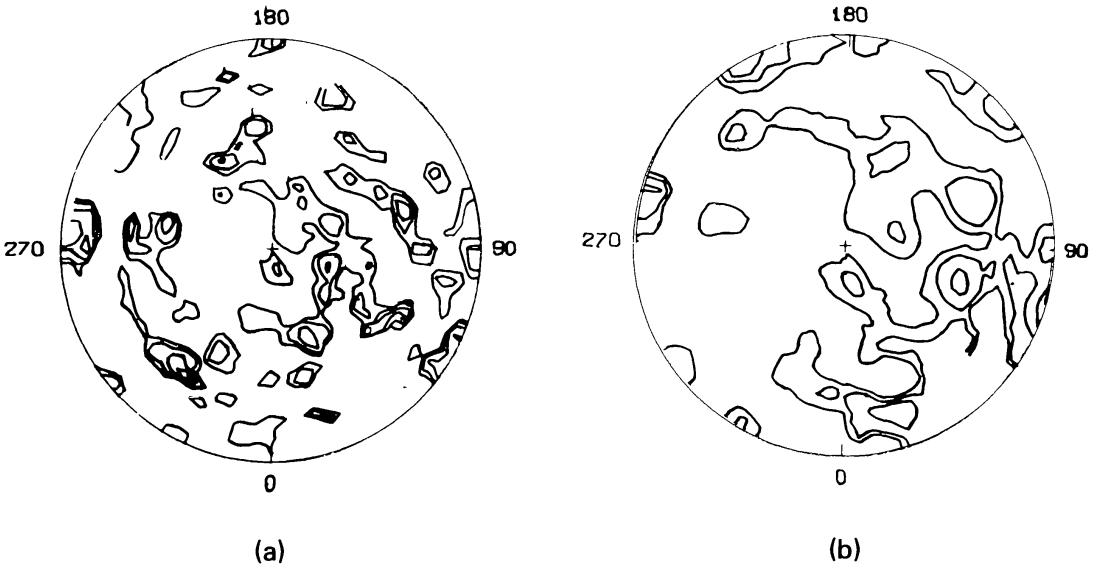

Fig. 9. Distribution of obscuring matter in the galactic plane (Lucke, 1978): (b) in the region 500 pc distance from the Sun (smoothed over 100 pc in a layer 50 pc thick); (a) in the region 2 kpc distance from the Sun (smoothed over 200 pc in a layer 200 pc thick). The contours stand for lines of equal values of dE_{B-V}/dr = 0.5, 1.0, 2.0, and 4.0 mag. kpc^{-1}.

to 2000 pc (Miller, 1937; Uranova, 1968; Kalandadze and Kolesnik, 1977). The matter inside the Great Rift seems to be concentrated in several large clouds (Kalandadze and Kolesnik, 1977; Lucke, 1978). Behind the Great Rift, up to 4 kpc, space is almost free of obscruring matter, after which line-of-sight enters the Persus I arm and obscuration increases (Pučinskas, 1982) (see Figure 3). The immediate vicinity of the Sun ($R \leq 100$ pc) is free of obscuring matter, as was pointed out in early studies (Müller and Hufnagel, 1935; Miller, 1937) and examined extensively by Lucke (1978) and Perry and Johnson (1982). More evidence to this effect is provided by the O VI ion lines observed in the spectra of the nearby stars 59 Cyg (250 pc) and 60 Cyg (380 pc) (Jenkins, 1978).

According to Perry and Johnson (1982), in the direction l = 65–90° there are several clouds of obscuring matter at distances of 50 to 100 pc from the Sun on either side of the galactic plane (galactic latitudes $b^{II} \approx +30°$ and $b \approx -45°$). The interstellar extinction is small near the galactic plane in the direction to Cygnus. It reaches a maximum value at 300 pc from the Sun in the region $l^{II} \approx 75°$, $b^{II} \approx -7.5$–0° with $E_{B-V} = 0^m.07$. Only at $l \approx 85$–90°, in the galactic plane at a distance of about 200 to 300 pc, there is a cloud with $A_V \approx 0^m.6$–$1^m.2$ (Müller and Hufnagel, 1935; Metik, 1961; Lucke, 1978).

The distribution of obscuring matter in the Great Rift is rather inhomogeneous, which has been pointed out by all those who investigated this region (see reference in Table VI). Consequently, the region of interest has to be broken down into rather small portions for a more complete examination of the obscuration. Pučinskas (1982) had to divide a region as small as 0.8 deg^2 into three portions. Obviously, in larger sky sectors one can use only averaged values of extinction.

Generally, at distances $r \leq 2$ kpc from the Sun toward the Cygnus superbubble, the obscuration near the galactic plane varies from about 2^m in the direction toward cluster

TABLE VI

Major studies into the spatial distribution of interstellar extinction in Cygnus region

Authors	Region under investigation	
	Area (deg^2)	Location
1. Wolf (1923)		Cyg Loop region (NGC 6960)
2. Wolf (1925)	1.51	North-America nebula
3. Müller and Hufnagel (1935)	14.3	Circle 4°.5 in diameter with its center at $l^{II} \approx 84°$, $b^{II} \approx 0°$ (around NGC 7000)
4. Miller (1937)	700	$50° \lesssim l^{II} \leq 87°$, $-10° \lesssim b^{II} \lesssim 15°$
5. Ikhsanov (1959)	30	Circle 6° in diameter with its center at $l^{II} \approx 80°$, $b^{II} \approx 4°$ (Cyg-X region)
6. Metik (1961)	42	Square with center at $l^{I} = 52°$, $b^{I} = +0°.5$, $80° \lesssim l^{II} \lesssim 87°$
7. Uranova (1968)		$65° \lesssim l^{II} \lesssim 77°$
8. Kalandadze and Kolesnik (1977)	18	Circle with its center at $l^{II} = 76°.9$, $b^{II} + 0°.6$ (in the direction to the stellar cluster NGC 6913)
9. Lucke (1978)	$\approx$ 42000	All over the sky
10. Pučinskas (1982)	0.8	Circle with its center at $l^{II} = 75°.4$, $b^{II} = +1°.3$ (in the direction to stellar cluster IC 4996)
11. Perry and Johnson (1982)	$\approx$ 20000	Northern hemisphere
12. Uranova (1985a, b)	350	$70 \lesssim l^{II} \lesssim 87°$, $-20° \lesssim b^{II} \lesssim 10°$

Range of distances (kpc)	Number of stars	Remarks
1.	2826	Stars counted up to $17^m.5$ in selected sectors with a total area of 0.03 deg^2
2.	10185	Stars counted up to 16^m in a region divided into three sectors according to the amount of obscuration
3. $\lesssim 1-2$	8000	Two-color photographic measurements of stars up to 15^m; the region is divided into 6 sectors according to the amount of obscuration
4.		88 selected sectors examined; photographic observations of stars in three colors
5. $\lesssim 1.5-2$	952	Cyg X region divided into 8 sectors; measurements in two colors
6. $\lesssim 4.4$	3403	Photographic measurements of OB2 stars in two colors
7. ≤ 4.0		
8. $\leq 2.5-4$	3213	Two-color measurements; the region is divided into 9 sectors
9. ≤ 2	4187	According to *UBV* magnitudes and spectral types
10. ≤ 7	888	Multicolor measurements; the region is divided into 3 sectors
11. ≤ 0.3	3450	According to data on bright A and F stars; resolution of about 25 pc in all three coordinates
12. $\lesssim 1.5-3$		Stars of known spectral classes and luminosities up to $12-14^m$; distribution along the z-coordinate in 8 sectors l at different distances from the Sun

IC 5996 (Pučinskas, 1982) and in some other directions to at least $3^m.5$–5^m (Müller and Hufnagel, 1935; Miller, 1937; Ikhsanov, 1959; Kalandadze and Kolesnik, 1977). The highest density of obscuring matter is observed at distances of 700 to 1200 pc from the Sun, where in many directions $dA_V/dr > 5^m$ kpc^{-1} and, in some cases, it can reach 15–34^m kpc^{-1} (Kalandadze and Kolesnik, 1977; Uranova, 1985a).

In some places, dense dark nebulae with extinction 5–6^m are observed (Lynds, 1962). Regions with pronounced obscuration ($A_V \geq 3^m$) extended along the galactic plane in the form of waves with $b^{II} < 0$ at $l^{II} \simeq 85°$ and $l^{II} = 67$–$72°$ and $b^{II} > 0$ at $l^{II} \approx 78°$. This wavy picture generally follows the z-variations of interstellar hydrogen distribution in the local arm, as discussed by Quiroga and Schlosser (1977), and seems to correspond to the departures of the interstellar matter distribution from the galactic plane in the local arm.

5.5.2. *Distribution of Obscuring Matter Along the z-Coordinate*

The density of the obscuring matter decreases with increasing galactic latitude. In the Cyg-X direction, as was pointed out by Ikhsanov (1959), the distance to the obscuring matter layer increases with the z-coordinate in the northern hemisphere of the Galaxy.

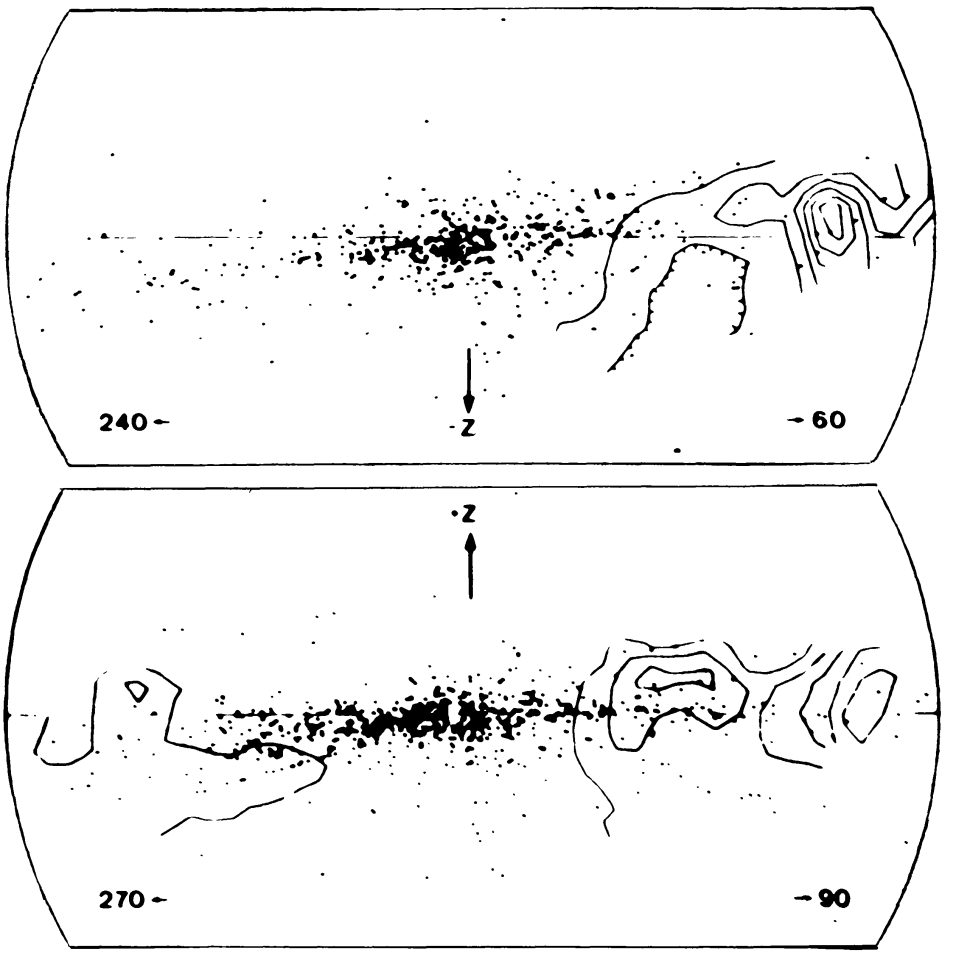

Fig. 10. Distribution of obscuring matter in cross sections normal to the galactic plane along galactic longitudes $l^{II} = 60°$ (a) and $l^{II} = 90°$ (b) (Lucke, 1978). Lines of equal values of color excesses E_{B-V} at distances of up to 1 kpc from the Sun are shown.

A more detailed examination by Lucke (1978) has shown that the leading edge of the Great Rift is almost vertical in the region $l = 90°$ (with the obscuring matter maximum being shifted into the northern hemisphere of the Galaxy by several tens of parsecs) and becomes oblique at $l^{II} = 60°$. Thus, obscuration begins at smaller distances from the Sun in the southern hemisphere and at larger ones in the northern hemisphere, but reaches maximum again in the northern hemisphere (Figure 10).

Careful analysis of the obscuring matter distribution along the z-coordinate in different longitudinal sectors and at different distances form the Sun (Uranova, 1985b) indicates that the obscuring matter is highly concentrated in the galactic plane, mainly in a layer 20 to 30 pc thick. In the center of the layer, the amount of obscuration along the tangent to the arm ($l^{II} = 78–80°$, $r \leq 1.5$ kpc) may be as high as tens of magnitudes at 1 kpc, but already at distances of 15 to 20 pc from the plane it is very much lower. This is why such large amounts of obscuration are not seen in Figure 9 which shows the average obscuration values in a layer 50 pc (Figure 9a) and 200 pc (Figure 9b) thick. Nor can it be seen in Figure 10 because of the low star density per unit sky area, taken from Lucke's work (1978).

At distances ranging from 1.5 to 3 kpc, the axis of the local arm is in direction $l^{II} = 77°$. In longitudinal sectors just a few degrees away from the arm axis, obscuration, even in the galactic plane, does not exceed 3 to 5^m kpc^{-1}. As was already mentioned in Section 3.1, according to Uranova (1985a), the obscuring matter has a cut-off with an almost vertical front on the outside of the local arm and with a distribution toward the inner edge.

5.5.3. *Optical Obscuration Along the Path to the Emission Nebulae*

Shklovskii (1960) notices that the interstellar absorption up to H II regions can be determined by comparing surface brightness in radio and optical ranges. Such first comparison for the Cyg-X region was made by Ikhsanov (1960a, b).

Dickel and Wendker (1978) made a more detailed investigation of the interstellar extinction in Cyg-X region by such a method. They constructed a map of the obscuration in the region $\alpha = 20^h08^m–20^h38^m$, $\delta = 38°.5–44°.3$ with angular resolution $11'$. The obscuration distribution turned out to be highly irregular, varying from 1^m to 4^m and reaching $5–6^m$ at some points. Comparison of these data with the spatial extinction distribution gives information about the spatial position of nebulae (although the extremely irregular obscuration makes such analysis difficult). According to Dickel and Wendker (1978), nebulae in Cyg X are most probably distributed along the line-of-sight in the local spiral arm and even beyond. This corroborates the conclusion, following directly from radio data (Section 4.3), that the Cyg-X region is a projection on the sky of objects located in the local arm at different distances from the Sun. As was pointed out in Section 5.2.2., Kapp-herr and Wendker (1972) used the same method to show that the filaments illustrated in Figure 2 do not form a continuous single spatial structure but are located on opposite sides from the system of obscuring clouds which form the Great Rift.

5.6. Interstellar polarization and orientation of magnetic fields

For magnetic field studies we selected stars belonging to the stellar associations in the Cygnus region – that is, groups of stars of the same origin spaced 1 to 2 kpc from the Sun. The distribution of stellar light polarization vectors indicating the direction of the magnetic field is presented in Figure 11. The polarization data were taken from Hall (1958) and Hiltner (1956).

Although in some cases, the polarization vectors are oriented along optical gas filaments, their distribution with respect to the filaments is chaotic. The only object in this region for which it can be said that its filaments extend along the magnetic field is the nebula S119. The polarization vector of 68 Cyg (which excites this nebula) indicates that the magnetic field is oriented in the same direction as the gas filaments of the nebula – that is, roughly along the galactic plane. Determination of the magnetic field strength

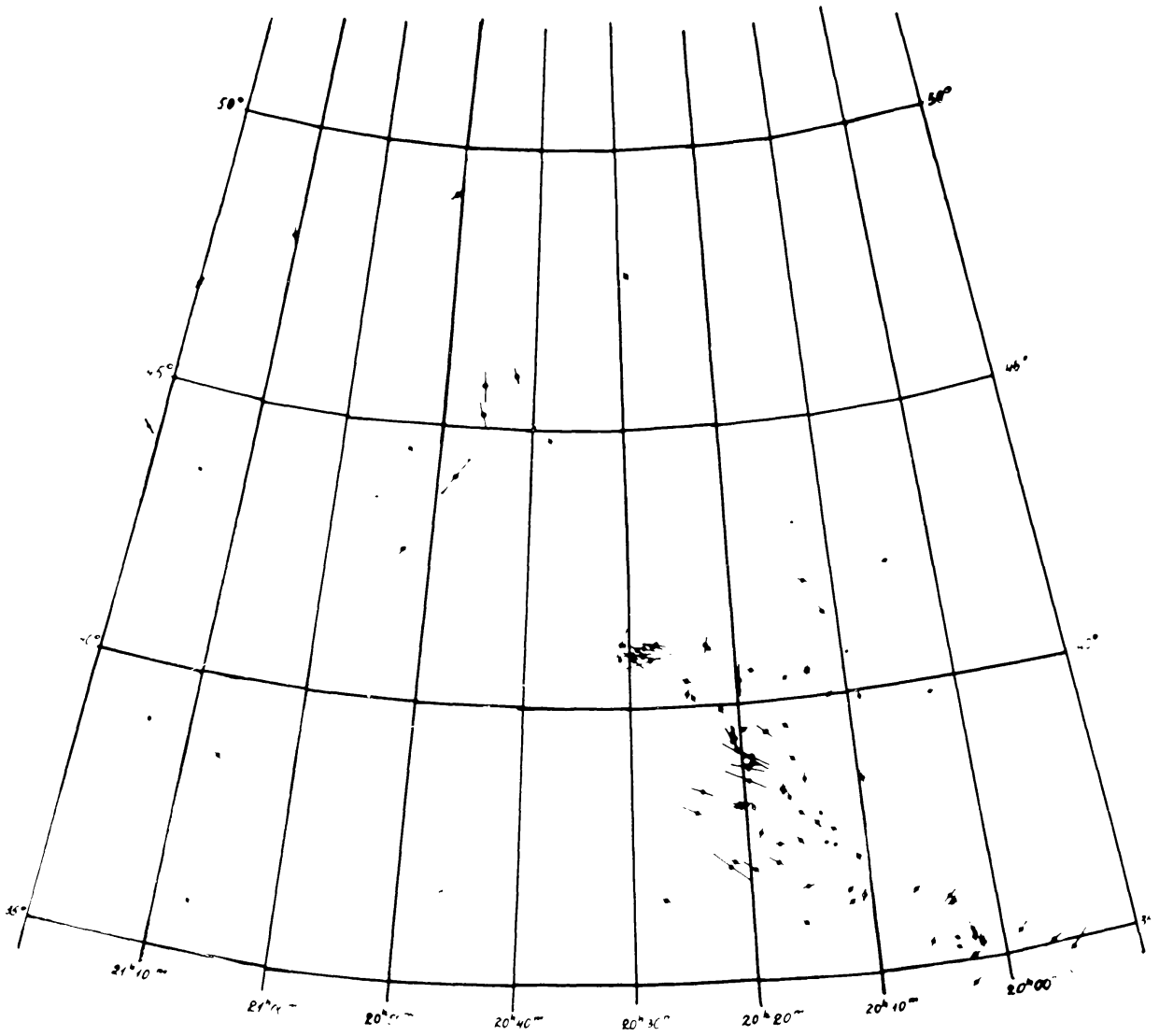

Fig. 11. Interstellar polarization of the light from stars located in the Cygnus superbubble region. Lengths and orientations of dashes show strength and direction of the *E*-vector of the interstellar polarization.

from Faraday rotation for nebula S119 gives a value of 20 μG (Heiles *et al.*, 1981). The magnetic field strength for the North-America nebula was also determined and found equal to 1–3 μG. In the molecular cloud, associated with this nebula, the magnetic field strength may reach 50 μG (Heiles *et al.*, 1981).

The available data are so poor that they cannot indicate a connection between the magnetic field direction, the orientation of filaments, and the stellar light polarization vector. Nevertheless, it seems likely that the giant gaseous structure of sinuous shape, described above in Section 5.1, may be a visible manifestation of the systematic galactic magnetic field (the interstellar matter is stretched along lines of force). The distribution of the polarization vectors of stars of young associations has not provided direct proof of this effect.

5.7. Summary

The optical emission from the region of interest includes the radiation of gaseous nebulae often super-imposed on one another. It includes a number of known bright H II regions, supernova remnants, and nebulae creates by stellar winds (Section 5.1, Table II). The expansion velocities of most objects are $|V| \leq (14–20)$ km s^{-1}. The western part of the region (to the north of the galactic equator, Figures 6 and 8) is notable for the bright sinuous gaseous structure extending along the galactic plane over 18°.

In the region under consideration, there are many elongated emission filaments. The ring of filaments, shown in Figure 2, is not a structural unit, as can be inferred from comparison of radio and optical measurements (Kapp-herr and Wendker, 1972) and, therefore, cannot be ascribed to the association Cyg OB2. Another argument against a relationship between Cyg OB2 and the ring is the longer dimension of the ring along the galactic plane, as compared to that across the plane (Section 5.2). We think that associated with Cyg OB2 may be a system of filaments with coordinates $\alpha = 20^h10^m–20^h30^m$, $\delta = 42–46°$ and $\alpha = 20^h50^m–21^h10^m$, $\delta = 37–41°$, extending across the galactic plane over about 10°.

Eight OB associations are located in the superbubble region, at distances of up to 2.5 kpc from the Sun. Brand and Zealey (1975) distinguished ring nebulae (giant loop structures, Section 5.2, Table IV) around some of them with a typical diameter of 100 pc. Five associations occupy crests and valleys of the sinuous system of gas filaments in the western part of the region (Figure 8) and are within 1.3 to 2 kpc of the Zun. The eastern part contains two less distant associations of large angular dimensions. These associations, taken together, form a horseshoe shaped figure similar to the superbubble (Table V, Section 5.3).

The associations contain 100 high-luminosity stars, including 55 supergiants of early spectral classes, about 20 Wolf–Rayet stars, and 16 Of stars characterized by a strong stellar wind (Section 5.4).

The interstellar extinction (Section 5.5) in the region of interest is highly irregular and is determined primarily by the Great Rift from 800 to 1200 pc distance from the Sun and consisting of several obscuring clouds (Figure 9). Up to 500–800 pc, the extinction amounts to about 1^m only in a few directions. On more distances near the galactic plane,

along the arm axis, the extinction exceeds $4–5^m$ kpc^{-1} (and even $10–30^m$ kpc^{-1} at some points) but then decreases sharply as the distance from the galactic plane increases. The decrease is slightly asymmetrical in the northern and southern hemispheres (Figure 10). Analysis of the interstellar absorption that lies in front of the nebulae in the Cyg-X region (Dickel and Wendker, 1978) suggests that the nebulae are spread along the line-of-sight at distances ranging from 1 to 2.5 kpc. Comparison of the distribution of interstellar polarization of the stellar light with the position of gas filaments does not reveal a clear correlation of the magnetic field and gas filaments except in the case of the nebula S119.

6. Infrared Emission

The region of interest (primarily Cyg X) was also investigated in near (Ackermann, 1970) and far (Hoffmann *et al.*, 1971) IR emission. Examination of the region of galactic latitudes 55° to 90° has shown that IR sources are concentrated in the region $l^{II} = 76–86°$; that is, where the maxima of the radio-emission of both the local CO and the H II regions occur (Scoville and Solomon, 1975; Burton *et al.*, 1975).

In the photographic IR range ($\sim 0.8–1\ \mu$), about 400 discrete IR sources have been detected. They are concentrated in the galactic plane and associated with dark clouds and prominent H II regions. Some of them seem to be highly obscured O stars.

Analysis of the early observations made in the far IR range ($100\ \mu$) had prompted Emerson (1976) to conclude that the seven far IR sources in the Cyg-X region are the brightest H II regions and can be identified with radio sources DR5, 6, 17, 21, 22, and 23.

Closer observations made by Campbell *et al.* (1980) have revealed in the Cyg-X region 49 emission sources in the range of 60 to $100\ \mu$, concentrated primarily in the Great Rift and stellar associations Cyg OB2 and Cyg OB9. The relationship between these IR sources and the objects emitting in the mid IR range ($\lambda \sim 20\ \mu$), the radio continuum, and the CO radio line ($\lambda \approx 2.6$ mm) was studied. The results of this study indicate that nearly 20 sources emit in all of the above-mentioned ranges. About one half of the detected sources correlate well with the radio-emission peaks at 2.7 GHz, observed by Wendker (1970). Others are probably associated with very young stars that have not yet created H II regins, or with stars of a luminosity not high enough to create a prominent H II region. At any case, the typical IR luminosity ($\sim 10^4 L_\odot$) of such sources corresponds to B1 stars which ionize hydrogen weakly but heat the dust well. Some of these sources correlate with the position of CO peaks. Their position is probably, on the boundary of the molecular cloud and the star-formation region indicates a young age of these objects.

IR observations indicate that the process of star formation is in progress in the region and that the Cygnus region contains other sites of star formation along with such well-known ones as DR21 (W75) (cf. Avedisova, 1981).

7. The Superbubble and Discrete X-Ray Sources

As was shown in the preceding sections, the optical, radio, and IR emissions from the Cyg region are due to a combination of various objects. Here we should like to consider the contribution of different known discrete sources of soft X-rays in the Cyg region to superbubble studies.

The constellation Cygnus abounds in soft X-ray sources, including three known strong binaries, eight supernova remnants, and so on. About 20 discrete sources in this region can be found in the catalogue compiled by Amnuel *et al.* (1982). Besides, this region is expected to contain more than a hundred weak sources of soft X-rays, associated with high-luminosity OB stars.

Before estimating the contribution of these sources to the X-ray emission from the superbubble let us have a look at the emission itself.

7.1. Irregularity of X-ray emission parameters over the superbubble surface

The extended X-ray source was treated briefly in Section 2.1. Here we should like to touch upon several more factors important in the analysis of the X-ray emission from the region of interest.

According to Cash *et al.* (1980), the sky sector occupied by the extended source has an area of about 250 square degrees. At the superbubble flux $F_x \approx 1.3 \times 10^{-9}$ erg cm^{-2} s^{-1} (after excluding four bright discrete soft X-ray sources: the Cyg Loop, G 65.2 + 5.7, Cyg X-1, and Cyg X-2), the sky brightness in soft X-ray emission, averaged over the entire region, is about 5×10^{-12} erg cm^{-2} s^{-1} deg^{-2}, or, within the instrumental resolution $1°.55 \times 2°.95$, about 2×10^{-11} erg cm^{-2} s^{-1}, which corresponds, at a typical spectral width of 0.5 keV, to 15 μJy.

The intensity of X-ray emission within the ring is inherently irregular. High-brightness regions, even without four discrete sources excluded by Cash *et al.* (1980), occupy about one third of the entire superbubble. The emission maximum coincides with the Cyg X-7 region. The sensitivity of the measurements carried out by Cash *et al.* (1980) is evidently somewhat higher than that determined from the mean emission intensity. An X-ray source producing a flux with a flux density as low as several μJy must already make a significant contribution to the observed picture (see Section 7.3, 4, 5).

Consider now the degree of irregularity of the superbubble emission spectrum. Two ring parts, Cyg X-6 and Cyg X-7, observed earlier can be taken for comparison.

One part of the superbubble, namely Cyg X-6, was first seen in a rocket experiment conducted by Coleman *et al.* (1971). It was later observed by Davidsen *et al.* (1977) in a rocket experiment and during the Apollo-Soyuz mission, when another ring part named Cyg X-7 was also examined.

Figure 12 shows the allowed values of column density N_H and gas temperature T, at a 90% coincidence limits derived from measurements with three different detectors in the case of Cyg X-6 and two detectors in the case of Cyg X-7 (Davidsen *et al.*, 1977). The range of permissible values of N_H and T, determined for the entire superbubble by

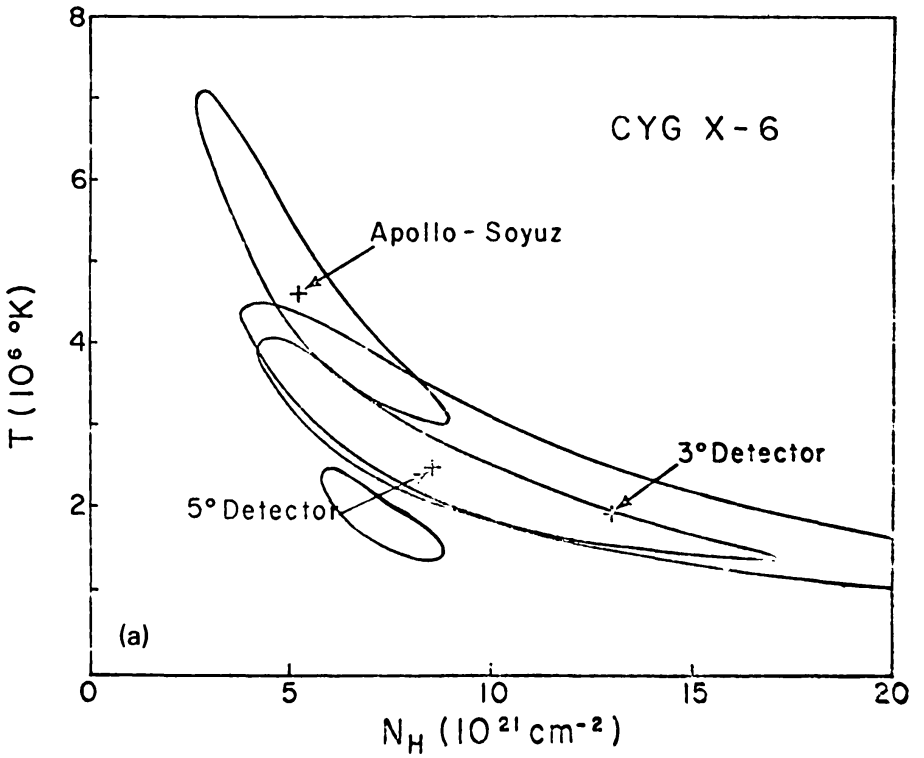

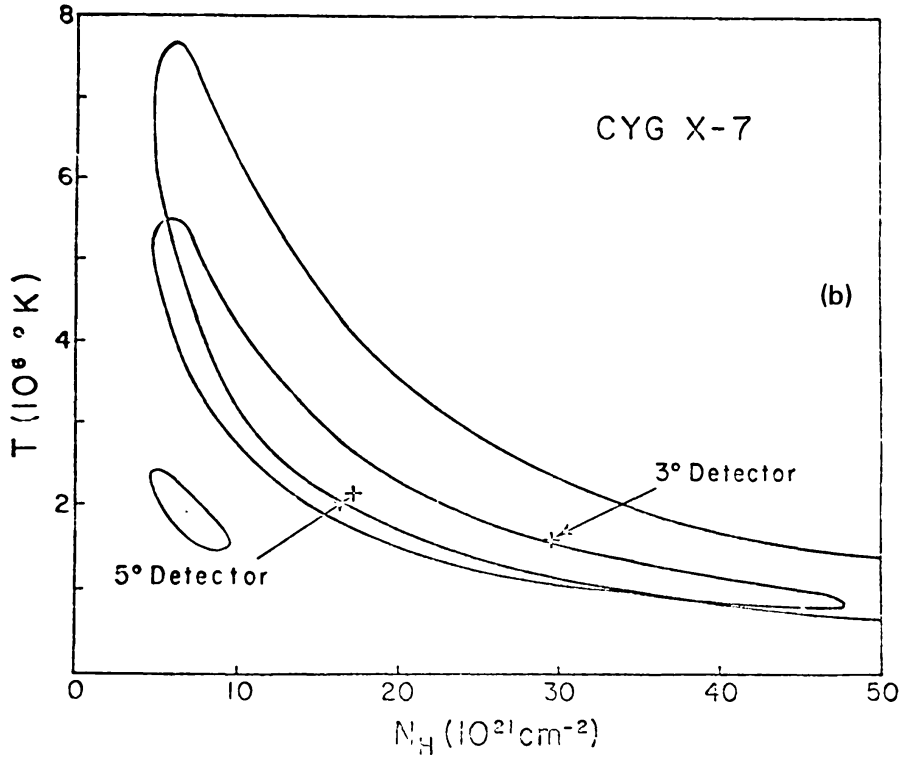

Fig. 12. Contour indicating allowed values of temperature T and column density N_H for portions of the superbubble known as Cyg X-6 (a) and Cyg X-7 (b) (Davidsen *et al.*, 1977). At the lower left portion of each diagram is shown the allowable T, N_H values for the superbubble as a whole derived by Cash *et al.* (1980).

Cash *et al.* (1980) also presented at the same level of significance. The range of permissible values of N_H and T for all the superbubble is beyond the regions of sôurces Cyg X-6 and Cyg X-7. Cyg X-7 and Cyg X-7 and Cyg X-6 are characterized either by a higher-emission temperature (when compared to the superbubble as a whole) or by a substantially greater value of N_H. Cyg X-7 has a higher observed surface brightness than the X-ray ring as a whole. These two facts suggest that the true surface brightness of Cyg X-7 is significantly above the average level. This difference results from the fact that Cyg X-7 is a discrete source not associated with the superbubble (see Section 7.3). The difference between Cyg X-6 and the entire superbubble is less pronounced.

Another argument in support of the different emission spectra produced by different parts of the superbubble is provided by Cordova *et al.* (1981). During the time that Cash *et al.* (1980) were making their observations they used the same LED-1 detector on board satellite HEAO-1 that Cash *et al.* (1980) did. They scanned in the slow mode, looking for X-rays from cataclysmic variables. According to Cordova *et al.* (1981), the star SS Cyg in the eastern portion of the superbubble had a much softer spectrum during the observations, than did the superbubble as a whole (see Section 7.4). Thus, the X-ray emission parameters (both intensity and spectrum) vary from one point to another over the superbubble.

7.2. Bright X-ray binaries

The superbubble region contains three known powerful sources of soft X-rays: Cyg X-1, Cyg X-2, and Cyg X-3. The first two make a significant contribution to the soft X-ray emission and are seen in Figure 1, between $\delta = 33°$ and $\delta = 40°$, as bright spots widened by the low resolution of the HEAO-1 detector. The contribution of Cyg X-3 to the soft X-ray range is insignificant because of the extremely high-hydrogen column density, $N_H = (5–10) \times 10^{22}$ cm^{-2} (Blissett *et al.*, 1981; Amnuel *et al.*, 1982) in the direction of Cyg X-3.

At least, one of these sources (Cyg X-1) is associated with the evolution of a binary system with components of very high mass (Bochkarev *et al.*, 1975; Balog *et al.*, 1981) and is about 2 kpc distant from the Sun (Margon *et al.*, 1973; Bregman *et al.*, 1973; Karitskaya, 1981). Therefore, it is situated in the region of interest and seems to be associated with the superbubble.

According to $N_H = (2–7) \times 10^{21}$ cm^{-2} (Bleeker *et al.*, 1972), the source Cyg X-2 is also spatially related to the Cyg superbubble. Cash *et al.* (1980) excluded these sources from calculations of the superbubble parameters.

7.3. X-ray emission from supernova remnants

Supernova remnants are powerful sources of thermal X-ray emission in the band of 0.5 to 2 keV and in the softer range of the spectrum. This emission arises behind the front of the blast shock in the diffuse interstellar medium.

Eight SNRs are located in the superbubble region (Section 4.1, Table I). The position of five supernova remnants are indicated by solid-line circles in Figure 13 (against the background of the X-ray picture of the superbubble).

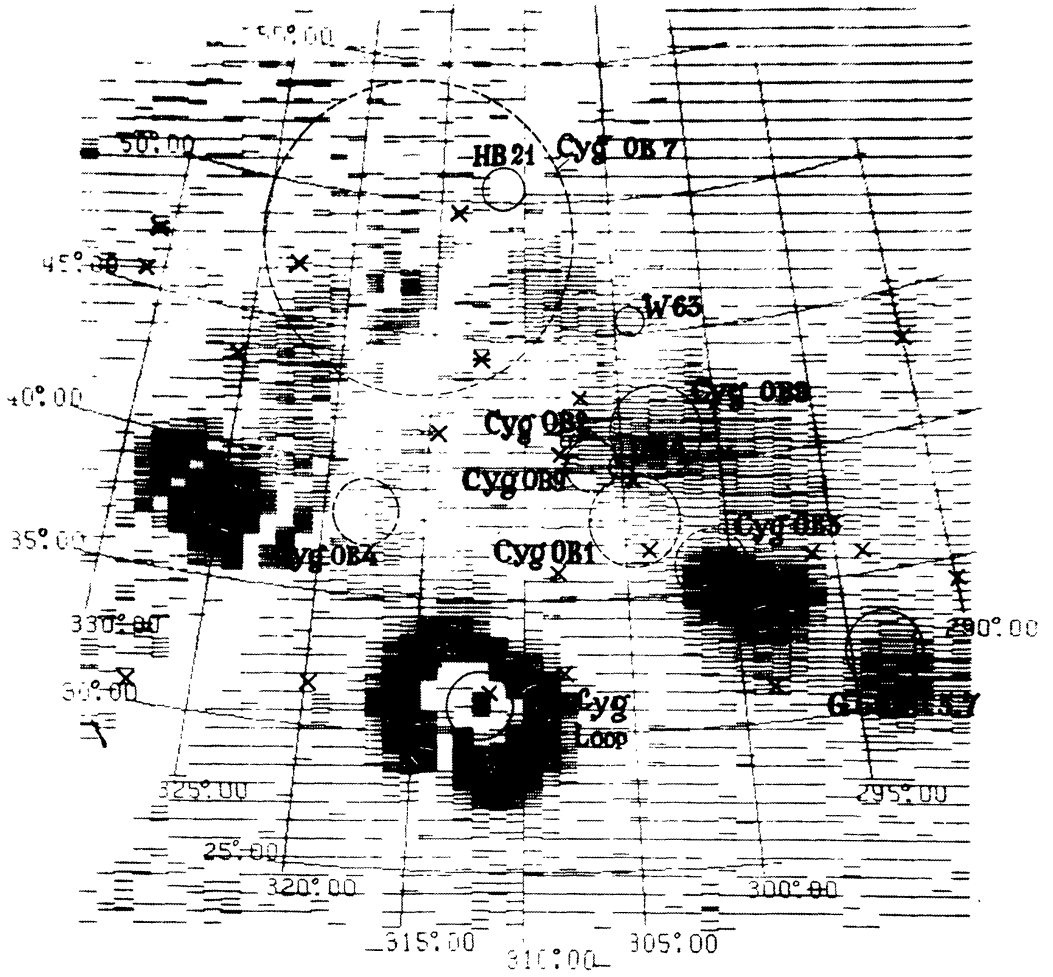

Fig. 13. Distribution of various X-ray sources in the Cygnus region. Solid circles on the X-ray picture of the superbubble (Figure 1) mark supernova remnants, dash circles indicate the approximate boundaries of stellar associations (but not the surrounding ring nebulae), and crosses mark the X-ray sources listed in the catalogue of Amnuel *et al.* (1982).

Cyg Loop and G 65.2 + 5.7. The brightest and best studied supernova remnant is the Cyg Loop (Bleeker *et al.*, 1972; Rappaport *et al.*, 1974). It is shown in the bottom of Figures 1 and 13 as a bright diffuse ring. The other bright supernova remnant, G 65.2 + 5.7 (see Section 5.1), can be seen on the right-hand sides of Figures 1 and 6 (α = 290–295°). The emission from these two sources, just as from Cyg X-1 and Cyg X-2, was subtracted by Cash *et al.* (1980) from the superbubble emission before the X-ray ring parameters were derived..

Also seen at a distance of up to 2 kpc from the Sun are supernova remnants HB21, W63, and DR4.

HB21. The possible contribution of supernova remnant HB21 to the emission from the superbubble does not exceed 3% because, according to Davidsen *et al.* (1977), the gas temperature $T \leq 2 \times 10^6$ K and the X-ray flux $F_x(0.5\text{–}1.5 \text{ keV}) \leq 4.1 \times 10^{-11}$ erg cm^{-2} s^{-1}. In the HEAO-1 observations this super-

nova remnant fell in a poorly observed region (light strip extending from the lower left corner of Figure 1).

W63. No reliable data on supernova remnant W63 are available although, as can be seen from Figures 1 and 13, a small portion of the X-ray emission from the Cygnus superbubble may be associated with this remnant. According to the rough estimates made by Clark and Culhane (1976), source W63 may produce a flux $F_x(0.5\text{–}1.5\ \text{keV}) \sim 10^{-9}\ \text{erg cm}^{-2}\,\text{s}^{-1}$ (without taking into account the interstellar absorption) at gas temperature $T \approx 4 \times 10^6$ K. These estimates seem to be too high. At the same time, it is to be expected that supernova remnant W63 may make a certain contribution to the observed flux of soft X-rays from the superbubble.

DR4. Davidsen *et al.* (1977) pointed out that the position of source DR4 correlates well with the Cyg X-7 region which is the brightest portion of the X-ray ring. The first uncertain detection of this source and its possible association with DR4 were described by Burginyon *et al.* (1973). According to Davidsen *et al.* (1977), supernova remnant DR4 may be responsible for the soft X-ray emission from Cyg X-7. Recently, Higgs *et al.* (1983) discovered X-rays emitted directly by supernova remnant G 78.2 + 2.1 = DR4. The X-ray flux observed at the *Einstein* Observatory from a region 32′ in diameter was found to equal $F_x(0.15\text{–}4.2\ \text{keV}) = 6 \times 10^{-11}\ \text{erg cm}^{-2}\,\text{s}^{-1}$. Using the angular diameter of object DR4 $\approx 62'$ (Table I), the soft X-ray flux may be estimate $F_x = 2.3 \times 10^{-10}\ \text{erg cm}^{-2}\,\text{s}^{-1}$. It is in good agreement with the flux derived for Cyg X-7 equal to $F_x(0.5\text{–}2\ \text{keV}) = (2.1 \pm 0.4) \times 10^{-10}\ \text{erg cm}^{-2}\,\text{s}^{-1}$ (Davidsen *et al.*, 1977). Thus, it becomes certain that the brightest feature in the superbubble observed by Cash *et al.* (1980) is emission from supernova remnant. This source provides about 15% of the superbubble X-ray emission.

Other supernova remnants. As was mentioned in Section 4.1, three supernova remnants (G 65.7 + 1.2, G 74.9 + 1.2, G 84.2 – 0.8) are distant objects. The X-ray flux from them may be strongly attenuated by the interstellar absorption and the long distances to the sources. Indeed, the observations made at the *Einstein* Observatory have shown that the column density on the way to G 74.9 + 1.2 = CTB87 = 1E2014.1 + 3702 is high ($N_{\text{H}} = (1\text{–}1.6) \times 10^{22}\ \text{cm}^{-2}$), whereas the X-ray flux ($F_x(0.15\text{–}3\,\text{keV}) = (0.74\text{–}0.86) \times 10^{-12}\ \text{erg cm}^{-2}\,\text{s}^{-1}$ (Wilson, 1980)) from it is too small to be of any significance in superbubble studies. As regards the other two remote supernova remnants, no reliable data are available.

Thus, the known supernova remnants in the Cygnus region, not excluded by Cash *et al.* (1980), account for at least 15% of the X-ray emission from this region.

7.4. The faint point X-ray sources

In addition to discussed above, the catalogue by Amnuel *et al.* (1982) contains 19 more permanently radiating discrete sources with low-density (< 100 μJy) fluxes, lying in the Cygnus superbubble region. They are indicated by crosses in Figure 13. It can be seen that the distribution on the sky of these sources replicates the shape of the superbubble. In this particular case, such shape is definitely a result of projection on the sky of sources

disposed primarily in the local spiral arm. Their absence in the central region must be due to the significant interstellar absorption of X-rays in the Great Rift.

SS Cyg. Among the weak sources in the Cygnus region we should first of all like to point out the nova-like star SS Cyg at a distance of only 150 pc. (Data on this star can be found, for example, in the work by Brandt and McClintock, 1983.) It is located in the north-eastern part of the regions ($\alpha_{1950} = 21^h40^m42.6$; $\delta_{1950} = 43°21'51''$). In the intervals between outbursts, SS Cyg produces a flux $F_x(1\text{–}3\ \text{keV}) \approx 3 \times 10^{-11}\ \text{erg cm}^{-2}\ \text{s}^{-1}$ (Heise *et al.*, 1978; Rickett *et al.*, 1979). This object was also observed by satellite HEAO-1 (Cordova *et al.*, 1981). The observation has made it possible to establish only the upper limit of the flux for the energy range of 0.48 to 2.8 keV, which was found to be $F_x < 7.8 \times 10^{-11}\ \text{erg cm}^{-2}\ \text{s}^{-1}$ (estimate at the 3σ level), whereas in the soft X-ray range, $F_x(0.18\text{–}0.48\ \text{keV}) \approx (0.82\text{–}1.4) \times 10^{-11}\ \text{erg cm}^{-2}\ \text{s}^{-1}$. Thus, the spectral flux density (F_ν) for SS Cyg during superbubble observation was not lower in the range of 0.18 to 0.48 keV than in the range to the 0.48 to 2.8 keV, which made the spectrum of SS Cyg distinctly different from that of the superbubble as a whole, as was already mentioned in Section 7.1. This means that during the observations, the sources SS Cyg was in the state of explosion. In that state there is a prominent soft component probably with $kT < 50$ eV (Cordova *et al.*, 1981). The contribution of SS Cyg to the emission from the Cyg superbubble amounts to 0.6–6%. Thus, the star SS Cyg must be responsible for an X-ray spot with a surface brightness close to the average over the X-ray ring.

V751 Cyg. Cordova *et al.* (1981) also discovered X-rays emitted from star V751 Cyg ($\alpha = 20^h49^m$, $\delta = 43°57'$). The flux from this star ($F_x(0.48\text{–}2.8\ \text{keV}) \approx \approx 1.2 \times 10^{-10}\ \text{erg cm}^{-2}\ \text{s}^{-1}$) accounts for about 9% of the emission from the superbubble.

Kukarkin *et al.* (1969) attribute V751 Cyg to the Orion variables of early spectral type. It s a $13^m.8\text{–}16^m.3$ object (Martynov and Kholopov, 1957) located in the faint nebula IC 5070. It has an almost continuous spectrum entering the UV range and features variable Balmer lines. According to Herbig (1958), V751 Cyg is either a B0 V star with absorption $A_V = 1^m.7$ or a hotter star of lower luminosity. The first possibility seems to be more likely. Consequently, the optical characteristics of V751 Cyg are typical of X-ray sources and Cordova *et al.* (1981) identification is very plausible.

Using the common relationship between A_V and column density, $N_H \approx 2 \times 10^{21} A_V\ \text{cm}^{-2}$ (Spitzer, 1978), we find that $N_H \approx 3.5 \times 10^{21}\ \text{cm}^{-2}$. The interstellar X-ray absorption (Grudace *et al.*, 1974) suggests that the emission in the range of ≤ 0.5 keV on the path to V751 Cyg must be strongly attenuated in agreement with the measurements made by Cordova *et al.* (1981), $F_x(0.18\text{–}0.48\ \text{keV}) \leq \leq 2.2 \times 10^{-11}\ \text{erg cm}^{-2}\ \text{s}^{-1}$ (at the 3σ level).

The brightest of the other sources in the range of 2 to 6 keV are 19540 + 319 ≡ 4U1954 + 31 and 21296 + 471 ≅ 4U2129 + 47 from the catalogue of Amnuel *et al.* (1982).

4U954 + 31 = EY Cyg. This source varies in its spectral flux density ($F_\nu = 50\ \mu\text{Jy}$) by a factor of 5 (Forman *et al.*, 1978). Vidal and Wickramasinghe (1974) identify it with

the star EY Cyg of the U Gem type. If the identification is correct, the distance to this object is about 700 pc, and the interstellar extinction (A_V) and, hence, X-ray absorption, must be low (see Section 5.5). The value of A_V cannot be determined from optical observations because of the composite nature of the spectrum of cataclysmic variables (Kraft, 1962). The X-ray flux of this star measured from HEAO-1 (Cordova *et al.*, 1981) is $F_x(0.48\text{–}2.8\ \text{keV}) = 1.3 \times 10^{-10}\ \text{erg cm}^{-2}\ \text{s}^{-1}$, which accounts for 10% of the emission from the superbubble. If the interpretation of the observations made by Cordova *et al.* (1981) is valid, this source is responsible for emission from that part of the superbubble which is to the south of the Cyg X-1 source.

4U2129 + 47. Source 21296 + 471 = 4U2129 + 47 has $F_\nu = 20\text{–}25$ μJy in the range of 2 to 6 keV (Forman *et al.*, 1978). HEAO-1 scans (Thorstensen *et al.*, 1979), made during a time close to that when Cash *et al.* (1980) carried out their observations of the Cygnus superbubble, have shown that the flux from this source was $F_x = (8.5 \pm 0.85) \times 10^{-11}\ \text{erg cm}^{-2}\ \text{s}^{-1}$ (6–7% of the emission from the superbubble). Thorstensen *et al.* (1979) identified it with a variable star with $m_V = 16.2\text{–}17.4$ and a light curve similar to that of HZ Her ≡ Her X-1. The star is characterized by He II and C III–N III emission lines, and variation of the Hβ and H and K Ca II lines which is typical for the optical components of X-ray sources. Therefore, the identification appears reliable. From optical observations of the optical component and background stars, Thorstensen *et al.* (1979) established that $A_V \geq 0^m.7$ (but not more than $1^m.5\text{–}1^m.9$). This A_V corresponds to $\log N_H = 21.15\text{–}21.16$ – that is, somewhat lower than for the superbubble as a whole according to Cash *et al.* (1980). In other words, the low-frequency cut-off of the 4U2129 + 47 spectrum emission lies approximately in the same region as in the case of other parts of the superbubble.

Hence, the emission from 4U2129 + 47 during the time of the observation accounted for 6 to 7% of that from the superbubble.

Other X-ray sources in the Cygnus region. In view of the lack of detailed spectral data and values of A_V to other sources listed in the catalogue of Amnuel *et al.* (1982), we made a rough estimation of their possible contribution of the superbubble emission assuming that the spectral flux density from them in the range of 0.2 to 3 keV is the same as in the range of 2 to 6 keV. Mean spectral flux densities were used for variable sources. The estimate achieved in this manner gives an overall spectral flux density value of $F_\nu \approx 150$ μJy for 17 faint discrete X-ray sources from the above-mentioned catalogue (with the exception of EY Cyg and 4U2129 + 47). This corresponds to a flux $F_x(0.5\text{–}1\ \text{keV}) \approx 1.9 \times 10^{-10}\ \text{erg cm}^{-2}\ \text{s}^{-1}$ (15% of the emission from the superbubble). This estimate is rather approximate because in some cases the source spectra may feature downward slopes in the range of energies less than 3 keV. In others, upward slopes in the soft range may occur. For example, the very faint source 19197 + 436 located near the superbubble region but beyond its boundaries and exhibiting, in the range of 2 to 6 keV, mean spectral density $F_\nu \approx 8$ μJy (Amnuel *et al.*, 1982) appears in the right-hand side of Figure 1 as a distinct spot so that its spectrum, at least, does not fall-off toward the soft region.

Stellar coronae. X-rays are also emitted in the range of 1 keV by bright stars (Harnden

TABLE VII

Known soft X-ray sources in Cygnus region

Source	α_{1950}	δ_{1950}	Type of source	Observation range (keV)	X-ray flux (erg cm^{-2} s^{-1})	Reference
G 65.2 + 5.7[a]	19^h31^m	31°10′	SNR			
G 74.9 + 1.2	19^h45^m	40°00′	SNR	0.15–3	$(0.74–0.86) \times 10^{-12}$	Wilson (1980)
EY Cyg	$19^h54^m02^s$	31°57′25″	S	0.48–2.8	1.3×10^{-10}	Cordova *et al.* (1981)
Cyg X-1[a]	$19^h56^m28.8^s$	35°03′54.5″	S			
Cyg X-7 (G 78.2 + 2.1, DR4)	20^h20^m	40°30′	SNR	0.15–4.2	2.4×10^{-10}	Higgs *et al.* (1983); Davidsen *et al.* (1977)
HB21	20^h43^m	50°30′	SNR	0.5–1.5	$\leq 4.1 \times 10^{-11}$	Davidsen *et al.* (1977)
Cyg Loop[a]	$20^h49^m45^s$	30°53′	SNR			
V751 Cyg	20^h49^m	43°57′	S	0.48–2.8	1.2×10^{-11}	Cordova *et al.* (1981)
Cyg X-6	21^h20^m	45°00′		0.5–2.0	4×10^{-10}	Davidsen *et al.* (1977)
4U2129 + 47	$21^h29^m34^s$	47°04′25″	S		8.5×10^{-11}	Thorstensen *et al.* (1979)
SS Cyg	$21^h40^m42.6^s$	43°21′51″	S	0.18–0.48	$\sim 1 \times 10^{-11}$	Cordova *et al.* (1981)
				0.48–2.8	$\lesssim 7.8 \times 10^{-11}$	Cordova *et al.* (1981)
Cyg X-2[a]	$21^h42^m36.91^s$	38°05′27.9″	S			
Cyg superbubble	0^h30^m	40°		0.1–3	1.3×10^{-9}	Cash *et al.* (1980)

[a] The X-ray emission from these sources was excluded by Cash *et al.* (1980) when the superbubble parameters were determined.
SNR, supernova remnant; S, star.

et al., 1979; Seward *et al.*, 1979; Long and White, 1980; Vaiana *et al.*, 1981). Emission from the brightest stars of the Cyg OB2 association including four Main-Sequence O-stars and a B5-supergiant was discovered at the *Einstein* Observatory (Harnden *et al.*, 1979). Subsequent analysis has shown that all OB-supergiants and Of stars seem to be sources of emission in the range of 1 keV with luminosity $L_x \gtrsim 10^{32}$ erg s^{-1} (Vaiana *et al.*, 1981; Cassinelli *et al.*, 1981). In the case of supergiants belonging to classes earlier than B1, L_x is about $10^{-7.2}$ of the bolometric luminosity (Cassinelli *et al.*, 1981). Evidently, all Main-Sequence O-stars also emit a lot of X-rays in the range of 1 keV (Vaiana *et al.*, 1981). However, in spite of the large number of such stars in the region of interest (Section 5.4), it is most unlikely that their coronae may account for more than 1% of the emission from the superbubble.

Thus, faint point X-ray sources account for 30 to 50% of the superbubble emission. The basic parameters of the above-described X-ray sources in the Cygnus region are given in Table VII.

7.5. Bright nebulae associated with stellar winds

The Cygnus region contains two bright nebulae S119 and NGC 6888 which were formed by the stellar winds and have been closely studied in the optical range. Theory predicts soft X-ray emission from such nebulae.

However, because no X-ray observations of these nebulae have been reported in the literature, one has to confine oneself to estimating X-ray emission parameters. Such

TABLE VIII

Basic parameters of the bright nebulae formed by stellar wind

Parameter	S119	NGC 6888
Exciting star	68 Cyg (HD 203064)	HD 192163
Spectral class of the star	O6f	WN6 (Willis and Wilson, 1978)
Angular dimension of the nebula	1°.4	15′ × 20′
Distance (kpc)	0.7 (Savage and Jenkins, 1972)	1.5–2.3 (Lozinskaya, 1980c)
Radius of the nebula (pc)	17	4 × 6
Expansion velocity (km s^{-1})	≤ 15 (filaments) (Esipov *et al.*, 1983)	110–120[a] (Lozinskaya, 1980c)
Column density N_H (cm^{-2})	1.5 × 10^{21} (Savage and Jenkins, 1972)	≈ 4 × 10^{21} (from A_V, Willis and Wilson, 1978)
Surrounding gas number density n (cm^{-3})	1–2 (Bochkarev and Lozinskaya, 1985)	1–2 (Lozinskaya, 1980c)
Emission flux density F_x ($E > 0.18$ keV) (erg cm^{-2} s^{-1})	≈ 1 × 10^{-11} (Bochkarev and Lozinskaya, 1985)	(1–2) × 10^{-11} (Bochkarev and Lozinskaya, 1985)
Stellar wind power L_w (erg s^{-1})	14 × 10^{36} (Kumar *et al.*, 1983)	30 × 10^{36} (Barlow *et al.*, 1981)

[a] Determined from the dispersion of velocities of the diffuse gas of the nebula.

estimations involving nebulae S119 and NGC 6888 were carried out by Bochkarev and Lozinskaya (1984). Table VIII summarizes the main results of observations of these nebulae and the X-ray emission parameters estimated from such observations. The flux emanating from NGC 6888 was estimated to be $F_x = (1\text{–}2) \times 10^{-11}$ erg cm^{-2} s^{-1} (0.8–1.5% of the superbubble emission).

The surface brightness in the soft X-range of nebula S119, which has angular dimensions greater than the beam of the detector used by Cash *et al.* (1980) (area of about 6 square degrees), is expected to equal approximately 0.3 of the average surface brightness of the superbubble ($F_x = 10^{-11}$ erg cm^{-2} s^{-1}; i.e., 0.8% of the emission from the superbubble) (Bochkarev and Lozinskaya, 1984). Thus, S119 may be responsible for part of the emission from the north-eastern part of the superbubble. Comparison of the distribution of optical (Figure 6) and X-ray (Figure 1) emission over the sky indicates that a small sector in the north-eastern part of the superbubble correlates well with the position of the bright filaments of nebula S119.

The spectra of these two nebulae, predicted by Bochkarev and Lozinskaya (1984), are similar to the superbubble spectrum observed by Cash *et al.* (1980).

7.6. Summary

As can be inferred from this section, the Cygnus superbubble region contains many discrete X-ray sources of various characteristics which make a great contribution to the soft X-ray flux (~ 1 keV) emergent from the superbubble. The basic parameters of the X-ray sources observed in the superbubble region are listed in Table VII. The largest contribution to the emission from the superbubble is made by supernova remnants and some dwarf binary systems.

As can be seen from Figure 13, the arrangement of discrete X-ray sources fits into the superbubble shape. This corroborates our earlier assumption that the superbubble is a result of projection of sources lying at different distances from the Sun on the sky. The absence of objects in the central part must be a consequence of the strong interstellar absorption of X-rays in the Great Rift.

Additional evidence supporting the discrete nature of the superbubble is provided by the irregular intensity and spectrum of its emission discussed in Section 7.1., as well as by the results reported by Cordova *et al.* (1981) who identified several superbubble parts with cataclysmic variables on the basis of the same observational data used by Cash *et al.* (1980) (see Section 7.4: point sources SS Cyg, EY Cyg, and V751 Cyg).

The total flux of soft X-rays from the above-discussed sources is about half that of emission from the superbubble (Bochkarev and Sitnik, 1983). About 30 to 50% of the observed flux is produced by faint point sources (Section 7.4), 15 to 20% by supernova remnants (Sectin 7.3), and approximately 2%, by the nebulae formed by stellar winds (Section 7.5).

Because of interstellar absorption, most of these objects are sources of relatively soft X-ray emission with low-frequency cut-offs in their spectra, in the range of hundreds of electron-volts. This makes their spectra similar to one another and to that of the

superbubble as a whole, although some differences of the sorts discussed in Section 7.1 must certainly occur.

To specify more accurately how much the discrete sources contribute to the emission from the superbubble requires more detailed observations of the X-rays from this region with a better angular resolution and an adequate sensitivity in the range of 0.5 to 1 keV.

Significantly, however, the known X-ray sources to not explain the entire emission from the superbubble, and about one half do one quarter of the observed flux must be of a different origin.

In the next section we shall discuss the nature of the remaining part of the X-ray emission from the superbubble.

8. Origin of the Diffuse X-Ray Emission from the Superbubble

We shall discuss here that part of the soft X-ray emission (25–50%) which cannot be ascribed to a combination of discrete sources (see Section 7).

8.1. Hot gas-filled caverns around stellar associations

The good excitation between the X-ray emission from the superbubble and the position of extended optical objects, such as stellar associations and gas filaments, especially in the western part of the region under consideration (Figures 8 and 13), suggests that soft X-rays may also be emitted from such sources in the superbubble (in addition to those described in Section 7) as the rarefied hot gas of the vast caverns observed in the stellar associations of Cygnus.

The gas filaments in the western part of the region form a cellular structure (Figures 6 and 7), as mentioned in Section 5.2. These cells, ranging in size from 2 to 4°, seem to be shells around young stellar associations. The most typical shell is the emission nebula Cyg 1 surrounding the Cyg OB1 association (Table IV; Figures 6 and 7). The shape of the nebula and the presence of at least nine stars with strong stellar winds in the association suggest that the ring structure Cyg 1 is a cavern blow out by the stellar wind and surrounded by emitting shell. In the case of other associations, the shells are not so clearly defined. Brand and Zealey (1975) distinguished bubbles around associations Cyg OB3 and Cyg OB9 (Table IV). A bubble is likely to surround association Cyg OB8 as well (Figures 6 and 8). There also may be a shell associated with Cyg OB2, although as was mentioned in Section 5.2, it does not have to coincide with the entire Cyg 4 structure or the ring of optical filaments shown in Figure 2.

Thus, the Cygnus region seems to contain at least four giant H II shells enveloping young stellar associations. The caverns inside these shells may be formed both by supernova explosions and by the stellar wind. (In Sections 7.3 and 7.5, we discussed the contribution of known supernova remnants and nebulae formed by the stellar wind around individual stars to the X-ray emission from the superbubble.)

The bubbles formed around individual stars in the central parts of young, sufficiently dense OB-associations soon coalesce to form a single object. Approximately the same takes place with supernova remnants in the interstellar medium (Cox and Smith, 1974).

As a result, a vast cavern is formed around the associations as a whole (Weaver, 1979; Bruhweiler *et al.*, 1980). In the general case, its formation is due both to the stellar wind and to supernova explosions.

The Cygnus region contains eight young OB associations. Let us assume that the hot gas caverns around the associations, confined by the above-mentioned emission ring nebulae, are responsible for the remaining (unrelated to the known X-ray sources) 25 to 50% of the emission from the superbubble. Then, the total X-ray luminosity of these caverns is $(1–3) \times 10^{36}$ erg s^{-1} at a distance of 2 kpc. Each of the eight associations, most of which are 1.3 to 2 kpc distant (see Table V), accounts for about $(1–4) \times 10^{35}$ erg s^{-1} of soft X-rays.

This estimate, however, is rather uncertain. The main uncertainty results from the difficulties arising in correction of the observed flux for the interstellar absorption of the X-rays. At a gas temperature of about 2×10^6 K, only a small part of the energy emitted in the range 0.5 to 1 keV because of exponential slope of the spectrum toward high frequencies. Cash *et al.* (1980) compared the results of their measurements with the spectrum of the isothermal optically thin plasma distorted by absorption. However, in the expanding bubbles, such as supernova remnants and nebulae blown out by the stellar wind, the plasma is non-isothermal (Pikel'ner, 1954; Cox, 1972; Pikel'ner and Shcheglov, 1968; Castor *et al.*, 1975; Weaver *et al.*, 1977).

The structure of the nebula formed by the stellar wind is such that the central parts of the slowed down stellar wind (region '*b*' according to Castor *et al.* (1975), that is, immediately behind the front of the internal shock wave) contain the most rarefied and hottest gas. The temperature and density distributions toward the edge of the nebula are determined by the electron conduction and almost constant pressures in all layers so that the density drops while the temperature rises to the center. The emission measure of the gas at a given temperature T in the nebula increases with decreasing T (Castor *et al.*, 1975). Therefore, the emission spectrum is steeper (with a more pronounced upward slope into the soft X-ray region) than for isothermal gas, so the factor of conversion to convert the value of the observed flux into the total flux must be greater than that used by Cash *et al.* (1980) (see, e.g., Bochkarev, 1984b).

Another indication that the spectrum of the superbubble is softer than that of isothermal plasma can be found in the low-energy part of the X-ray spectrum observed by Cash *et al.* (1980). The slope of the spectrum found by Cash *et al.* (1980) is much less steep than the slope of an isothermal plasma spectrum. The discrepancy between the model spectrum computed by Cash *et al.* (1980) and the observed one increases with decreasing photon energy. However, for a more reliable quantitative estimate of the factor to convert the observed flux into total flux it is desireable to repeat the deconvolution procedure performed by Cash *et al.* (1980) and to compare the result with synthetic spectra of non-isothermal plasmas.

An accurate account of the non-isothermal nature of the nebula may significantly change (increase) the estimated value of its flux E_x, hence, of its luminosity L_x. We took into account Bochkarev's (1984b) numerical results of the detailed calculations of the X-ray spectrum of gaseous caverns blown by stellar winds. He used the density and

temperature distributions for the model of a gaseous cavern (Castor *et al.*, 1975) and spectrum for optically thin rarefied plasma, by Raymond and Smith (1977), i.e., the same model spectrum as Cash *et al.* (1980). Bochkarev (1984b) has taken into account the interstellar absorption determined by Ride and Walker (1977) (Model A). Using Bochkarev's (1984b) results we found that in the case of a bubble having central temperature $T_c = 2.5 \times 10^6$ K and column density $\log N_H = 21.85$ (that is, at parameters corresponding to the observations made by Cash *et al.* (1980), only $\frac{1}{90}$ of the emission in the photon-energy range $E > 280$ eV reaches the observer. At lower T_c, even a smaller part of the emission reaches to observer. Cash *et al.* (1980) took the spectrum reduction factor equal to 7.7. Thus, they may underestimate the luminosity of the superbubble by more than an order of magnitude.

Let us now consider what conditions may be formed a cavern with the observed characteristics around a stellar association.

8.2. Conditions of formation of hot caverns responsible for the diffuse X-ray emission from the superbubble

The parameters of the stellar wind emanating from individual stars vary in the course of their evolution, increasing considerably at the supergiant and, especially, Wolf–Rayet star stages. Moreover, within an association the number of stars that have powerful stellar winds decreases at the evolution of the most massive stars is about to end. The interstellar medium in which the cavern develops is not homogeneous. Yet, for rough estimations, it seems to be sufficient to use the solutions by Avedisova (1971), Castor *et al.* (1975), and Weaver *et al.* (1977) for a snowplow stage in which the nebular matter flows into a homogeneous medium. Supernova explosions occur from time to time in associations with age $t \gtrsim 2 \times 10^6$ yr (i.e., associations in which the most massive stars have already passed through all evolutionary stages) may also produce pronounced homogeneities in the flow of matter. Let us assume, according to Bruhweiler *et al.* (1980), that supernova explosions do not radically alter the structure of the nebula produced by continuous stellar winds. In that case we shall use the solutions offered by Castor *et al.* (1975) and Weaver *et al.* (1977).

The observed cavern characteristics include X-ray luminosity L_x, emitting gas temperature T, and cavern dimensions. By resorting to the self-consistent solutions by Castor *et al.* (1975) and Weaver *et al.* (1977) and the observed Cavern parameters, one can easily derive the stellar wind power (L_w), its duration (t), density of undisturbed interstellar gas (n_0), and that of the gas in the center of region 'b' of the cavern (n_c):

$$
\begin{aligned}
L_w &= 10^{36}\left(\frac{R}{33.7\ \mathrm{pc}}\right)\left(\frac{T_c}{2\times 10^6\ \mathrm{K}}\right)^{7/2}\ \mathrm{erg\ s^{-1}}\,,\\
t &= 10^6\left(\frac{R}{33.7\ \mathrm{pc}}\right)^{1/2}\left(\frac{T_c}{2\times 10^6\ \mathrm{K}}\right)^{-11/4}\left(\frac{L_x}{k\times 10^{34}\ \mathrm{erg\ s^{-1}}}\right)^{1/2}\ \mathrm{yr}\,,\\
n_0 &= \left(\frac{R}{33.7\ \mathrm{pc}}\right)^{-5/2}\left(\frac{T_c}{2\times 10^6\ \mathrm{K}}\right)^{-19/4}\left(\frac{L_x}{k\times 10^{34}\ \mathrm{erg\ s^{-1}}}\right)^{3/2}\ \mathrm{cm^{-3}}\,,\\
n_c &= 0.012\left(\frac{R}{33.7\ \mathrm{pc}}\right)^{-3/2}\left(\frac{T_c}{2\times 10^6\ \mathrm{K}}\right)^{-1/4}\left(\frac{L_x}{k\times 10^{34}\ \mathrm{erg\ s^{-1}}}\right)^{1/2}\ \mathrm{cm^{-3}}\,.
\end{aligned}
\qquad (1)
$$

Here, R is the radius of the external shock wave, determined by the size of the observed giant bubble, T_c is the temperature (in the center of the nebula in the '*b*' region according to Castor *et al.*, 1975), and L_x is the X-ray luminosity of the nebula. We have introduced the coefficient k into the above formulae, equal to the ratio between the total luminosity of the nebula and its luminosity due to the free-free emission for which Castor *et al.* (1975) made appropriate calculations. In general, the coefficient k depends on temperature, which will slightly alter the temperature dependences derived by Avedisova (1971), Castor *et al.* (1975), and Weaver *et al.* (1977). To take the temperature dependence of $k(T)$ into account calls for numerical calculations. However, as can be inferred from the calculations by Tucker and Blumenthal (1974), it is appropriate to take $k = 4.3$: over the temperature region of interest, k is essentially independent of T.

In the subsequent calculations of the X-ray luminosity we shall use the value $L_x = 4 \times 10^{35}$ erg s^{-1}. As was pointed out at the end of Section 8.1, L_x may have been markedly underestimated by Cash *et al.* (1980). This is why the value of L_x adopted here should be regarded primarily as the lower cavern luminosity limit. Let us take radius $R = 50$ pc as a typical dimension of the cavern, which is close to the average dimension of the emission shell discovered by Brand and Zealey (1975) around associations Cyg OB1 (see Section 5.2).

The gas temperature derived by Cash *et al.* (1980) equals (1.6–2.5) $\times 10^6$ K. This is an effective value averaged throughout the volume of the emitting region. As was indicated in Section 8.1, the structure of a nebula formed by flow of matter is such that, when the emission from the nebula is approximated by the spectrum of optically thin isothermal gas, as was done by Cash *et al.* (1980), the derived effective temperature is slightly below T_c (see, also Bochkarev, 1984b). Thus, the temperature determined by Cash *et al.* (1980) is a lower limit of the temperature T_c in the center of the cavern, which is incorporated into the expressions of Castor *et al.* (1975) and Weaver *et al.* (1977). Yet, the true value of T_c cannot be much higher than the observed average, since only the harder portion of the emission from the cavern can be observed. The major contribution to this emission is made by the central region, which is the most rarefied and the hottest.

As can be seen from (1), all parameters except n_c depend strongly on T_c. To obtain reliable values of the nebular parameters one must compare the observed X-ray spectrum of the Cygnus superbubble with a spectrum integrated in terms of density and temperature distributions in the gas in the interior of the bubble formed by the stellar wind. However, formulae (1) are quite sufficient for the estimates. We carried out our estimates for two values $T_c = 2 \times 10^6$ K and 2.5×10^6 K from Equations (1). For the first case ($T_c = 2 \times 10^6$ K):

$$L_w \approx 1.5 \times 10^{36} \text{ erg s}^{-1},$$

$$t \approx 3 \times 10^6 \left(\frac{L_x}{4 \times 10^{35} \text{ erg s}^{-1}} \right)^{1/2} \text{yr}, \tag{2}$$

$$n_0 \approx 11 \left(\frac{L_x}{4 \times 10^{35} \text{ erg s}^{-1}} \right)^{3/2} \text{cm}^{-3},$$

and for the second ($T_c = 2.5 \times 10^6$ K):

$$L_w \approx 3.3 \times 10^{36} \text{ erg s}^{-1},$$
$$t \approx 2 \times 10^6 \left(\frac{L_x}{4 \times 10^{35} \text{ erg s}^{-1}} \right)^{1/2} \text{yr}, \tag{3}$$
$$n_0 \approx 4 \left(\frac{L_x}{4 \times 10^{35} \text{ erg s}^{-1}} \right)^{3/2} \text{cm}^{-3}.$$

Since the adopted value of L_x should be regarded as the lower limit (see above) while the actual values may be several times higher, the value of n_0 may be well above 4–11 cm^{-3}.

The mass of the bubble formed by the interstellar gas driven from a sphere 50 pc in radius is equal, at the surrounding interstellar medium densities according to (2)

$$M \sim (3\text{–}9) \times 10^4 \left(\frac{L_x}{4 \times 10^{35} \text{ erg s}^{-1}} \right)^{3/2} M_\odot .$$

At $L_x = 4 \times 10^{35}$–4×10^{36} erg s^{-1}, the computed mass corresponds to the average parameters of giant molecular clouds (Scoville and Solomon, 1975). Hence, it may be assumed that the association are generated in a giant molecular cloud and that the wind produced by the stars shaped the molecular cloud from which they formed into a shell.

The velocity of expansion of a typical bubble formed by the stellar wind with the parameters (2) and (3) equals 7 to 10 km s^{-1}, which agrees well with the low velocity values in the region of the sky investigated (see Table III).

Estimates of the bubble age, derived from (2) and (3), are close to the lifetime of the most massive stars in the associations of the constellation Cygnus (see Table V). Thus, a cavern about 100 pc in diameter, heated to $T_c \sim (2\text{–}2.5) \times 10^6$ K, and exhibiting X-ray luminosity $L_x \gtrsim 4 \times 10^{35}$ erg s^{-1} might have been formed over a period of several million years in the interstellar medium with density $(4\text{–}10) \times (L_x/4 \times 10^{35} \text{ erg s}^{-1})^{3/2}$ cm^{-3} under the influence of a stellar wind with a power of several units times 10^{36} erg s^{-1}. A combination of such caverns may explain the 'background' emission from the superbubble.

It is quite possible that the caverns are formed in collapsing rather than quiescent clouds. Dopita *et al.* (1981) studied the superbubble N70 in the Large Magellanic Cloud, ranging from 110 to 120 in diameter, and demonstrated that the best agreement between observations in different spectral range is achieved in a model in which the cavern is blown out by the stellar wind produced by an OB-association in a collapsing cloud.

Although the parameters of the stellar associations and the bubbles they create may differ one case to another, the X-ray spectra of the hot gas caverns created by them may be similar because the only parameter determining the shape of the emission spectrum is T_c (see Castor *et al.*, 1975; Weaver *et al.*, 1977), it is only weakly dependent on L_w, t, and n_0. An increase in N_H as compared to the average for the superbubble region at fixed T_c, will lead to an exponential attenuation of the emission from the corresponding

association, whereas a decrease in N_H will shift the maximum toward lower photon energies but very slowly by the law $(T_c \times N_H)^{1/4}$. That is, in the case of N_H varying toward less than average values, possibly occurring in Cygnus associations (see Sections 5.3 and 5.5), the position of the maximum must shift insignificantly from one association to another.

8.3. The Role of the Stellar Wind in Cavern Formation

According to Equations (1) stellar wind power L_w, which is sufficient to create the above-described caverns is independent of the adopted value of L_x and is determined only by the size of the cavern and the gas temperature in its center. According to Equations (2) and (3), the average stellar wind power in the cavern must be maintained at $L_w \approx (1.5\text{–}4) \times 10^{36}\ erg\ s^{-1}$ over a period of several million years, and at an even higher value if $T_c > 2.5 \times 10^6$ K. The question whether the stellar wind power in an association may be maintained at such a level as long as two or three million years is currently being debated.

Abbott *et al.* (1981) found the total stellar wind power of the five brightest Cyg OB2 stars $L_w \approx 10^{38}$ erg s^{-1}; they proposed that L_w has been constant at that high value over a period of two million years. However, the association Cyg OB2 is not typical in many respects (see Section 5.3); it contains, for example, several superluminous stars. Yet, the stellar wind power specified by Abbott *et al.* (1981) could hardly have been maintained at the high value observed for 2×10^6 yr. Almost all L_w is currently being sustained in Cyg OB2 by the five supergiants. They are extremely high-mass stars in the range $(60\text{–}120)M_\odot$ (de Jager, 1980). Before they became supergiants, the luminosity of the association was much lower since stars occupying the supergiant branch were absent. In view of the close relationship between L_w and stellar luminosity (see, for example, Abbott *et al.*, 1981), the lower luminosity also means a lower stellar wind power.

According to Johnson (1980), who investigated stars of high luminosity in symmetrical nebulae, the power of the wind from bright stars can be maintained over an extended period of time only at the level $L_w \sim 10^{35}$ erg s^{-1}. This estimate, however, may be somewhat low if part of the stellar wind breaks through between nebular filaments so that the velocities of the filaments, just as in the case of supernova remnants, do not represent that of the shock front (Bochkarev and Lozinskaya, 1985).

L_w might have been maintained at a permanently high level in Cyg OB2 only if the high-mass stars had formed at times that deferred by about 2×10^6 yr, corresponding to the age of the association. This, however, is not likely in such a dense association as Cyg OB2 (see Section 5.3) because the appearance of the first hot stars excludes forming new massive stars in the close environment before the first generation of massive stars has completed its evolution – that is, within a period of about 10^7 yr.

The history of variations in $L_w(t)$ in an association is determined primarily by the evolution of the most massive stars. If the most massive stars were not components of binary systems which remained bound after the evolution of one of the components was over, we cannot establish from observations whether such stars have been in the

association, because they do not leave any observable remnants. This problem is further aggravated by the uncertainty and the non-universality of the initial mass function (Freeman, 1977; Zasov and Demin, 1979), especially in the range of stas with the highest mass, as well as by the small number of stars in individual associations, which must result in a wide statistical spread of the parameters of the brightest stars even at a fixed mass function.

Thus, although it seems impossible to reconstruct the evolution of an association (consequently, impossible to know the mean value of L_w throughout the evolution) without resorting to the data on the gaseous cavern around it, it still appears unlikely that any association could maintain L_w at a level above 10^{36} erg s^{-1} over a period of several million years. To reverse the situation requires the presence of stars with extremely high masses in all associations, which seems improvable particularly in poor associations.

A major contribution to the mean value of L_w may be made by the stellar wind from Wolf–Rayet stars (see below, Section 8.5). However, in view of the fact that the Wolf–Rayet phase lasts only about 10^5 yr (see, for example, Massevich and Tutukov, 1981; Yungel'son and Massevich, 1983) – that is, a period of time much shorter than the lifetime of the association – such an energy influx is essentially instantaneous and must have the same consequences as explosions of supernovae whose role will now be discussed.

8.4. Supernova remnants in hot caverns

The most massive stars of an association in the end of their evolution must explode as supernovae. The propogation of the shock wave initiated by this explosion within the hot cavern has several peculiarities.

In the rarefied gas heated by the stellar wind, the shock wave formed by the supernova completes its existence at the adiabatic stage of the evolution because the wave is no longer supersonic, when the temperature of the gas in SNR shock front drops to the temperature of the cavern gas (i.e., several million degrees). Furthermore, the undisturbed gas had already been strongly ionized. Therefore, the supernova remnant is faint in emission lines, which reduces its energy output.

Electrons in the cavern ahead of the shock are preheated to $T \approx 2 \times 10^6$ K. Most of the supernova remnant energy is radiated at the end of the evolution, when the volume of the remnant is maximal and the temperature is close to that ahead of the shock. In calculating the radiative losses one might not reasonably assume the equality of electron and ion temperatures throughout the evolution of the supernova. In this case, in an approximation of a strong shock wave with a compression by the factor of 4, the emitting gas may be considered as concentrated within a spherical layer having a volume equal to one quarter of the entire nebula. $V \approx 0.25(4\pi/3)R^3$. Then, as follows from the Sedov self-consistent solution for the adiabatic stage of the shell evolution, the total radiation loss up to the moment t is

$$E = 4.4 \times 10^{46}\, k \left(\frac{t}{10^3 \text{ yr}}\right)^{8/5} \left(\frac{\varepsilon}{0.75 \times 10^{51} \text{ erg}}\right)^{4/5} \left(\frac{n_0}{1 \text{ cm}^{-3}}\right)^{6/5} \text{erg}\,, \qquad (4)$$

where ε is the kinetic energy of the SNR, n_0 is the number density of the gas in which the shock wave propagates, and k is the same coefficient as in (1). The maximum age of the SNR derived from the equality of the velocities of the shock wave and the thermal motions in the gas, is

$$t_{\max} = 70 \times 10^3 \left(\frac{\varepsilon}{0.75 \times 10^{51}\ \text{erg}}\right)^{1/3} \left(\frac{n}{1\ \text{cm}^{-3}}\right)^{-1/3} \left(\frac{T}{10^6\ \text{K}}\right)^{-5/6} \text{yr},$$

which gives, at the same parameters as in (2) and a typical SNR energy $\varepsilon = 10^{50.5}$ erg s^{-1} (Lozinskaya, 1980a, b), $t_{\max} \approx 10^5$ yr and $E \lesssim 0.01\varepsilon$. These estimates suggest that we are dealing with the upper limit of the amount of energy expended in radiation. That is instead of the usual situation in the interstellar medium (Spitzer, 1978), the supernova remnant really ceases to exist inside the hot cavern at the adiabatic stage of the evolution and transfers almost all of its kinetic energy into the bubble expanding under the influence of the stellar wind and thereby pushes the bubble. At the end of the supernova remnant evolution in a cavern its radius approaches 50 pc, according to Cox (1972).

The supernova remnant inside the cavern may not be observable in the optical range because the shock propagates in a low-density gas already preheated to about 10^6 K and ionized. The density inside cavern is determined from (1) and is equal to about 0.02–0.03 cm^{-3} in the cavern center and about 0.1 cm^{-3} behind the supernova shock front. Its emission measure is much lower than 1 pc cm^{-6}. Since the shock wave quickly traverses the rarefied gas, the supernova remnant is most likely to become observable at the period of interaction with the bubble structure.

The radio-emission from the supernova remnants in the caverns of the Cygnus region has several interesting features. In view of the large sizes of the caverns, the surface radio brightness of the supernova remnants is low, and they must be observed on the background of the thermal radio-emission from the numerous H II regions in Cygnus. This is probably why we do not see large-scale nonthermal ring radio sources around associations in Cygnus. The North-Polar Spur is a rare example of a supernova remnant visible in radio and X-ray emissions from inside the hot gas probably blown out by the old Sco-Cen association (Weaver, 1979).

At the end of its evolution, a supernova remnant transmits the kinetic energy of the supernova explosion to the shock front of the expanding cavern. Let us assume that several supernova explosions have taken place throughout the evolution of an association. Then, such an additional source of kinetic energy may be regarded as continuously distributed in time. It may also be assumed that the cavern structure remains the same as in the case of the stellar wind alone (Bruhweiler *et al.*, 1980). L_w must represent the total strength of the stellar wind from the association plus the average amount of kinetic energy supplied by supernova explosions.

It is impossible to determine exactly the relative contributions of the stellar wind and supernova explosions to the transmission of the impulse and energy from stellar associations into the interstellar medium because of uncertainties of the number of the most massive stars originating in the associations (Section 8.3). Thus, the frequency of

supernova explosions in stellar associations remains uncertain. The kinetic energy of the explosion of the most massive stars ε is also very uncertain.

The transfer of kinetic energy from supernova explosions into the interstellar medium, averaged over the Galaxy, is greater than a similar transfer from stellar winds by about one order of magnitude (Salpeter, 1979). However, in stellar associations this ratio must be lower because in an association the relative number of stars producing powerful stellar winds normally far exceeds that of such stars in the Galaxy as a whole. (The stellar wind power increases sharply with stellar luminosity, while, at the same time, supernovae of type I are absent in associations.) The contributions of energy from supernova explosions and from stellar winds to the formation of giant shells and hot gas caverns around associations seem to be approximately the same.

If the energy of a supernova explosion is $\varepsilon = 10^{50.5}$ erg (value derived from the data on many optically observed supernova remnants (Lozinskaya, 1980a, b)), then a single supernova explosion in an association over a period of 3×10^6 yr corresponds to an average $L_w = 3 \times 10^{36}$ erg s^{-1}. In other words, it could have provided all the energy necessary to form a cavern. During evolution of most associations listed in Table V, several supernovae must have been exploded in each. Yet the most prominent giant loop structures Cyg 1, 2, and 3 (see Table IV) surrounding stellar associations in Cygnus definitely are not supernova remnants because no nonthermal emission is produced by them. If the proposed interpretation of the diffuse component of X-ray emission from the Cygnus superbubble is valid, this implies that the explosion of massive stars adds much less energy to the kinetic energy of the shell than was found by Lozinskaya (1980) for an average supernova remnant. It is most likely that $\varepsilon \sim 10^{49}$ erg s^{-1}. If ε is much smaller, the contribution of supernova to cavern formation will be insignificant.

8.5. The Role of Wolf–Rayet Stars in Cavern Formation

Wolf–Rayet stars, just a supernova explosions, are capable of injection a great amount of kinetic energy within a short period of time into an expanding cavern. For example, at stellar wind strength $L_w = (1\text{–}5) \times 10^{37}$ erg s^{-1}, such as is produced by star HD 192 163 in the center of NGC 6888 (discussed in Section 7.5: see Table VIII; Bochkarev and Lozinskaya, 1985), or by star V444 Cyg discussed in details by Cherepashchuk (1982). During the Wolf–Rayet stage, which lasts about 10^5 yr (Massevich and Tutukov, 1981; Yungel'son and Massevich, 1983), a star produces about 10^{50} ergs of energy, which exceeds the total stellar wind energy of an ordinary massive star during its lifetime, and is only half an order lower than the kinetic energy of an average supernova (Lozinskaya, 1980a, b). The nebula around a Wolf–Rayet star with such an energy output (if it is formed inside a cavern) may escape observation for the same reasons that supernova remnants inside hot caverns are invisible (Section 8.4). However, if inhomogeneities exist in the coronal gas of the initial cavern, the increasing stellar wind will compress them, as is the case, for instance, with planetary nebulae (Pikel'ner, 1973). If the resulting filaments become sufficiently dense (≥ 10 cm^{-3}) and the radiation cooling time, becomes shorter than the lifetime of the nebula ($\sim 10^5$ yr), they will be

compressed, in the process of cooling to $T \approx 10^4$ K, to densities of hundreds cm^{-3} and form an optically visible nebula.

Johnson's (1980) analysis of his observations of the nebulae around Wolf–Rayet stars indicates that in some cases the wind power from Wolf–Rayet stars does not exceed 10^{36} erg s^{-1}. However, in Section 8.3 we point out that Johnson's (1980) estimates may be too low. If the difference is real, it may be understood in terms of the evolution of close binaries (see, for example, Massevich and Tutukov, 1981; Yungel'son and Massevich, 1983). The Wolf–Rayet phase may involve a single star or a star paires with an ordinary star, or binaries containing relativistic companions. The low-mass companions of Wolf–Rayet stars are, in some cases, already been found (see, for example, Antokhin *et al.*, 1982). The maximum wind power seems to be associated with the presence of a close relativistic companion of such stars.

According to the evolutionary schemes for close binaries with massive components, the number of Wolf–Rayet stars with relativistic companions must be somewhat greater than the number without such companions, hence, most Wolf–Rayet stars may produce very strong stellar winds. Thus, in addition to supernovae, Wolf–Rayet stars may serve as sources of energy for hot gas caverns. The total energy available to the cavern from a Wolf–Rayet star is comparable to that of the other energy sources described above in Sections 8.3 and 8.4.

8.6. Summary

We associate the diffuse component of soft X-ray emission from the superbubble (about 25–50% of the total flux described by Cash *et al.* (1980) and not attributable to discrete sources (Section 7)) with the emission of the hot ($T \approx 2 \times 10^6$ K) and rarefied ($n \approx 0.03$ cm^{-3}) gas in the caverns formed around stellar associations by combined action of the stellar wind and supernova explosion. The region of interest contains eight stellar associations distributed on the sky in approximately the horseshoe shape of the superbubble (Figures 1 and 13). The hot-gas caverns are confined by loop-shaped emission nebulae described by Brand and Zealey (1975) and having the form of giant shells. As regards Cyg OB2, we assume that the bubble does not coincide with the system of filaments referred to as Cyg 4 (Section 5.2). The typical radius of a giant shell surrounding a hot cavern is about 50 pc. Their soft X-ray luminosity is $L_x \gtrsim (1\text{–}4) \times 10^{35}$ erg s^{-1} (Section 8.1).

Such caverns can be formed by stellar wind with the average power $L_w > (1.5\text{–}4) \times 10^{36}$ erg s^{-1}, maintained in the stellar association for a period of two to five million years. This particular power level is maintained both by the Main-Sequence stars and supergiants (Section 8.3) and by supernova explosions (Section 8.4) as well as a strong wind produced by Wolf–Rayet stars (Section 8.5). The contributions of all these three types of sources to L_w are approximately equal.

The shell formed in a cavern by a supernova does not produce an optically bright nebula. Its emission measure seems to be less than 1 pc cm^{-6} (Section 8.4). The supernova shell expands rapidly and has not time to radiate its kinetic energy before it becomes as big as the cavern and transmits its kinetic energy to the shock wave

confining the cavern. In the Cygnus region, the radio-emission from such supernovae is likely to be lost against the background of the thermal radio-emission from numerous H II regions in the same region. The kinetic energy of the shell formed by the explosion of a massive star appears to be much lower than the average for supernova remnants and may be approximately 10^{49} erg (Section 8.4).

The same conclusions related to the difficulty of observing the shell created by a supernova holds for the nebulae created by Wolf–Rayet stars provided, however, that dense filaments have no time to be formed in them (Section 8.5).

The mass of the gas involved in a bubble is approximately the same as that in a giant molecular cloud (see Section 8.2) – that is the cloud from which the association producing the bubble originated.

Although associations may differ in age, in the number of stars producing strong winds and, possibly, the parameters of the molecular cloud from which they originated, the X-ray spectra of the caverns around associations are closely similar (Section 8.2).

9. Spatial Distribution of the Objects Constituting Cygnus Superbubble

The observation results described in the preceding sections have led us to the conclusion that the X-ray superbubble discovered by Cash *et al.* (1980) is not a single structure but a projection on the sky of a combination of several points and extended X-ray sources. The distances to these sources vary from about 150 pc to 2–2.5 kpc (Sections 7 and 8) – that is, the numerous objects in the Cygnus region lie within the local spiral arm (Section 3.1). The shape of the superbubble both in X-ray and in optical emission is defined by the projection of the local spiral arm on the sky and by the effects of interstellar extinction.

As can be seen from Figure 3, the local spiral arm is curved in the galactic plane in such a manner that more distant objects are visible at smaller galactic longitudes. Accordingly, the objects forming the eastern part of the superbubble are closer to the Sun than those on the western edge.

An extensive system of obscuring gas-dust clouds that form the Great Rift is an important part of this picture. It is responsible for bifurcation of the Milky Way in the constellation Cygnus and, as was pointed out by Cash *et al.* (1980), obscuration of the X-rays from the central part of the superbubble, which gives it a horseshoe shape. The near edge of the Great Rift is about 0.5 to 0.8 kpc distant from the Sun; the distance to the far edge ranges from 1.2 to 2 kpc (Section 5.5). The most extensive complex of dust clouds is at a distance of 0.8 to 1.2 kpc and produces very high obscuration near the galactic plane.

All objects responsible for the X-ray and optical emission from the eastern part of the superbubble are concentrated to the near edge of the Great Rift at distances less than 1 kpc. The objects of the eastern part include: stellar associations Cyg OB4 and Cyg OB7 (Section 5.3), nebulae S119 and S117 (Sections 5.1 and 7.5), the Cyg Loop SNR (Sections 4.1 and 7.3), two H I supershells (Section 4.3), and the nova-like star SS Cyg (Section 7.4). The distances to these objects are given in Table IX. It can be seen that the main objects are localized within 0.5 to 1 kpc from the observer.

TABLE IX

Objects associated with the eastern part of the superbubble (southern hemisphere of the Galaxy)

Object	Distance R (kpc)	Reference
Stellar associations:		
Cyg OB7	0.8	Humphreys (1978)
Cyg OB4	1.0	Humphreys (1978)
Supernova remnant:		
Cyg Loop	0.8	Milne (1979)
Nebulae:		
North America	0.4–1.2	Becker (1964); Georgelin and Georgelin (1970)
S119	0.72	Savage and Jenkins (1972)
H I envelopes:		
GS 087 + 03 + 19	0.5	Heiles (1979)
GS 088 + 04 + 17	0.5	Heiles (1979)

The western part of the region consists of the following objects: five stellar associations (Table IV), several star clusters, dust clouds, an H I supershell (Section 4.3), five supernova remnants (Table I), the multicomponent extended radio source Cyg X (Section 4.2), and the X-ray source Cyg X-1 (Table VII). All these sources are at distances exceeding 1 kpc; the main objects that form the visible superbubble are less than 2.5 kpc distant (see Table X). The radio source Cyg X is the result of projection on the sky of many objects that lie within the local spiral arm (at distances from 1 to 4 kpc) and, probably, several objects belonging to the Perseus arm (see Section 4.2 and 5.5; Dickel *et al.*, 1969; Dickel and Wendker, 1978). Most of the components of radio source Cyg X are 1 to 2.5 kpc distant (Dickel *et al.*, 1969).

Thus, the majority of the objects in the western half of the region are at distances of 1 to 2.5 kpc. We probably observe only those objects that are sufficiently far from the galactic plane to be visible above the layer of the obscuring matter concentrated in the galactic plane (see Section 5.5, Figure 10).

Table XI gives column densities N_{H} (cm^{-2}) in the direction of some of the objects in the superbubble. The values of N_{H} have, in some cases, been derived from X-ray observations (marked by X in the fourth column of Table XI), in others, from radio data (marked by R), UV measurements of the Lα-line (marked by U), or values of interstellar extinction A_V (or E_{B-V}) and N_{H}, extinction relationship (Spitzer, 1978): $N_{\mathrm{H}} \sim 6 \times 10^{21} E_{B-V}$ (V in the fourth column). As can be seen from Table XI, different objects lying within the superbubble region are characterized by N_{H} values varying by more than one order of magnitude.

The optical emissions from the eastern and western parts of the superbubble, situated in the southern and northern hemisphere of the Galaxy, respectively, are markedly different in morphology (Figure 6). Objects in the eastern part represent separate nebulae

TABLE X

Objects associated with the western part of the superbubble (northern hemisphere of the Galaxy)

Object	Distance (kpc)	Reference
Stellar associations: Cyg OB1, OB2, OB3, OB8, OB9	1.2–2.3	Humphreys (1978)
Star clusters: NGC 6866, 6871, 6883, 6910, 6913, 7062; Ba6; IC 4996	1.2 – 2.1	Becker and Fenhart (1971)
Dust clouds	1–2	Kalandadze and Kolesnik (1977)
Supernova remnants: G 65.2 + 5.7, DR4, W63, HB21	1–1.6	Gull *et al.* (1975); Milne (1979)
Most of the ~90 emission nebulae in the Cyg-X region	(>1)–2.4	Dickel *et al.* (1969); Dickel and Wendker (1978)
H I envelope: GS 075 – 01 + 39	2.6	Heiles (1979)

TABLE XI

Column densities N_H for objects in Cygnus region

Object	Distance R (kpc)	$\log N_H$ (cm^{-2})	Determination method	Reference
Cyg superbubble	~2	21.85 ± 0.1	*X*	Cash *et al.* (1980)
Cyg Loop	~0.8	≈20.7	*X*	Rappaport *et al.* (1974)
S119	0.7	21.2	*U*	Savage and Jenkins (1972)
Cyg X-6		~22.0	*X*	Davidsen *et al.* (1977)
α Cyg (A2Ia)	0.6	20.37	*X*	Casinelli *et al.* (1981)
55 Cyg (B3Ia)	1.1	22.38	*X*	Casinelli *et al.* (1981)
Cyg OB2	1.8	22.0–22.2	*X*	Harnden *et al.* (1981)
Cyg X-7 = DR4		22.1–22.3	*X*	Davidsen *et al.* (1981)
HB21		21.7	*R*	Kaftan-Kassim (1961)
W63		~21.5	*V*	Wendker (1971)
NGC 6888	1.5–2	21.6	*V*	Willis and Wilson (1978)
Cyg X-1	≈2	21.8	*V*	Walborn (1973)
Cyg X-2		21.3–21.85	*X*	Bleeker *et al.* (1972)
G 65.2 + 5.7		20.4–22.4	*X*	Amnuel *et al.* (1982)
4U2129 + 4.7	1.4–1.6	21.15–21.6	*V*	Thorstensen *et al.* (1979)
V751 Cyg		21.5	*V*	Herbig (1958)

or filaments visible on the background of, or through, dust. Diffuse gas is observed in the northern part of the region, near the North-America nebula. The western part of the area leaves an impression of a continuous structure extending along the galactic plane and overlying it several degrees above (see Section 5.1, Figures 6 and 8). It is saturated with bright dense H II regions as well as intertwined gas and dust filaments.

Thus, the eastern and western parts of the Cygnus region are localized at distances < 1 kpc and > 1 kpc, respectively, and differ in morphology.

10. Origin of the Objects Forming the Cygnus Superbubble

In this section we shall discuss some aspects of star formation in the Cygnus region as well as formation of gas-dust shells around caverns; we shall also discuss the nature of the extended radio component detected in Cyg X.

10.1. Associations in the Western Part of the Superbubble

A giant system of gas and dust filaments, extending in the form of a two-crest wave along the galactic plane is observed in the western part of the Cygnus region (see Sections 9 and 5.1, Figure 6). Five associations, Cyg OB1, OB2, OB3, OB8, and OB9 occupy the crests and valleys of this wave (Figure 8). All associations but the last one are spatially close to one another – within 500 pc. The peculiar arrangement of the young associations with respect to the sinuous gaseous structure suggests that we are dealing with a star-formation region resulting from development of a Rayleigh–Taylor–Parker instability.

Pikel'ner (1970) demonstrated that the Rayleigh–Taylor instability may form a stellar association with a highly dense core which may be gravitationally bound. The highly dense and bright stellar association Cyg OB2 may look like an object originating in such an instability. Cyg OB2 seems to be the only known galactic object similar to the young globular clusters in the Magellanic clouds.

The Rayleigh–Taylor instability may have developed in the local spiral arm to the stage where compact associations of the Cyg OB2 type were formed. This happened, most probably, because the local arm does not, for some reason, have a spiral shock wave that might have stimulated star formation in giant molecular clouds before the Rayleigh–Taylor instability created a sufficiently dense object (Bochkarev, 1984a, c) for star formation. The absence of a spiral shock wave in the local arm may also account for the other peculiarities of the arm described in Section 3.1. The absence of a spiral shock wave in the local arm is also consistent with the explorations of Georgelin and Georgelin (1976), Mishurov *et al.* (1979), Pavlovskaya and Suchkov (1980), indicating that the Sun is in a region between major spiral arms.

We tried to check the hypothesis according to which the western part of the superbubble region originated from development of the magnetic field vectors derived from the interstellar polarization (see Section 5.6, Figure 11). In the case of a Rayleigh–Taylor instability, one might expect that the sinuous form of optical filaments would follow the orientation of the magnetic field (see Section 10.2). However, comparison of the distri-

bution of interstellar polarization vectors with the optical picture of the region indicates that the distribution of polarization vectors relative to the filaments is not regular as a whole. In any case, the available data do not show magnetic field-filament orientation correlation. The lack of correlation may be the result of lack of information.

An argument in favor of the above picture may be the distribution of high-latitude atomic hydrogen with low radial velocities (Heiles and Jenkins, 1976). It indicates that the region of the galactic longitudes from 70 to 90° in the northern hemisphere of the Galaxy contains a system of oblique H I filaments, which may be a reflection of the upper parts of the magnetic arcs resulting from the Rayleigh–Taylor instability.

10.2. Gas-dust envelopes around the caverns blown out by the stellar wind from associations and interstellar polarization

According to the calculations by Castor *et al.* (1975), a dense H I envelope forms around a cavern created by a stellar wind from a star in an advanced stage of evolution. According to (2) and (3), the column density in such an envelope is given by

$$N_{\mathrm{H}} = n_0 R/3 \sim 10^{21}\ \mathrm{cm}^{-2}\,.$$

Thus it may be expected that part of the neutral gas along the path to the sources of diffuse X-rays is concentrated immediately around the hot bubbles from which the X-rays originate.

Since the compressed gas must also contain interstellar dust, a dust ring may also form. From the usual relation between column density N_{H} and the interstellar extinction A_V (Spitzer, 1978), one may compute that the extinction in the thin envelope around the giant shell is about $0^{m}.5$, this value being greater when the observation is made along the tangent to the bubble. Thus, calculations of the parameters of the envelopes around caverns blown out by the stellar wind clearly suggest that dust rings of the Cyg 5 type (see Table IV) may exist around sufficiently dense stellar associations that produce strong winds. They are also likely to be observed in the far IR (~ 100 μm).

The gas density in the envelope blown out by the stellar wind from the association must be approximately 10^2 to $10^3\ \mathrm{cm}^{-3}$ (at $T \approx 10^2$ K). In view of the fact that the intensity of the magnetic field in compressed gas increases approximately in proportion to $n^{2/3}$, that of the field in such an envelope may be as high as tens and even hundreds of micro-oersteds. In such fields one should expect pronounced Zeeman-splitting of the 21 cm line. But if giant molecular clouds are formed by compression along field lines, the intensity of the magnetic field may be significantly lower (Mouschovias, 1976; Chaisson and Vrba, 1978).

The field lines must be oriented primarily along the surfaces of the formed envelopes. Since the orientation of dust particles in the gas flow by the Dolginov and Mitrofanov (1976) mechanism is very fast (about 10^2 yr under such conditions) and most of the dust along the line-of-sight to the stars of these associations may be concentrated in the envelopes around them, the orientation of the interstellar polarization vectors must follow that of the filaments around the associations.

As as mentioned above (Section 5.6), the observed orientation of polarization vectors

in this region is indeed markedly different from regular in the Galaxy (see Figure 11). However, we could not obtain any definite results, which seems to be due, as was already mentioned, to the complex structure of the filaments, a certain degree of the disturbance of the interstellar polarization by the dust between the observer and filaments, and the scant observational data.

10.3. Extended radio component in the Cyg X region

After having excluded all discrete components from the Cyg-X region, Wendker (1970) detected there an extended structure with dimensions ranging from 4 to 6°, correlating well with the position of the Cyg OB2 association (see Section 4.2). We believe that this association may be related to the system of optical filaments which extends across the galactic plane over almost 10° (Section 5.2). Brand and Zealey (1975) associate it with the dust envelope Cyg 5, which is about 8° in diameter (Table IV). In this section, we shall discuss the possible origin of the extended radio source discovered by Wendker (1970).

Let us assume that the extended radio source has a thermal emission spectrum. Then, taking into account the brightness temperature $T_b \approx 1$ K at 2.7 GHz it is easy to determine the emission measure of the nebula responsible for this source from

$$EM = 1.6 \times 10^4 \frac{T_b T^{1/2}}{\lambda^2 \langle gz^2 \rangle} \text{ pc cm}^{-6},$$

where λ is the wavelength, T is the gas temperature, and $\langle gz^2 \rangle$ is the Gaunt factor averaged in terms of the ion abundance. The source of the thermal emission may be either the hot ($T \sim 10^6$ K) coronal gas or the H II region around the association ($T \sim 10^4$ K). For $\lambda = 11$ cm, $\langle gz^2 \rangle = 6$ at $T = 10^4$ K and $\langle gz^2 \rangle = 10$ at $T = 10^6$ K. It can be easily seen, however, that radio-emission cannot be associated with the hot coronal gas. Indeed, at $T = 10^6$ K, $EM \simeq 10^4$, which can be seen from (1), is about five orders of magnitude above the value for the nebulae responsible for the diffuse emission from the superbubble. Thus, if the emission is thermal, it should be ascribed to the H II region around the association. In this case, $T \sim 10^4$ K and $EM \approx 2000$. The optical emission from such a nebula may invisible because of the strong interstellar extinction in the direction to Cyg OB2 ($A_V \approx 5$–6^m, Reddish *et al.*, 1966; see also Table XI). In view of the fact that the distance to the nebula is about 2 kpc, its radius must be $R \approx 100$ pc, hence, the number density must be $n_e \approx (EM/2R)^{1/2} \approx 3$ cm^{-3}.

For a nebula with such parameters it is necessary to have $N_{L_c} = \alpha n^2 \frac{4}{3}\pi R^3 \approx 3 \times 10^{50}$ L_c-photons per second. Here, $\alpha \approx 3 \times 10^{-13}$ cm^3 s^{-1} (Spitzer, 1978) is the hydrogen recombination coefficient. At the ionizing photon wavelength $\lambda \sim 600$ to 700 Å, the ionizing emission power must be about 10^{40} erg s^{-1}, which corresponds to an object with absolute bolometric magnitude $M_{\text{bol}} = -11^m$. This value roughly corresponds to the total emission from Cyg OB2 stars since this association contains several hot ($T = (40$–$50) \times 10^3$ K) stars with $M_{\text{bol}} \approx -10^m$ (Abbott *et al.*, 1981; Humphreys, 1978). Almost all of the emission from them falls into the Lyman continuum.

The mass of such a nebula must be about $2.5 \times 10^5 M_\odot$ – that is of the same order of magnitude as that of a giant molecular cloud. Thus, the interpretation of Wendker's (1970) observations of the thermal emission from the H II region around Cyg OB2 provides an estimate consistent with the optical data on the association. Eaerlier, a similar interpretation of the Cyg-X region was discussed by Veron (1965) among others.

The dimensions of the cavern blown by the stellar wind from the association must be similar to those of the H II region. From the expression dervied by Castor *et al.* (1975) for the cavern radius, age $t = 2 \times 10^6$ yr (Abbott *et al.*, 1981), $n = 3\ \mathrm{cm}^{-3}$, as was determined above from the radio data presented by Wendker (1970), and $L_w = 10^{37}$–$10^{38}\ \mathrm{erg\ s}^{-1}$ (see discussion of this value in Section 8.3), we have $R = 50$–80 pc. Thus the H II region around Cyg OB2 must have the shape of an envelope.

Another possible interpretation of Wendker's (1970) observations is based on hypothesis of a supernova remnant inside the cavern blown by the stellar wind from association Cyg OB2. In any event, surface radio brightness $\Sigma \approx 2 \times 10^{-21}\ \mathrm{erg\ m}^{-2}\ \mathrm{sr}^{-1}\ \mathrm{Hz}^{-1}$ agrees well with the $\Sigma - D$ relation for SNRs (Shklovskii, 1976; Lozinskaya, 1981). In this case, the size of the bubble blown by the association is assumed to be larger than the one derived above and to correspond to that of the optical filaments described earlier or to that of the dust ring Cyg 5 (Table IV). To verify the hypothesis that this is a supernova remnant requires examination of the spectrum of the radio-emission from this object.

Finally, it may be assumed, following the discussion in Section 8.3, that the power of the stellar wind in this association increased sharply within a relatively recent period of time, after the massive stars left the initial Main Sequence and supergiants and the Wolf–Rayet stars appeared in this association (Reddish, 1968). In this case, it may be expected that a new filamentary nebula blown out by the powerful stellar wind will start emerging inside the already formed cavern. In a gas with density $n \simeq 0.03\ \mathrm{cm}^{-3}$, a wind with power $L_w \approx 10^{38}\ \mathrm{erg\ s}^{-1}$ may blow out a cavern with a radius of 50 to 100 pc over a period of about 3×10^5 yr. In all likelihood, the stellar wind must compress the inhomogeneities that developed earlier in the nebula, as is the case, for instance, with planetary nebulae (Pikel'ner, 1973). The dense matter cools down, is compressed further, and may probably form a fine-filament nebula with the observed parameters. In this case, as opposed to SNR, nonthermal radio-emission will be absent.

Thus, for investigation of the nature of the extended radio component detected by Wendker (1970) in Cyg X, spectral radio observations of this component are required as well as investigation of its spatial structure.

10.4. Summary

In this section we speculated that the sinuous system of filaments and associations in the western part of the Cygnus region, remote from the galactc plane, have emerged emerged as a result of development of the Rayleigh–Taylor instability of the galactic gas disk (Section 10.1). Development of the Rayleigh–Taylor instability to a stage where such dense associations as Cyg OB2 are formed seems to be possible only in the absence

of a spiral shock wave in the local spiral arm. This conclusion is consistent with a number of investigators on the grand design of the Galaxy.

As was shown in Section 10.3, all observations of the extended radio component in the Cyg-X region, detected by Wendker (1970), may be interpreted either (1) as thermal emission from the H II shell around association Cyg OB2 with an average number density equal to 3 cm^{-3}, (2) as a supernova remnant, or else (3) as a filamentary nebula formed by a stellar wind with an intensity that has increased considerably over the past 3×10^5 yr, inside the already-formed, large, hot-gas cavern around Cyg OB2, confined by dust envelope Cyg 5 and/or a system of gas filaments, as discussed in Section 5.2. To know which of the above alternatives is true calls for spectral radio observations and investigation of the structure of the radio component in question.

In Section 10.2, we showed that the dust enveloped discussed by Brand and Zealey (1975) around some associations are a natural result of development of bubbles around the associations. Such gas-dust envelopes may exhibit pronounced Zeeman-splitting of the 21 cm line. The filaments of these envelopes must be oriented along the magnetic field.

To verify the hypotheses described in Section 10.2 requires further extensive studies of the correlation between the orientation of gas filaments and the interstellar polarization in the western portion of the Cygnus region.

11. Conclusion

This work summarizes and analyzes a wealth of observational data obtained in radio (Section 4), optical (Section 5), infrared (Section 6), and X-ray (Section 7) emissions from an extensive region of the galactic disk in which the Cyg superbubble is located (Section 2.1). An interpretation of these data is offered in Sections 8 through 10.

The main results of analysis of the emission in each range are summarized at the end of a respective section (see Sections 4, 5, and 7) and reviewed below in Section 11.1. The main conclusion from the entire work is that the superbubble observed by Cash *et al.* (1980) is not a single structure but a projection of many objects on the sky. The major arguments in favor of this conclusion are presented in Section 11.2. Section 11.3 covers the results of analysis of the contribution of various discrete X-ray sources to the emission from the superbubble, while Section 11.4 discusses the results of analysis of the nature of that part of the emission which cannot be explained by discrete sources. Section 11.5 summarizes the results of analysis of the spatial arrangement of the emission sources. Our main conclusions regarding the origin of some objects forming the Cygnus superbubble can be found in Section 11.6. Finally, Section 11.7 offers some other conclusions.

11.1. Basic characteristics of the region of interest

The sky sector occupied by the X-ray superbubble is essentially a gigantic aggregation of gas, dust, and high-luminosity stars within a region $\approx 15 \times 25^\circ$ in size; it is especially rich in terms of the emission nebulae it contains. At a distance of up to 2.5 kpc from

the Sun, the region contains 8 young stellar associations (Section 5.3) with about 110 stars of very high luminosity (including 55 supergiants of early spectral classes), about 20 Wolf–Rayet stars, 16 Of stars, many nebulae of different types (Tables II and IV; Sections 5.1, 5.2; Figures 6 and 7), and sinuous system of filaments, extending over about 20° along the galactic plane, with about five stellar associations occupying its 'valleys' (Section 5.1, Figure 8). The interstellar light extinction in this region is high (up to $3–5^m$ kpc^{-1} and more) and irregular (Section 5.5). It is determined primarily by the Great Rift which causes a bifurcation of the Milky Way and is 0.8 to 1.2 kpc distance from the Sun. The interstellar polarization of star light is irregular and, because of scant data, does not reveal a clear relationship between the orientations of the magnetic field and gas filaments, with the exception of the nebula S119 (Section 5.6). The velocities of expansion of most nebulae are small: $|v| \lesssim 20$ km s^{-1} (Section 5.1, Table III).

Radio-emission from this region is intense and inhomogenous. The western portion of the superbubble is superimposed and the extensively studied multicomponent radio source Cyg X (Sections 4.2 and 4.3) which was found to be a projection on the sky of many sources, mostly of thermal nature, spaced along the local spiral arm from 1 to 4 kpc (mainly 1 to 2.5 kpc). They are associated with molecular clouds (Section 4.3) and star-formation regions, such as W75 and others, where the star formation process is still continued (Section 6). The irregular thermal radio-emission forms a background against which non-thermal emission from eight supernova remnants is prominent (Section 4.1). There are also several H I supershells (Section 4.3).

The far IR emission is associated with prominent H II regions and dark clouds, while the near IR emission can be ascribed to stars reddened to a high degree (Section 6).

The superbubble region contains more than 20 X-ray sources listed in the catalogye compiled by Amnuel *et al.* (1982), including several bright binaries (Section 7.2), supernova remnants (Section 7.3), and numerous faint sources (Sections 7.4 and 7.5).

11.2. Arguments against the superbubble being a single structure

The main conclusion from this work is that the superbubble is not a single structure but a projection on the sky of many points as well as extended sources of soft X-rays. These sources are located mainly at distances ranging from 0.5 to 2 kpc from the Sun, in the local spiral arm (Section 3.1), to which the line-of-sight toward the constellation Cygnus is tangent.

That the superbubble is made up of a variety of objects is supported by the following facts:

(1) The observed dimensions of the superbubble are 18° along the galactic plane, 13° across it. This shape is hard to reconcile with its origin from a single center. At a distance of 2 kpc (Cash *et al.*, 1980) its physical dimension along the plane is more than 500 pc; its dimension perpendicular to the plane is 450 parsecs, a value greater than the thickness of the galactic gas disk (200–300 pc). One would expect to observe for an expanding superbubble, a dimension across the galactic plane greater than the dimension along the plane.

The observed shape follows naturally if the subject is not a single entity but made up

the projection of several objects distributed at different distances in the spiral arm, which is oblate in cross section and curved in the plane.

(2) The system of optical filaments, observed around the Cyg-X region by Ikhsanov (1960b), Dickel *et al.* (1969), and Brand and Zealey (1975), is not a continuous object but a combination of gas filaments spread over a distance of at least 1 kpc along the line-of-sight. This follows from comparison of radio and optical data on this ring of filaments, carried out by Kapp-her and Wendker (1972) (see Section 5.2).

(3) The hypothesis stating that the superbubble is a result of the explosion of one (Blinnikov *et al.*, 1982) or several (Cash *et al.*, 1980) supernovae is refuted by the absence of a nonthermal radio source with dimensions corresponding to those of the X-ray superbubble. On the contrary all evidence concerning the Cyg-X region and the surrounding objects suggests that, with the exception of eight supernova remnants (Table I) 3 to 4° in diameter, no sources of nonthermal radio-emission have been found in the region of interest. All the numerous radio sources with examined spectra attest to the thermal nature of the emission (Section 4).

(4) There seems to be nothing in common between the X-ray superbubble and H I superbubble GS 081–05–37 discovered by Heiles (1979) and associated, according to Cash *et al.* (1980), with the X-ray superbubble. The bubble found by Heiles is much more distant than the sources of soft X-rays (Section 4.3).

(5) The emission spectrum of the superbubble is irregular. This was brought to light (Section 7.1) by comparison of the data reported by Cash *et al.* (1980) and the observations of different parts of the superbubble carried out by other workers.

(6) The extensively studied radio source Cyg X (Sections 4.2, 4.3, and 5.5) is not a spatially coherent object with which the X-ray superbubble might be associated, but a projection on the sky of many, primarily thermal, radio sources located, with rare exceptions, at distances ranging from 1 to 4 kpc (mostly 1 to 2.5 kpc) in the local spiral arm.

11.3. Contribution of discrete sources to the superbubble radiation

As was shown in Section 7, 50 to 75% of the X-ray emission from the superbubble is produced by several dozens of known faint discrete X-ray sources not excluded from observations by Cash *et al.* (1980). These sources are located in the local arm. They repeat the horseshoe shape of the superbubble in projection on the sky by virtue of the fact that the central part of the region is obscured by the Great Rift. Fifteen percent of the emission can be ascribed to supernova remnant DR4 (Cyg X-7) from which X-rays were detected at the *Einstein* Observatory (Higgs *et al.*, 1983). Other supernova remnants account for a small portion of the X-ray emission (see Section 7.3). About 20% of the X-ray emission from the superbubble are attributable to cataclysmic variables (Section 7.4): EY Cyg (10%), V751 (9%), and SS Cyg (0.6–6%). The other faint sources included in the catalogue compiled by Amnuel *et al.* (1982) account for about 20% of the emission from the superbubble (Section 7.4). The most intense source is 4U2129 + 47 (6–7%). The X-rays emitted by the coronas of more than 100 high-luminosity and superluminous stars (Sectin 5.4) in the region under investigation seem

to account for not more than 1% of the emission from the superbubble. The bright nebulae S119 and NGC 6888 formed by the wind from stars of types O6f and WN6 may contribute about 2% to the emission from the superbubble (Bochkarev and Lozinskaya, 1985; Section 7.5).

Most of the above objects are sources of relatively soft X-rays and are characterized by low-frequency slopes in their spectra. This is caused by interstellar absorption in the range of hundreds of electron-volts, which makes their spectra similar to one another and to that of the superbubble as a whole. The critical point here is that (1) the position of the maximum in the spectrum of thermal sources is only weakly dependent on N_H and T (related as $(N_H T)^{1/4}$, Section 8.2), and (2) the column density N_H to objects associated with the superbubble varies by only slightly more than one order of magnitude (Table XI).

In spite of the importance of the contribution of discrete sources to the emission from the superbubble, at most $\sim 50\%$ of the emission can be attributed to them. To elucidate the contribution made by discrete sources calls for thorough observations of the entire region with a higher angular resolution and an adequate sensitivity in the range of 0.5 to 1 keV.

11.4. Origin of the Diffuse Emission from the Superbubble

We attribute 25 to 50% of the X-rays from the superbubble, which cannot be explained by discrete sources, to the emission from the hot ($T \approx 2 \times 10^6$ K) rarefied ($n \approx 0.03$ cm^{-3}) gas in the caverns formed around stellar associations by joint action of the stellar wind and supernova explosions (Section 8).

The Cygnus region contains eight stellar associations which, when projected on the sky, repeat the horseshoe shape of the superbubble (Figures 13 and 8). The caverns are confined by ring nebulae described by Brand and Zealey (1975). The typical radius of a cavern is $R = 50$ pc, their luminosity in soft X-ray emission is $L_x = (1\text{–}4) \times 10^{35}$ erg s^{-1} or more, and the number density of undisturbed gas is 4 to 10 cm^{-3} or more (see Section 8.1). The mass of the swept-up gas is roughly the same as that of a giant molecular cloud. It takes several million years for a cavern to evolve, which corresponds to the ages of the associations in the Cygnus region. Their theoretically derived expansion velocity is about 7 to 10 km s^{-1}, which agrees well with the low expansion velocities of the nebulae observed in the same region (Section 5.1, Table III).

Formulation of such caverns requires the injection of kinetic energy with average power $L_w \approx (1.5\text{–}4) \times 10^{36}$ erg s^{-1} (Section 8.2). This seems to exceed the average strength of the stellar wind from stars of a typical association (Section 8.3). The wind from supergiants and stars of the Main Sequence (Section 8.3), supernova explosions (Section 8.4), and the strong wind from Wolf–Rayet stars (Section 8.5) make approximately equal contributions to the kinetic energy required to form the caverns.

Although the stellar population differs from association to association and the immediately surrounding interstellar medium is different in each case, X-ray spectra of bubbles around the associations must be similar (Section 8.2) because, among other things (Section 11.3), the position of the maximum in the spectrum is only weakly

dependent on the parameters N_H and T which define the shape of the observed spectrum.

11.5. Spatial arrangement of emission sources

The emission sources whose projection on the sky produces the observed picture of the superbubble lie in the local spiral arm and are located mainly at distances of 0.5 to 2.5 kpc from the Sun (Section 9). The form and curvature of the spiral arm causes the eastern part of the superbubble to be formed mainly by objects less than 1 kpc distant from the Sun (Table IX) that lie in front of the Great Rift. This portion of the superbubble is connected with associations Cyg OB7 and Cyg OB4. Objects in the western part of the superbubble are 1 to 2.5 kpc distant from the Sun. They lie behind the main molecular clouds constituting the Great Rift (Table X), and are linked mostly with associations Cyg OB1, 2, 3, 8, and 9.

11.6. Origin of the large-scale objects in the Cygnus superbubble

In the western part of the superbubble the distribution of the stellar associations relative to the galactic plane and the observed sinuous system of filaments, led to the suggestion that these associations originated in Rayleigh–Taylor–Parker instabilities in the galactic disk.

The extended radio source discovered by Wendker (1970) seems to be related to the Cyg OB2 association. The nature of its radio-emission remains unknown (Section 10.3): it may be both thermal radio-emission from the low-density ($n \approx 3\ \mathrm{cm}^{-3}$) H II region around association Cyg OB2 and emission from the nebula formed either by a supernova explosion or by the stellar wind from association Cyg OB2, whose intensity may have increased substantially over the past 3×10^5 yr. To understand the origin of the radio-emission requires studies of the spectrum and structure of this radio source. We hypothesize (Section 5.2) that the oval system of filaments, extending across the galactic plane over about 10° (the main filaments occupy regions with coordinates $\alpha = 20^h10^m$–20^h30^m, $\delta = 42$–$46°$, and $\alpha = 20^h50^m$–21^h10^m, $\delta = 37$–$41°$) may be a continuous object connected with association Cyg OB2. To verify this hypothesis calls for comparison of the radio and optical emissions from these filaments.

The giant dust rings distinguished by Brand and Zealey (1975) around some associations are a natural consequence of development of envelopes around OB associations (Caster *et al.*, 1975) (Section 10.2) and must lead to systematic orientation of interstellar polarization.

11.7. Some other conclusions

(1) The remnants of supernova exploding in coronal gas caverns must exhibit certain peculiarities (Section 8.4): their evolution is over at the adiabatic stage when almost all of their kinetic energy is transmitted to the shock wave forming the coronal gas cavern. Their optical emission must be very faint. The radio-emission, on the other hand, may be pronounced (as seems to be the case with the North-Polar Spur (Weaver, 1979) and,

probably, the extended radio source in Cyg X (Sections 10.3 and 11.6), although against the background of numerous bright radio sources in the constellation Cygnus it may as well remain unnoticed.

(2) The expulsion of the envelope or the strong wind from Wolf–Rayet and other stars, occurring inside coronal gas caverns, does not necessarily form the observed nebulae if the gas has insufficient time to produce dense condensations (Section 8.5).

(3) The kinetic energy of the supernova remnants formed by the most massive stars does not seem to exceed 10^{49} erg (Section 8.4).

(4) The dense gas-dust envelopes formed at late stages of the evolution of the caverns around OB associations (Sections 10.3 and 11.6) can have magnetic fields with a strength of dozens or even hundreds of micro-oersteds, and their observation is may be possible through both the Zeeman-splitting of the 21 cm hydrogen line and interstellar polarization of star light.

Acknowledgements

The authors gratefully thank I. S. Shklovskii for useful discussions, Harold Weaver for discussion and editing of the article, and W. Cash for submission of the figure with distribution of X-ray radiation from the Cygnus superbubble on the sky.

References

Abbott, D. C., Bieging, J. H., and Churchwell, E.: 1981, *Astrophys. J.* **250**, 645.
Ackermann, G.: 1970, *Astron. Astrophys.* **8**, 315.
Amnuel, P. R., Guseinov, O. H., and Rakhamimov, Sh. Yu.: 1982, *Astrophys. Space Sci.* **82**, 3.
Antokhin, I. I., Aslanov, A. A., and Chrerepashchuk, A. M.: 1982, *Pis'ma Astron. Zh.* **8**, 290 (*Soviet Astron. Letters* **8**, 156).
Avedisova, V. S.: 1971, *Astron. Zh.* **48**, 894 (*Soviet Astron.* **15**, 708).
Avedisova, V. S.: 1977, *Pis'ma Astron. Zh.* **3**, 405 (*Soviet Astron. Letters* **3**, 217).
Avedisova, V. S.: 1981, *Catalogue of Star Formation Regions in the Galaxy*, Part 1, Observational Data, Supplement to the Collection, Nauchnye Informacii, iss 47, Riga, Zinatne.
Balog, N. I., Goncharskij, A. V., and Cherepashchuk, A. M.: 1981, *Astron. Zh.* **58**, 67 (*Soviet Astron.* **25**, 38).
Barlow, M. J., Smith, L. J., and Willis, A. J.: 1981, *Monthly Notices Roy. Astron. Soc.* **196**, 101.
Becker, W.: 1964, *Z. Astrophys.* **58**, 202.
Becker, W. and Fenkart, R.: 1971, *Astron. Astrophys. Suppl. Ser.* **4**, 241.
Berkhuijzen, E. M.: 1971, *Astron. Astrophys.* **14**, 359.
Bleeker, J. A. M., Deerenberg, A. J. M., Yamashita, K., Hayakawa, S., and Tanaka, Y.: 1972, *Astrophys. J.* **178**, 377.
Blinnikov, S. I., Imshennik, V. S., and Utrobin, V. P.: 1982, *Pis'ma Astron. Zh.* **8**, 671 (*Soviet Astron. Letters* **8**, 361).
Blissett, R. J., Mason, K. O., and Culhane, J. L.: 1981, *Monthly Notices Roy. Astron. Soc.* **194**, 77.
Bochkarev, N. G.: 1984a, *Pis'ma v. Astron. Zh.* **10**, 184 (*Soviet Astron. Letters* **10**, 76).
Bochkarev, N. G.: 1984b, *Soviet Astron.*, in press.
Bochkarev, N. G.: 1984c, in 'Local Interstellar Medium', *IAU Colloq.* **81**.
Bochkarev, N. G. and Lozinskaya, T. A.: 1985, *Astron. Zh.* **61**, No. 1 (*Soviet Astron.* **28**, No. 1).
Bochkarev, N. G. and Sitnik, T. G.: 1983, *Soviet Astron. Circ.* **1261**, 1.
Bochkarev, N. G., Karitskaya, E. A., and Shakura, N. I.: 1975, *Pis'ma Astron. Zh.* **1**, No. 12, 13 (*Soviet Astron. Letters* **1**, 118).
Bok, B. J.: 1959, *Observatory* **79**, 58.
Bok, B. J. and Bok, P. F.: 1957, *The Milky Way*, Harvard Univ. Press, Cambridge, Massachusetts.

Bolton, J. G. and Westford, K. C.: 1950, *Australian J. Sci. Res.* **A3**, 251.
Brand, P. W. J. L. and Zealey, W. J.: 1975, *Astron. Astrophys.* **38**, 363.
Brandt, H. V. D. and McClintock, J. E.: 1983, *Ann. Rev. Astron. Astrophys.* **21**, 13.
Bregman, J., Butler, D., Kemper, E., Koski, A., Kraft, R. P., and Stone, R. P. S.: 1973, *Astrophys. J.* **185**, L117.
Bruhweiler, F. C., Gull, T. R., Kafatos, M., and Sofia, S.: 1980, *Astrophys. J.* **238**, L27.
Burginyon, G., Hill, R., Palmieri, T., Scudder, J., Seward, F., Stoering, J., and Toor, A.: 1973, *Astrophys. J.* **179**, 615.
Burton, W. B., Gordon, M. A., Bania, T. M., and Lockman, F. J.: 1975, *Astrophys. J.* **202**, 30.
Bychkov, K. V. and Pikel'ner, S. B.: 1975, *Pis'ma Astron. Zh.* **1**, 29 (*Soviet Astron. Letters* **1**, 14).
Bychkov, K. V. and Lebedev, V. C.: 1979, *Astron. Astrophys.* **80**, 167.
Byl, J. and Ovenden, M. W.: 1978, *Astrophys. J.* **225**, 496.
Campbell, M. F., Hoffmann, W. F., Throuson, H. A. Zr., and Harvey, P. A.: 1980, *Astrophys. J.* **238**, 122.
Cash, W., Charles, P., Bowyer, S., Walter, F., Garmire, G., and Riegler, G.: 1980, *Astrophys. J.* **238**, L71.
Cassinelli, J. P., Waldron, W. L., Sanders, W. T., Harnden, F. R., Rosner, R., and Vaiana, G. S.: 1981, *Astrophys. J.* **250**, 677.
Castor, J., McCray, R., and Weaver, R.: 1975, *Astrophys. J.* **200**, L107.
Chaisson, E. J. and Vrba, F. J.: 1978, in T. Gehrels (ed.), *Protostars and Planets,* Univ. of Arizona Press, Arizona, p. 189.
Cherepashchuk, A. M.: 1982, *Astrophys. Space Sci.* **86**, 299.
Churchwell, E., Mezger, P. G., and Huchtmeier, W.: 1974, *Astron. Astrophys.* **32**, 283.
Clark, D. H. and Culhane, J. L.: 1976, *Monthly Notices Roy. Astron. Soc.* **175**, 573.
Coleman, P. L., Bunner, A. N., Kraushaar, W. L., and McCammon, D.: 1971, *Astrophys. J.* **170**, L47.
Cordova, F. A., Nugent, J. J., Klein, S. R., and Garmire, G. P.: 1980, *Monthly Notices Roy. Astron. Soc.* **190**, 87.
Cordova, F. A., Jensen, K. A., and Nugent, J. J.: 1981, *Monthly Notices Roy. Astron. Soc.* **196**, 1.
Courtès, G., Cruvellier, P., and Georgelin, J.: 1966, *J. Obs.* **49**, 329.
Cox, D. P.: 1972, *Astrophys. J.* **178**, 143.
Cox, D. P. and Smith, B. W.: 1974, *Astrophys. J.* **189**, L105.
Cruddace, R., Paresce, F., Bowyer, S., and Lampton, M.: 1974, *Astrophys. J.* **187**, 497.
Davidsen, A. F., Henry, R. C., Snyder, W. A., Friedman, H., Fritz, G., Naranan, S., Shulman, S., and Yentis, D.: 1977, *Astrophys. J.* **215**, 541.
Davidsen, A., Shulman, S., Fritz, G., Meekins, J. F., Henry, R. C., and Friedman, H.: 1972, *Astrophys. J.* **177**, 629.
Davies, R. D. and Matthews, H. E.: 1962, *Monthly Notices Roy. Astron. Soc.* **156**, 253.
de Jager, C.: 1980, *The Brightest Stars,* D. Reidel Publ. Co., Dordrecht, Holland.
Dickel, H. R. and Wendker, H. J.: 1977, *Astron. Astrophys. Suppl.* **29**, 209.
Dickel, H. R. and Wendker, H. J.: 1978, *Astron. Astrophys.* **66**, 289.
Dickel, H. R., Dickel, J. R., Wilson, W. J., and Epstein, E. E.: 1974, *Bull. Am. Astron. Soc.* **6**, 221.
Dickel, H. R., Wendker, H., and Bieritz, J. H.: 1969, *Astron. Astrophys.* **1**, 270.
Dieter, N. H.: 1967, *Astrophys. J.* **150**, 435.
Dolginov, A. Z. and Mitrofanov, I. G.: 1976, *Astrophys. Space Sci.* **43**, 257.
Dopita, M. A., Ford, V. L., McGregor, P. J., Mathewson, D. S., and Wilson, I. R.: 1981, *Astrophys. J.* **250**, 103.
Doroshenko, V. T., Sakhibov, F. Kh., and Sitnik, T. G.: 1982, *Astron. Zh.* **59**, 699 (*Soviet Astron.* **26**, 427).
Downes, D. and Rinehart, R.: 1966, *Astrophys. J.* **144**, 937.
Dyson, J. E. and de Vries, L. L.: 1972, *Astron. Astrophys.* **20**, 223.
Emerson, J. P.: 1976, *Monthly Notices Roy. Astron. Soc.* **177**, 113P.
Esipov, V., Klement'eva, A. Yu., Kovalenko, A. V., Lozinskaya, T. A., Lyutyi, V. M., Sitnik, T. G., and Udal'tsov, V. A.: 1982, *Astron. Zh.* **59**, 965 (*Soviet Astron.* **26**, 582).
Forman, W., Zones, C., Cominsky, L., Julien, P., Murray, S., Peters, G., Tananbaum, H., and Giacconi, R.: 1978, *Astrophys. J. Suppl. Ser.* **38**, 357.
Freeman, K. C.: 1977, in B. M. Tinsley and R. B. Larson (eds.), *The Evolution of Galaxies and Stellar Populations*, New Haven, Yale Univ. Obs., p. 133.
Georgelin, J. P. and Georgelin, J. M.: 1970, *Astron. Astrophys.* **6**, 349.
Georgelin, J. M. and Georgelin, J. P.: 1976, *Astron. Astrophys.* **49**, 57.

Georgelin, J. M., Georgelin, J. P., and Sivan, J.-P.: 1979, in W. B. Burton (ed.), 'The Large-Scale Characteristics of the Galaxy', *IAU Symp.* **84**, 65.
Goss, W. W.: 1968, *Astrophys. J. Suppl. Ser.* **137**, 131.
Goudis, C.: 1976, *Astrophys. Space Sci.* **44**, 281.
Goudis, C.: 1982, in *The Orion Complex: A Case Study of Interstellar Matter*, D. Reidel Publ. Co., Dordrecht, Holland.
Goudis, C. and Meaburn, J.: 1978, *Astron. Astrophys.* **68**, 189.
Gull, T. R., Kirshner, R. P., and Parker, R. A. R.: 1977, *Astrophys. J.* **215**, L69.
Hall, J. S.: 1958, *Publ. U.S. Naval Obs. Ser.* **17**, 275.
Harnden, F. R., Jr., Branduardi, G., Elvis, M., Gorenstein, P., Grindlay, J., Pye, J. P., Rosner, R., Topka, K., and Vaiana, G. S.: 1979, *Astrophys. J.* **234**, L51.
Heiles, C.: 1979, *Astrophys. J.* **229**, 533.
Heiles, C.: 1984, *Astrophys. J. Suppl. Ser.* **55**, No. 4.
Heiles, C. and Jenkins, E. B.: 1976, *Astron. Astrophys.* **46**, 333.
Heilkes, C., You-Hua-Shu, and Troland, T. H.: 1981, *Astrophys. J.* **247**, L77.
Heise, J., Mewe, R., Brinkman, A. C., Gronenshield, E., Boggende, A., Schrijver, J., Parsignault, D. R., and Grindlay, J. E.: 1978, *Astron. Astrophys.* **63**, L1.
Herbig, G. H.: 1958, *Astrophys. J.* **128**, 259.
Higdon, J. C.: 1981, *Astrophys. J.* **244**, 88.
Higgs, L. A.: 1966, *Monthly Notices Roy. Astron. Soc.* **132**, 67.
Higgs, L. A., Brotten, N. W., Medd, W. J., and Raghavrao, R.: 1965, *Monthly Notices Roy. Astron. Soc.* **127**, 367.
Higgs, L. A., Landecker, T. L., and Seward, F. D.: 1983, in J. Danziger and P. Gorenstein (eds.), 'Supernova Remnants and Their X-Ray Emission', *IAU Symp.* **101**, 281.
Hiltner, W. A.: 1956, *Astrophys. J. Suppl. Ser.* **2**, 389.
Hoffmann, W. F., Frederick, C. L., and Emery, R. J.: 1971, *Astrophys. J.* **170**, L89.
Humphreys, R. M.: 1976, *Publ. Astron. Soc. Pacific* **88**, 647.
Humphreys, R. M.: 1978, *Astrophys. J. Suppl. Ser.* **38**, 309.
Icke, V.: 1979, *Astron. Astrophys.* **78**, 352.
Icke, V.: 1981, *Astrophys. J. Suppl.* **45**, 585.
Ikhsanov, R. N.: 1959, *Izv. Krymsk. Astrophys. Obs.* **21**, 257.
Ikhsanov, R. N.: 1960a, *Astron. Zh.* **37**, 275 (*Soviet Astron.* **4**, 258).
Ikhsanov, R. N.: 1960b, *Astron. Zh.* **37**, 988 (*Soviet Astron.* **4**, 923).
Jefferts, K. B., Penzias, A. A., and Wilson, R. W.: 1970, *Astrophys. J.* **161**, L87.
Jenkins, E. B.: 1978, *Astrophys. J.* **219**, 845.
Jenkins, E. B. and Meloy, D.: 1974, *Astrophys. J.* **193**, L121.
Johnson, H. M.: 1980, *Astrophys. J.* **235**, 66.
Kaftan-Kassim, M. A.: 1961, *Astrophys. J.* **133**, 821.
Kalandadze, N. B. and Kolesnik, L. N.: 1977, *Astrometrija Astrofizika* **32**, 57.
Kaplan, S. A. and Pikel'ner, S. B.: 1970, *The Interstellar Medium,* Harvard University Press, Cambridge.
Kaplan, S. A. and Pikel'ner, S. B.: 1979, *Physics of the Interstellar Medium*, Nauka, Moscow.
Kapp-herr, A. V. and Wendker, H. J.: 1972, *Astron. Astrophys.* **20**, 313.
Karitskaya, E. A.: 1981, Thesis, Sternberg State Astronomical Institute, Astronomical Council, Moscow.
Kraft, R. P.: 1962, *Astrophys. J.* **135**, 408.
Kukarkin, B. V., Khopolov, P. N., Efremov, Yu. N., Kukarkina, N. P., Kurochkin, N. E., Medvedeva, G. I., Perova, N. B., Fedorovich, V. P., and Frolov, M. S.: 1969, *General Catalogue of Variable Stars,* USSR Acad. Sci., Moscow.
Kumar, C. K., Kallman, T. R., and Thomas, R. J.: 1983, *Astrophys. J.* **272**, 219.
Long, K. S. and White, R. L.: 1980, *Astrophys. J.* **239**, L65.
Lozinskaya, T. A.: 1972, *Astron. Zh.* **49**, 265 (*Soviet Astron.* **16**, 219).
Lozinskaya, T. A.: 1975, *Astron. Zh.* **52**, 515 (*Soviet Astron.* **19**, 315).
Lozinskaya, T. A.: 1980a, *Pis'ma Astron. Zh.* **6**, 350 (*Soviet Astron. Letters* **6**, 193).
Lozinskaya, T. A.: 1980b, *Astron. Zh.* **57**, 707 (*Soviet Astron.* **24**, 407.
Lozinskaya, T. A.: 1980c, *Astron. Astrophys.* **84**, 26.
Lozinskaya, T. A.: 1981, *Pis'ma Astron. Zh.* **7**, 29 (*Soviet Astron. Letters* **7**, 17).

Lozinskaya, T. A.: 1982, *Astrophys. Space Sci.* **87**, 313.
Lozinskaya, T. A. and Lomovskij, A. I.: 1982, *Pis'ma Astron. Zh.* **8**, 224 (*Soviet Astron. Letters* **8**, 119).
Lozinskaya, T. A. and Sitnik, T. G.: 1978, *Pis'ma Astron. Zh.* **4**, 509 (*Soviet Astron. Letters* **4**, 274).
Lozinskaya, T. A., Klement'eva, A. Yu., Zhukov, G. V., and Shenavrin, V. I.: 1975, *Astron. Zh.* **52**, 682 (*Soviet Astron.* **19**, 416).
Lucke, P. B.: 1974, *Astrophys. J. Suppl. Ser.* **28**, 73.
Lucke, P. B.: 1978, *Astron. Astrophys.* **64**, 367.
Lynds, B. T.: 1962, *Astrophys. J. Suppl.* **7**, 1.
Margon, B., Bowyer, S., and Stone, R. P. S.: 1973, *Astrophys. J.* **185**, L113.
Martynov, D. Ya. and Kholopov, P. N.: 1957, *The Variable Stars* **11**, 222 (USSR Acad. Sci.).
Massevich, A. G. and Tutukov, A. V.: 1981, 'Physics and Evolution of Stars', *Sci. Reviews, Ser. Cosmical Researches* **17**, VINITI, Moscow.
Mathewson, D. S. and Ford, V. L.: 1971, *Mem. Roy. Astron. Soc.* **74**, 139.
Mathewson, D. S., Large, M. I., and Haslam, C. G. T.: 1960, *Monthly Notices Roy. Astron. Soc.* **120**, 242.
McCutcheon, W. H. and Shuter, W. L. H.: 1970, *Astron. J.* **75**, 910.
McKee, C. F. and Ostriker, J. P.: 1977, *Astrophys. J.* **217**, 148.
Meaburn, J.: 1980, *Monthly Notices Roy. Astron. Soc.* **192**, 365.
Metik, L. P.: 1961, *Izv. Krymsk. Astrophys. Obs.* **26**, 386.
Miller, F. D.: 1937, *Ann. Harv. Coll. Obs.* **105**, 297.
Miller, J. S.: 1968, *Astrophys. J.* **151**, 473.
Milne, D. K.: 1979, *Australian J. Phys.* **32**, 83.
Mishurov, Yu. N., Pavlovskaya, E. D., and Suchkov, A. A.: 1979, *Astron. Zh.* **56**, 268 (*Soviet Astron.* **23**, 147).
Morgan, W. W.: 1955, *Astrophys. J.* **121**, 611.
Mouschovias, T. Ch.: 1976, *Astrophys. J.* **207**, 141.
Müller, D. K.: 1979, *Z. Astrophys.* **9**, 331.
Müller, H. and Hufnagel, L.: 1935, *Z. Astrophys.* **9**, 331.
Parker, R. A. R., Gull, T. R., and Kirshner, R. P.: 1979, *An Emission-Line Survey of the Milky Way,* NASA, SP-434.
Pashchenko, M. I.: 1973, *Astron. Zh.* **50**, 685 (*Soviet Astron.* **17**, 438).
Pavlovskaya, E. D. and Suchkov, A. A.: 1980, *Astron. Zh.* **57**, 280 (*Soviet Astron.* **24**, 164).
Pedlar, A. and Davies, R. D.: 1972, *Monthly Notices Roy. Astron. Soc.* **159**, 129.
Pedlar, A. and Matthews, H. E.: 1973, *Monthly Notices Roy. Astron. Soc.* **165**, 381.
Perry, C. L. and Johnson, L.: 1982, *Astrophys. J. Suppl. Ser.* **50**, 451.
Piddington, J. H. and Minnett, H. C.: 1952, *Australian J. Sci. Res.* **A5**, 17.
Pike, E. M. and Drake, F. D.: 1964, *Astrophys. J.* **139**, 545.
Pikel'ner, S. B.: 1954, *Izv. Krymsk. Astrophys. Obs.* **12**, 93.
Pikel'ner, S. B.: 1970, *Astron. Zh.* **47**, 254 (*Soviet Astron.* **14**, 208).
Pikel'ner, S. B.: 1973, *Astrophys. Letters* **15**, 91.
Pikel'ner, S. B. and Shcheglov, P. V.: 1968, *Astron. Zh.* **45**, 953 (*Soviet Astron.* **12**, 757).
Pučinskas, A.: 1982, *Vilneians Astron. Obs. Biuletenis* **61**, 3.
Quiroga, R. J. and Schlosser, W.: 1977, *Astron. Astrophys.* **57**, 455.
Rappaport, S., Petre, R., Kayat, H., Evans, K., Smith, G., and Levine, A.: 1974, *Astrophys. J.* **227**, 285.
Raymond, J. C. and Smith, B. W.: 1977, *Astrophys. J. Suppl. Ser.* **35**, 419.
Reddish, V. C.: 1968, *Observatory* **88**, 139.
Reddish, V. C., Lawrence, L. C., and Pratt, N. M.: 1966, *Publ. Roy. Obs. Edinburgh,* **5**, 111.
Reifenstein, E. C., Wilson, T. L., Burke, B. F., Mezger, P. G., and Altenhoff, W. J.: 1970, *Astron. Astrophys.* **4**, 357.
Reynolds, R. J.: 1980, *Bull. Astron. Am. Soc.* **12**, 860.
Reynolds, R. J. and Ogden, P. M.: 1979, *Astrophys. J.* **229**, 942.
Rickett, M. J., King, A. R., and Raine, D. J.: 1979, *Monthly Notices Roy. Astron. Soc.* **186**, 233.
Ride, S. K. and Walker, A. B. C.: 1977, *Astron. Astrophys.* **61**, 339.
Rydbeck, O. E. H., Kollberg, E., Hjalmarson, A., Sume, A., Ellder, J., and Irvine, W. M.: 1976, *Astrophys. J. Suppl. Ser.* **1**, 333.
Sabbadin, F.: 1976, *Astron. Astrophys.* **51**, 159.
Salpeter, E. E.: 1979, in W. B. Burton (ed.), 'The Large-Scale Characteristics of the Galaxy', *IAU Symp.* **84**, 245.

Sato, F.: 1968, *Publ. Astron. Soc. Japan* **20**, 303.
Savage, B. D. and Jenkins, E. B.: 1972, *Astrophys. J.* **172**, 491.
Scheuer, P. A. S. and Ryle, M.: 1953, *Monthly Notices Roy. Astron. Soc.* **113**, 3.
Schraml, J. and Mezger, P. G.: 1969, *Astrophys. J.* **156**, 269.
Scoville, N. Z. and Solomon, P. M.: 1975, *Astrophys. J.* **199**, L105.
Sedov, L. I.: 1957, *Methods of Similarity and Dimension in Mechanics*, Gostekhizdat, Moscow.
Seward, F. D., Forman, W. R., Giacconi, R., Griffiths, R. E., Harnden, F. R., Jr., Zones, C., and Pye, J. P.: 1979, *Astrophys. J.* **234**, L55.
Sharov, A. S.: 1982, *The Andromeda Nebula,* Nauka, Moscow.
Shklovskii, I. S.: 1960, *Cosmic-Radio Waves*, Harvard Univ. Press, Cambridge.
Shklovskii, I. S.: 1976, *Supernovae and Problems Connected with Them*, Nauka, Moscow.
Snyder, W. A., Davidsen, A. F., Henry, R. C., Shulman, S., Fritz, G., and Friedman, H.: 1978, *Astrophys. J.* **222**, L13.
Spitzer, L., Jr.: 1978, *Physical Processes in the Interstellar Medium*, Wiley and Sons, New York.
Struve, O.: 1957, *Sky Telesc.* **16**, 118.
Terzian, Y. and Parrish, A.: 1973, *Astron. J.* **78**, 894.
Thorstensen, J., Charles, P., Bowyer, S., Briel, U. G., Doxsey, R. E., Griffiths, R. E., and Schwartz, D. A.: *Astrophys. J.* **233**, L57.
Tucker, W. H. and Blumenthal, G. R.: 1974, in R. Giacconi and H. Gursky (eds.), *X-Ray Astronomy*, D. Reidel Publ. Co., Dordrecht, Holland, p. 99.
Turner, B. E.: 1973, *Astrophys. J.* **186**, 357.
Uranova, T. A.: 1968, *Astron. Zh.* **45**, 1318 (*Soviet Astron.* **12**, 1041).
Uranova, T. A.: 1985a, *Pis'ma v. Astron. Zh.* **11** (*Soviet Astron. Letters* **11**).
Uranova, T. A.: 1985b, *Astron. Zh.*, in press.
Vaiana, G. S., Cassinelli, J. P., Fabbiano, H., Giacconi, R., Golub, L., Gorenstein, P., Haisch, B. H., Harnden, F. R., Jr., Johnson, H. M., Linsky, J. L., Maxson, C. W., Mewe, R., Rosner, R., Seward, F., Topka, K., and Zwaan, C.: 1981, *Astrophys. J.* **245**, 163.
Vanäs, E.: 1941, Uppsala Medd., No. 81.
Van der Hucht, K. A., Conti, P. S., Lundström, I., and Stenholm, B.: 1981, *Space Sci. Rev.* **3**, 227.
Veron, P.: 1965, *Ann. Astrophys.* **28**, 391.
Vidal, N. V. and Wickramasinghe, D. T.: 1974, *Astron. Astrophys.* **36**, 306.
Walborn, N. R.: 1973, *Astrophys. J.* **180**, L35.
Weaver, H.: 1979, in W. B. Burton (ed.), 'Large-Scale Characteristics of the Galaxy', *IAU Symp.* **84**, 295.
Weaver, R., McCray, R., Castor, J., Shapiro, P., and Moore, R.: 1977, *Astrophys. J.* **218**, 377.
Wendker, H. J.: 1967, *Z. Astrophys.* **66**, 379.
Wendker, H. J.: 1970, *Astron. Astrophys.* **4**, 378.
Westerhout, G.: 1958, *Bull. Astron. Inst. Neth.* **14**, 215.
Willis, A. J. and Wilson, R.: 1978, *Monthly Notices Roy. Astron. Soc.* **182**, 559.
Wilson, A. S.: 1980, *Astrophys. J.* **241**, L19.
Wilson, W. J., Schwartz, R. P., Epsteine, E. E., Johnson, W. A., Etcheverry, R. D., Mori, T. T., Berry, G. G., and Dyson, H. B.: 1974, *Astrophys. J.* **191**, 357.
Wolf, M.: 1923, *Astron. Nachr.* **219**, 109.
Wolf, M.: 1925, *Astron. Nachr.* **223**, 89.
Yang, K. S. and West, L. A.: 1964, *Astron. J.* **69**, 246.
York, D. G.: 1974, *Astrophys. J.* **193**, L127.
York, D. G.: 1977, *Astrophys. J.* **213**, 47.
Yungel'son, L. R. and Massevich, A. G.: 1983, in R. A. Sunyaev (ed.), *Astrophysics and Space Physics Reviews, Soviet Scientific Reviews,* Section E, Harwood Academic Publ., New York, Vol. 2, p. 29.
Zasov, A. V. and Demin, V. V.: 1979, *Astron. Zh.* **56**, 941 (*Soviet Astron.* **23**, 941).